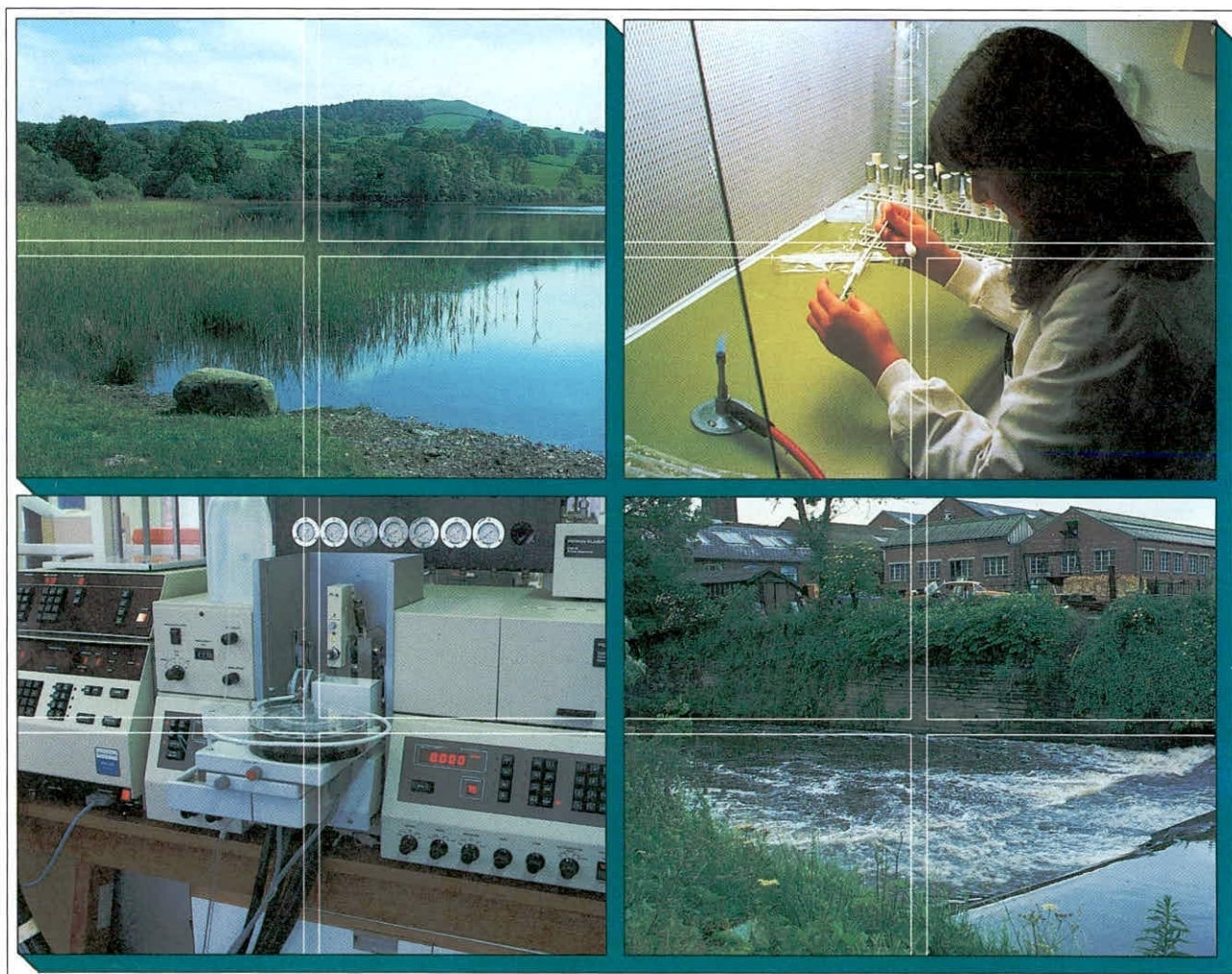# Institute of Freshwater Ecology

Towards a functional model of radionuclide transport in freshwaters

J. Hilton
M.C. Vaz Carreiro
A. Cremers
L. Foulquier
U. Sansone

R. Blust
J. Fernandez Garcia
R.N.J. Comans
T. Forseth

Natural Environment Research Council

Towards a functional model of radionuclide transport in freshwaters

1.	J. Hilton	NERC
2.	M.C. Vaz Carreiro	DGA
3.	A. Cremers	Univ. Leuven (KUL)
4.	L. Foulquier	CEA
6.	U. Sansone	ANPA
7.	R. Blust	Univ. Antwerpen (RUCA)
8.	J. Fernandez Garcia	Univ. Malaga (UMAG)
10.	R.N.J. Comans	ECN
11.	T. Forseth	NINA

INTELLECTUAL PROPERTY RIGHTS

CONFIDENTIALITY STATEMENT

Final Report

Contract: F13P-CT92-0029

Title: Towards a functional model of radionuclide transport in freshwaters.

1)	Hilton	NERC
2)	Ortins	DGA
3)	Cremers	Univ. Leuven (KUL)
4)	Foulquier	CEA
6)	Sansone	ANPA
7)	Blust	Univ. Antwerpen (RUCA)
8)	Fernandez	Univ. Malaga (UMAG)
10)	Comans	ECN
	Forseth	NINA

Summary

Measurement and Prediction of radiocaesium distribution coefficient (K_d)

The distribution coefficient (K_d) is a fundamental parameter in mathematical models of radionuclide transport in aquatic systems. Measured values in the literature range from 10^2 to 10^5. Because of this wide range the use of an estimated K_d is very prone to error. The ion-exchange theory of sorption suggests that in the presence of a major competitor the K_d is given by:

$$K_d = \frac{K_c[sites]}{[M^{a+}]}$$

where K_c is the selectivity coefficient, [sites] is the number of sites in terms of equivalents per gramme of solid and $[M^{a+}]$ is the concentration in solution of the major competitor (with the same charge as the material of interest) for sites on the solid. For radiocaesium, previous work has shown that the selectivity of the so-called frayed edge sites (FES) on illite particles is so high that these sites define the sorption of caesium, even in mixed mineral systems. Under aerobic conditions K^+ is the major competing ion for these specific sites and under anaerobic conditions NH_4 competes. Studies in the present programme have focused on the extension of our understanding of the parameters defining K_d.

Because of the high selectivity of FES for Cs, it is necessary to know the FES if the K_d in any chemical scenario is to be predicted. In a previous study a complex masking technique using silver thiourea was developed. As a result of new work by KUL this method has been replaced by a single measurement of K_d in a defined medium (Ca^{2+}: 100 mM; K^+: 5 mM). Under these chemical conditions all the potassium and caesium will be confined to the FES. Hence, knowing the K^+ concentration in solution and the K_d it is possible to calculate the product K_c.[FES]. By measuring this in a series of similar, mixed Ca: K: NH_4 or Na solutions, it is possible to measure K_c.[FES] for the ammonium and sodium systems, respectively. From these constants and a knowledge of the in situ [K], [NH_4] and [Na] it

was possible to predict the K_d for a range of soils and sediments to within a factor of 3 in laboratory experiments where K_d covered the range 50 - 50000 l kg^{-1}. Using the same approach, DGA/DPSR were able to predict K_d's of suspended solids and bottom sediments in field samples to within a factor of 2.

A detailed set of measurements of K_d's in sediment cores taken from a number of locations has confirmed that the ion-exchange equation is valid over a wide range of ammonia concentrations: a very good relationship is seen between log ammonium concentration and log total K_d. A similar plot of exchangeable (i.e. ammonium extractable) K_d, however, which should according to the fixation theory (see later) be a better estimate of the field K_d, gives a much lower correlation. This suggests that, contrary to expectation, over the time scale of years, the total K_d is a better predictor of Cs mobility than the exchangeable K_d.

For caesium there is a general assumption that the concentrations in natural waters are so low that it is possible to assume the simplifying conditions of trace levels, compared to the major competitor, potassium. Previously there were very few measurements of stable Cs in the literature to confirm this assumption. A study by IFE of stable Cs concentrations in 21 lakes covering a wide range of K and Ca concentrations showed that concentrations range between 1 -13 ng l^{-1} ($\equiv$0.01 - 0.1 nM) and, unlike Sr, are independent of major ion concentrations. At these levels, the assumption of trace concentrations is valid. Measurements of K_d made in the laboratory by the addition of radionuclide containing carrier Cs, however, are likely to be biased underestimates. The bias will increase with increasing amounts of carrier.

From a study of the properties of sediments taken from rivers in France, CEA showed that the Cs concentration on the solid was a linear function of the proportion of fine silt and the percentage organic matter, i.e. the K_d increased with increasing fractions of fine silts and organic matter. This is a result of a combination of the increased area available for sorption, relative to the sample weight, for fine silts and the presence of higher concentrations of illites in the smaller size ranges. The relationship with organic matter is probably a result of a co-correlation between fine silt deposition and organic matter deposition, since both need slow flowing waters to deposit. A detailed study of a single river by ENEA suggested that the total K_d can be predicted from a weighted mean of the K_d's measured on individual size fractions.

Reversibility of caesium and strontium sorption

On the basis of frayed edge site studies it appears to be possible to predict values of radiocaesium K_d after short equilibration times (24 hours). Following a fallout event, however, caesium slowly moves to less available sites on the solid phase, a process commonly known as "fixation". Desorption studies were carried out by DGA/DPSR on sediments spiked with ^{90}Sr and ^{137}Cs and then left for a period of three days. After this time, it was found that all of the strontium could be removed from the solid by a concentrated solution of a competing ion (Ca^{2+}), but that only 40-50% of the caesium was removed by one of its competitors (K$^+$), implying "fixation" of 50-60% of the caesium. Further studies showed that after 4 days adsorption in solutions containing different competing ions, fractions of ^{137}Cs in the fixed phase were 20-35% in K$^+$ solution, 40-55% in Na$^+$, and 60-75% in Ca^{2+} solution. It appears that the poorly hydrated ions competing with Cs for the FES (K$^+$, NH$_4^+$) also inhibit transfers to fixed sites.

Measurements of radiocaesium in the environment, mainly resulting from the Chernobyl accident and thus aged for around 7 years, were carried out by ECN and IFE. It was found that in freshwater sediments only 1-10% of the ^{137}Cs could be desorbed by an ammonium acetate extraction. After removal of all of the exchangeable ^{137}Cs, two of the sediments were then left in ammonium acetate solution for one year. After this period it was found that a further 1-2% of the ^{137}Cs was de-sorbed from the solid, implying that there is a slow transfer of activity from the so-called "fixed" phase back into solution. An approximate rate constant for the reverse reaction was calculated from these data, giving a half-life for the transfer of around 80 years.

It appears, then, that the "fixation" of ^{137}Cs is not a truly irreversible process. Short term (timescale days) laboratory desorption experiments can give a measurement of that fraction of the radiocaesium which is available for transport and uptake by biota on a similar timescale. On longer timescales (years-decades), however, it is necessary to take account of the slow movement of ^{137}Cs to and from "fixed" sites.

Transfers of radiocaesium across the sediment-water interface

A model based on the advection-diffusion equation has been developed by IFE and ECN to determine the mobility of radiocaesium in the bottom sediments of lakes and rivers. In many freshwater systems the bottom sediments act as an important sink for radionuclides since activiy in the water column accumulates in the sediments via the settling of suspended particles or direct diffusion across the sediment-water interface. Settling of contaminated particles is relatively simple to measure using sediment traps, or calculating mass accumulation of bottom sediments. The direct diffusion process, however, is controlled by the thickness of the benthic boundary layer, a thin layer of laminar flow water overlying the sediment. To our knowledge, few measurements of this boundary layer have been made in lakes. A method has been developed to measure this layer both *in situ* using gypsum plates, and by studying the diffusion of ions to sediments in an experimental flow chamber. *In situ* measurements in Esthwaite Water, UK gave a value of 0.43 mm for the boundary layer thickness, of the same order as suggested from a model of radiocaesium removal from Devoke Water. In the experimental chamber it was shown that boundary layer thickness varied between 0.27-0.56 mm, and was inversely proportional to the mean velocity of the overlying water.

Previous work has shown that radiocaesium may be remobilised from bed sediments, particularly when sediments become anoxic, resulting in high ammonium concentrations. The model takes account of changes in short-term K_d as ammonium concentrations change down the sediment profile, and of long term movement of activity to and from "fixed" sites. Model predictions showed that remobilisation of activity from Hollands Diep and Ketelmeer sediments resulted in loss rates of around 2.5% of the sediment inventory per year shortly after the Chernobyl accident, and around 0.15% per year 30 years after the accident. In agreement with the experimental studies, it was found that in order to fit the observed field data, it was necessary to include a rate constant for transfers of activity from the fixed phase. The model fitted value of this constant gave a half-life for this process of around 10 years, lower than, but of the same order as the experimentally determined value.

Mechanisms and models of radionuclide transfer in aquatic food chains

The objective of this part of the project was the study of the kinetics and mechanisms of radionuclide uptake and accumulation in aquatic plants and animals. Special attention was given to the effects of environmental conditions on these processes. The results have been used to construct mechanistic models for the accumulation of radionuclides by aquatic organisms which can account for the effects of chemical speciation and ionic composition on the accumulation of the radionuclides in aquatic organisms. The results reported here are based upon the complementary work performed by the five groups participating in the biological part of the project. The work consisted of three work packages which together provided new insights into the mechanisms of radionuclide uptake and transfer in aquatic ecoystems. Most studies were performed with caesium or cobalt as model radionuclides. The information provides the basis for the development of a new generation of models for the prediction of the transfer of radionuclides in aquatic food chains. Briefly, the work packages dealt with the following:

1 Development of mechanistic models for the uptake of radionuclides in plants and animals.Experimental characterisation of the transport systems involved in the translocation of radionuclides across biological interfaces (RUCA/UMAG)..

2.Determination of the effects of environmental and metabolic factors on the accumulation of radionuclides by aquatic plants and animals. Special attention was paid to key factors such as ion composition, complexation capacity and temperature (DGA/NINA/RUCA/UMAG)..

3. Determination of the transfer of radionuclides in model food chains to determine the relative importance of water and food in different environments. Effect of metabolic activity and growth rate on radionuclide accumulation in top level predators (CEA/DGA/NINA)..

Radionuclide uptake depends on the biological availability of the radionuclides in the environment and the systems involved in the uptake of the radionuclide by the organisms. To model the effects of environmental conditions on the chemical speciation of radionuclides a model was developed which allows the calculation of the activities of radionuclide species in aquatic environments taking into account the effects of changes in ionic compositin and complexation capacity on the behaviour of the radionuclides in the environment. The model has been used to predict the effect of changes in water composition on the biological availability of radionuclides. In general only the free metal ion appears to be taken up by aquatic organisms. Much of the variation observed in radionuclide uptake from water is explained when uptake is expressed on a free metal ion activity scale rather than a total metal activity scale.

Radionuclides do not permeate biological interfaces by simple permeation but require gating systems which facilitate their uptake. For caesium, potassium channels and for strontium and cobalt, calcium channels have been implicated to be the major pathways for uptake of the radionuclides. Within the framework of this project it has been shown that indeed these channels are involved in the uptake of these radionuclides by a variety of aquatic organisms. Based upon a fundametal appreciation of the processes being

involved, a model has been developed to account for the effect of environemtal conditions on the accumulation of caesium and cobalt.

The effects of key environmental conditions on the uptake of caesium was studied in *Riccia fluitans* as a model plant and *Cyprinus carpio* as model animal. As expected caesium was taken up by a potassium transport system. The results of the experimental work were used to construct a mechanistic model from which radiocaesium concentration factors in freshwater plants can be predicted as function of the potassium concentration in the water. The models considers two systems for the uptake of potassium. One is opperative under potassium limitation and one when potassium supply is not a constraint. In the latter case, radiocaesium is accumulated by plants through potassium channnels. The concentration of caesium in plants reached at equilibrium is determined by the electrochemical potential gradient which exists across the membrane interface and can be predicted from the Nernst equation. The cellular caesium concentration reaches equilibrium when the Nernst potential for caesium equals the membrane potential. Thus, the concentration factor of caesium in plants can be predicted from the membrane potential which in turn depends on the concentration of potassium in the environment. When potassium concentrations in the environment are limiting, an active system is invoked which has a higher affinity for caesium then the channel system. In this case, uptake displays saturation kinetics which can be described by a Michaelis-Menten type transport model. The same approach has been used to describe the uptake of caesium and other radionuclides by fish, which present the highest trophic level. In fish the situation is somewhat more complex since radionuclides are accumulated from both water and food sources but the principals remain the same. To model the accumulation of radionuclides by aquatic plants and animals a clearance constant based pharmacokinetic model has been developed which uses membrane transport kinetics to describe the fluxes of the radionuclides in an out of the organisms. The model accounts for the effect of changes in chemical speciation on the biological availability of the radionuclides and the selectivity of the transport systems involved in the uptake of the radionuclides.

The effect of environmental conditions such as dissolved organic carbon, water ion composition and temperature have been determined under a variety of conditions in experimental food chains. These experiments provided essential information on the long term accumulation kinetics and relative importance of water and food at different trophic levels. These food chains include a variety of plant and animal species, i.e. unicellular algae, insects, crustaceans and bivalves and different fish. The results of the uptake and accumulation experiments have been combined to construct mechanistic models from which the effect of environmental conditions on the accumulation kinetics can be predicted. For each trophic level information is required on the absorption efficiencies, feeding rates, growth rates and excretion rates. Effects of environmental conditions on absorption efficiencies from water and food are described by membrane transport models. As such these models provide truely mechanitic descriptions that can be used to model the long term fate of radionuclides in aquatic food chains under combinations of conditions that have not been studied experimentally.

For example, experiments conducted concerning the uptake of caesium by *Chondrostoma* under different potassium and caesium regimes showed that the model developed for the interaction between potassium and caesium almost perfectly

described the observed variation in caesium accumulation under the different exposure regimes. Similar results were obtained for the interaction between calcium and cobalt to explain the variation in cobalt accumulation by *Cyprinus*.

In conclusion this joint effort has cumulated in the development and experimental validation of a set of mechanistic models for the uptake and accumulation of radionuclides in aquatic organisms of distinct structural and functional organisation. The results obtained so far provide very evidence that it is possible to integrate the different models into one robust system that can be used to predict the fate of radionuclides in entire food chains. Although it has been shown that the approach works for some plants and fish under a variety of conditions, essential information is still lacking concerning the kinetics of radionuclide uptake at intermediate trophic levels to allow the construction of a bottom to top food chain pharmacokinetic model

Head of project 1: Dr. J. Hilton

II. Objectives

(a) To measure the rates of diffusional transport of radionuclides from water to bottom sediments and the mobility within, and remobilization from, contaminated sediments.

(b) To assess the influence of stable Sr and Cs concentrations on the solids/aqueous distribution of their radioactive isotopes, and to relate these to the concentrations of competing ions.

III. Progress achieved including publications

(a) Studies on the sediment/water interface

The transfer of radioactive pollutants into and out of the bottom sediments of lakes and rivers occurs both in the solid phase by the sedimentation and resuspension of particles, and in the aqueous phase, by the diffusion of ions across the sediment/water interface. The importance of diffusive transfers, however, is not yet well understood. The aim of our work was to quantify this latter process by measuring the thickness of the benthic boundary layer, a thin layer in which the flow is laminar or stagnant, so that vertical transport within the layer occurs only by molecular diffusion. Based on these measurements, a model has been developed (in collaboration with ECN) for the remobilisation of ^{137}Cs from freshwater sediments.

The boundary layer has been measured in two ways: the first using the rate of dissolution of gypsum plates to make an *in situ* estimate in Esthwaite Water, Cumbria, and the second using a flow chamber to assess the effects of flow rate on the boundary layer thickness.

Gypsum Plate Method

The gypsum plates were made by heating gypsum ($CaSO_4.2H_2O$) at 130 °C for 5 hr to form $CaSO_4.(1/2H_2O)$. This was then mixed with water at a ratio of 5 parts $CaSO_4.(1/2H_2O)$ to 3 parts water (by weight) forming a smooth paste. Small (5.2 cm diameter) petri dishes were then filled with the paste until a clear meniscus was seen over the rim of the dish. The dishes were then dried at 40 °C for 24 hr, then smoothed to a flat surface with coarse sandpaper. Residual dust was removed by blowing compressed air over the surface of the plates, before returning them to the oven for a further 24 hr. Apparatus holding 7 plates was constructed to lower the plates to the sediment surface, a moveable lid being used to protect the plates during deployment and retrieval of the apparatus. This apparatus was deployed in Esthwaite Water, Cumbria, the boundary layer thickness being calculated from the rate of dissolution of the plates over a 50 hour period. Results showed that the mean boundary layer thickness was 430μm, within the range 370-2000μm obtained by other workers using both this method and benthic flux chambers (Santschi *et al.* 1983; Hesslein 1987; Devol 1987).

Flow chamber studies

An experimental flow chamber (see Fig. 1) has also been used to study chemical fluxes across the sediment/water interface under controlled conditions (House *et al.* 1995). Because of radiation safety regulations, it was not, at that time, possible to use a radioactive element in this experimental setup, so a stable isotope, the phosphate (HPO_4^{2-}) ion was used. A spike of phosphorus was added to the water overlying the sediment, and aqueous phosphorus concentrations were measured as the phosphorus was absorbed by the sediment over a 24 hr period. The experiment was carried out for different flow rates of the overlying water.

The diffusive flux, *F*, across a boundary layer of thickness z is proportional to the concentration gradient across the boundary, leading to the following equation for the change in water concentration over time (House *et al.* 1995):

$$C_w = C_w(0) e^{-kt} + C_i(1 - e^{-kt}) \tag{1}$$

where

$$k = \frac{D_0}{z\bar{d}} \tag{2}$$

and C_w is the water concentration, z the boundary layer thickness, $\bar{d}$ the mean depth of water, and D_0 the diffusion coefficient of the HPO_4^{2-} ion.

Equation (1) was fitted to the measurements of C_w vs time by varying the unknown boundary layer thickness, z to give the best least squares fit to the data (Fig. 2). It is clear from Fig. 2 that the flux to the sediments is increased at higher water flow velocities. Fig. 3 shows a clear linear proportionality (correlation coefficient R^2 = 93.1 %) between the best fit boundary layer thickness and the inverse of the flow velocity. The intercept of the regression line is not significantly different to zero, so we can write:

$$z \approx \frac{2500}{v} \tag{3}$$

where z is measured in μm and v is the mean flow velocity in cm/s.

A further experiment was carried out in order to compare boundary layer estimates from the phosphorus flux model with those obtained using gypsum plates. Four gypsum plates were placed in the flow chamber so that their surfaces were level with the surface of the sediment. The plates were left to dissolve into the flowing water for a period of 98 hrs, then removed and the loss of gypsum calculated to give a boundary layer estimate of 380 μm, in reasonable agreement with the phosphorus flux measurements.

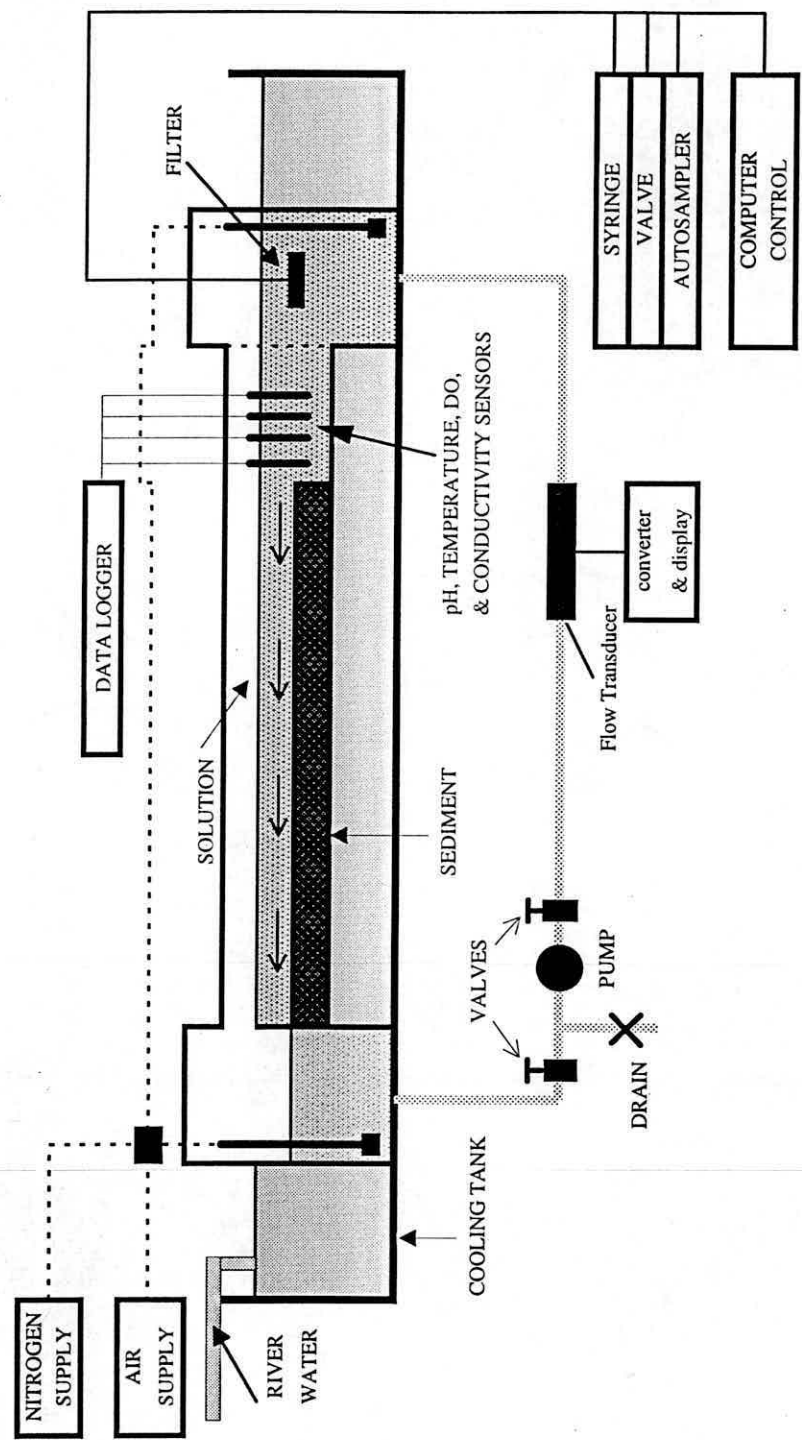**FIGURE 1.**

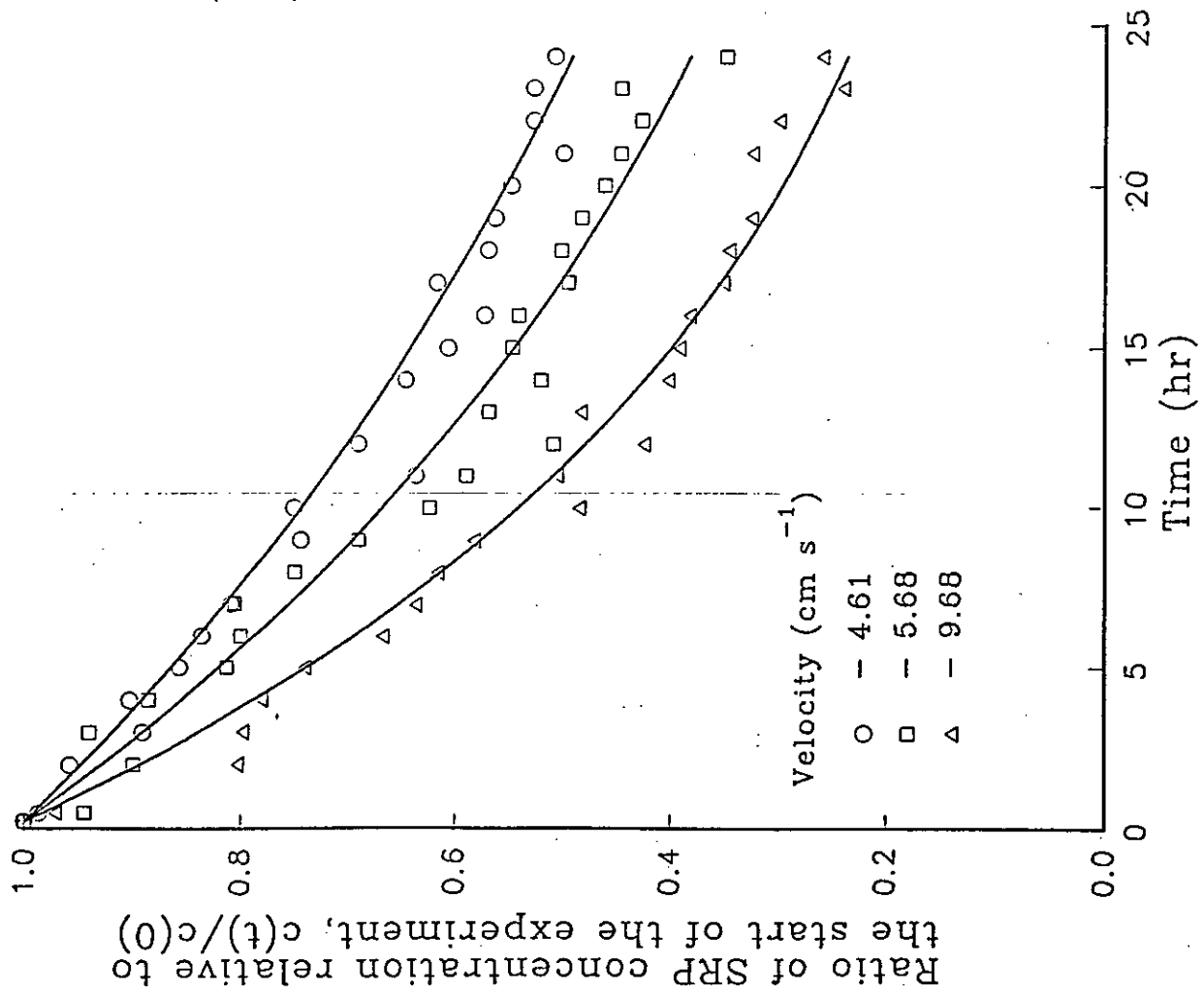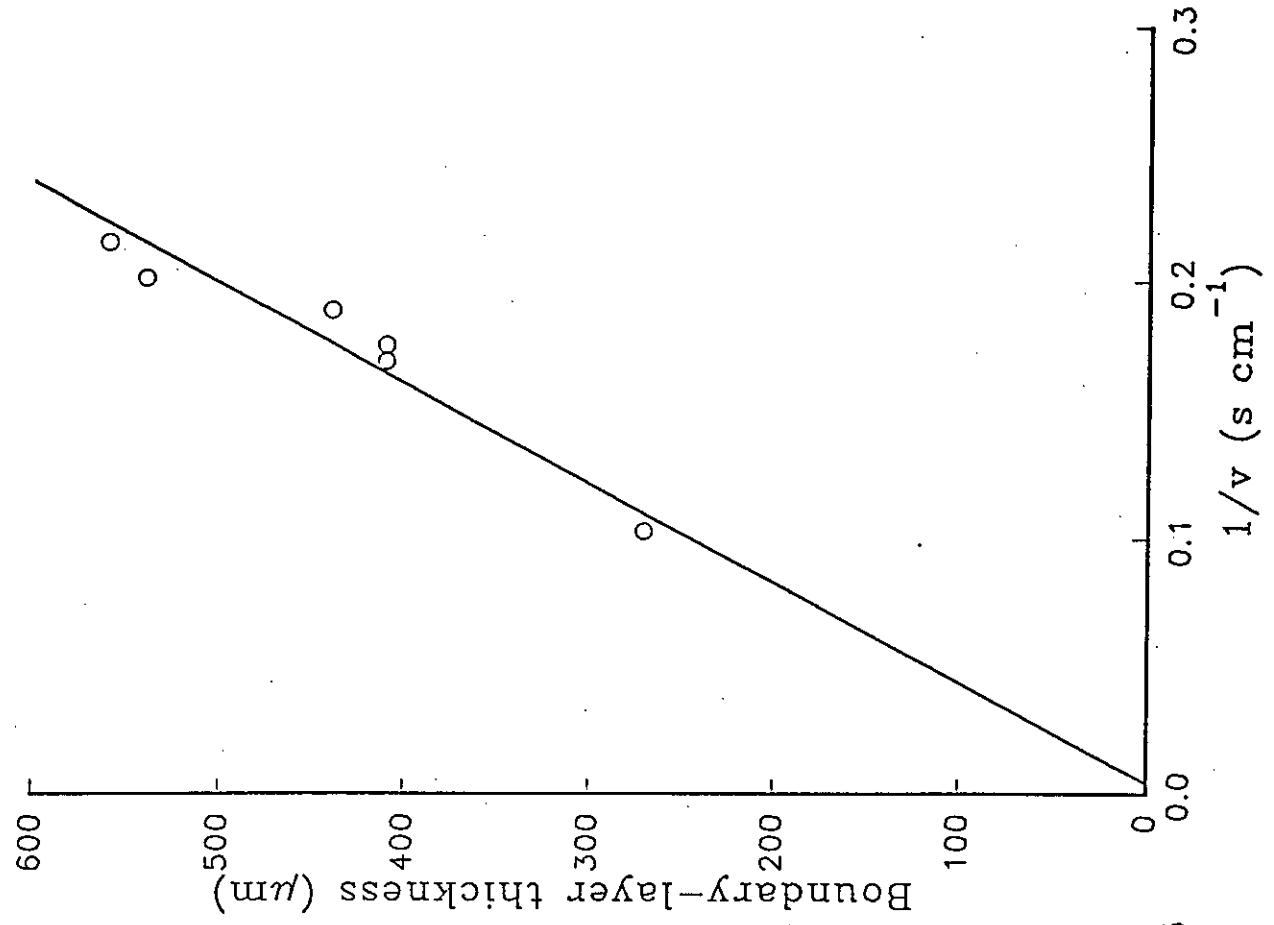Fluvarium channel for bed-sediment flux studies.

FIGURE 3

FIGURE 2

Boundary-layer thickness (μm)

$1/v$ (s cm^{-1})

Time (hr)

Ratio of SRP concentration relative to the start of the experiment, c(t)/c(0)

Velocity (cm s^{-1})
○ — 4.61
□ — 5.68
△ — 9.68

Modelling diffusional removal to bottom sediments.

A simple box-type model has been used to analyse data on aqueous ^{137}Cs concentrations in Devoke Water, Cumbria for several years following the Chernobyl accident. It was found that, in the long term (90 days - 6 years) after the accident, the concentrations of ^{137}Cs in the water column can be explained by measurements of inputs from the catchment (Hilton *et al.* 1993), and by flushing of the lake. In the initial period, however, there is a significant loss of dissolved activity to the sediments which cannot be explained by particulate settling alone. The results suggest that this is due to diffusional uptake by the bottom sediments across a boundary layer of thickness around 1000 μm, of the same order as that obtained in the experimental studies.

Modelling remobilisation from contaminated sediments.

Clearly, diffusional fluxes across the boundary layer are not constant with time, but will change as the concentration gradient across the boundary changes. As ^{137}Cs builds up in the sediment pore waters, the diffusional uptake will reduce, and this may lead to remobilization of activity from sediments back into the water column, particularly during periods where sediments become anoxic. In collaboration with ECN a model has been developed to predict changes in ^{137}Cs concentration in aqueous, exchangeable and fixed phases within the sediment, and rates of remobilisation to the water column.

Let C_w (Bqcm^{-3}) represent the radiocaesium activity in the aqueous phase, C_s (Bqg^{-1}) the exchangeably sorbed activity and C_i (Bqg^{-1}) the activity which is "fixed" in the mineral lattice (see Fig.). The aqueous $\Leftrightarrow$ exchangeable reaction is believed to be of order minutes, so that these two phases can be assumed to be in instantaneous equilibrium with distribution coefficient

$$K_d^e = \frac{C_s}{C_w}. \tag{4}$$

It has been shown that the ammonium ion directly competes with ^{137}Cs for exchange sites on clay minerals. We have therefore assumed that the K_d^e varies with depth in inverse proportion to the ammonium concentration, C_{NH4}:

$$K_d^e(x) = K_d^e(0) \frac{C_{NH4}(0)}{C_{NH4}(x)}. \tag{5}$$

Transfers of activity to and from the "fixed" phase are modelled by first-order rate constants k_f, k_b (s^{-1}). The final phase is termed "fixed" since on the timescale of most laboratory sorption/desorption experiments (weeks-months) no reverse reaction has been determined, although it will be shown that there is evidence to suggest that the reaction is reversible on a timescale of several years.

The equations describing the transport of trace elements in sediments have been described

elsewhere (Berner 1980). Full details of modelling methods and assumptions can be found in Smith & Comans (1995), so a brief outline only will be given.

In the coupled aqueous/exchangeable phase, transport occurs both by diffusion in the sediment pore waters, and by advection as sediment layers accumulate. These processes are described by:

$$\frac{\partial C_e}{\partial t} = \frac{\partial}{\partial x}\left[\phi\psi D_0\frac{\partial}{\partial x}\left(\frac{C_e}{\phi + sK_d^e(x)}\right) - rC_e\right] - k_fC_e + k_bsC_i - \lambda C_e. \quad (6)$$

where D_0 is the diffusion coefficient of the free ion in water ($1.45 \times 10^{-5}cm^2s^{-1}$ at $10\,^oC$), ϕ is the porosity of the sediment and r the (constant) mean sedimentation rate (cms^{-1}). ψ is a dimensionless factor (< 1) to take account of the tortuosity of path an ion must follow in diffusing through the sediment. Tortuosity is estimated by

$$\psi \approx \phi^2. \quad (7)$$

The transport of activity in the fixed phase is described by:

$$s\frac{\partial C_i}{\partial t} = -sr\frac{\partial C_i}{\partial x} + k_fC_e - k_bsC_i - \lambda sC_i. \quad (8)$$

For the case of diffusion across the upper boundary, the boundary condition is:

$$F_e(0,t) = -\phi\psi D_0\frac{\partial}{\partial x}\left(\frac{C_e}{\phi + sK_d^e}\right) + rC_e(0,t) - \frac{D_0}{z}\left(\frac{C_e}{\phi + sK_d^e} - C_a\right) \quad (9)$$

where z is the thickness of the non- turbulent flow "boundary layer" and C_a the concentration in the water column. For the fixed phase the condition is

$$F_i(0,t) = rsC_i(0,t) \quad (10)$$

where $F_e(0,t)$ is the flux of activity to the sediment in the aqueous/exchangeable phase, and $F_i(0,t)$ the flux in the "fixed" phase. The above equations are solved by a simple explicit finite-difference method. Computer codes were written in FORTRAN and run on a SUN workstation. Inputs to the sediment from the Chernobyl event were modeled using a smoothed short duration spike, those from the weapons fallout followed the history of atmospheric depositions, a smoothed spike corresponding to the relative deposition (corrected for decay) being input each year. Activities were scaled to the total inventory of each profile.

Fig. 4 Ketelmeer Cs-137. Model fits shown as solid lines.
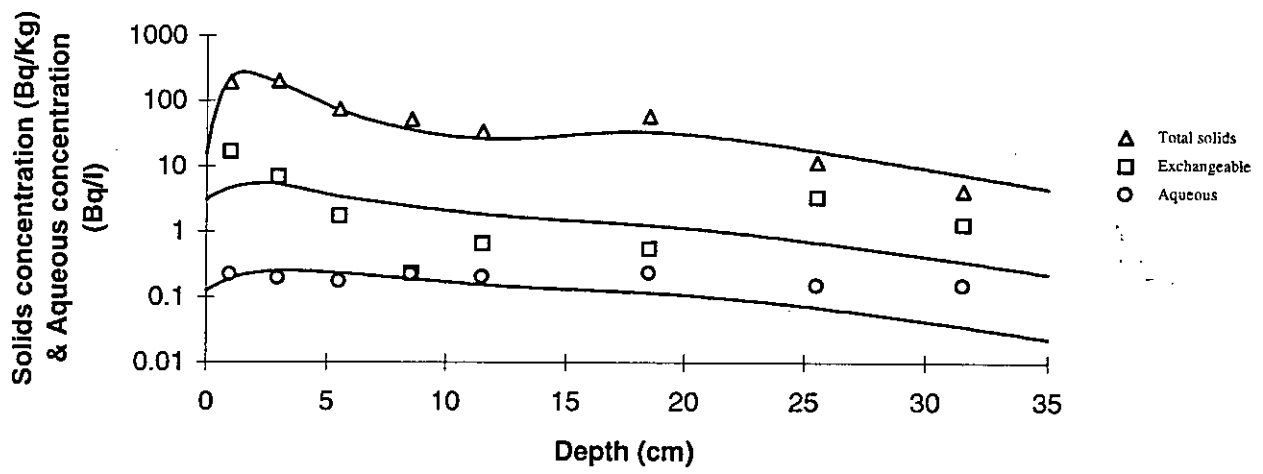
Model results

The above model was applied to measurements of ^{137}Cs concentrations in the aqueous, exchangeable, and fixed phases of the sediments of two Dutch lakes, Ketelmeer and Hollands Diep. Parameter values were varied to get the best chi-squared fit to the data. Fig. 4 shows the best model fit to the measurements from Ketelmeer.

The transport of activity to less-exchangeable sites on illites has been demonstrated in many ^{137}Cs sorption experiments and the forward rate constants, k_f, estimated by the model fits $(T_{1/2}= 50$ and 125 d) are in good agreement with experimental observations of 35-150 d (Comans & Hockley 1992) and with an estimate of 100d made by Comans & Hockley (1992) from data obtained by Evans and co-workers (Evans *et al.* 1983). Because of the very long timescale on which it operates, a reverse rate constant for this reaction has not been established experimentally, although exchangeable ^{137}Cs has been found in sediments more than 15 years after the contamination event (Evans *et al.* 1983). Using the exchangeability measurements made by Evans & co-workers (85% "fixed", 15% exchangeable), and a forward rate constant of half-time 100d, we calculate a reverse rate constant, k_b, of half-time around 600 days. This is lower than, but of the same order as, our model estimates of 3000 and 4000 days for Ketelmeer and Hollands Diep respectively.

Values of the boundary layer thickness, z we have measured and obtained from a literature survey range between 0.37 and 2.0 mm (Santschi *et al.* 1983; Hesslein 1987; Devol 1987). Within this range, the remobilisation flux did not vary significantly since, on the timescales of interest here, remobilisation is limited by diffusion rates within the sediment rather than across the boundary layer. Using the best-fit parameters, and assuming that $C_a = 0$ (ie giving a maximum estimate) we have made tentative predictions for remobilization rates resulting from the Chernobyl fallout event for times between 1 and 30 years after the time (1.5y after the accident) at which the cores were taken. Remobilization rates, quoted as a percentage of the core inventory at the time of coring, for Hollands Diep changed from 2.8% per year after 1 year to 0.2% per year after 30 years, and for Ketelmeer from 2.4% per year after 1 year to 0.1% per year after 30 years.

(b) Stable Cs and Sr concentrations in freshwaters in Northern England and their effect on estimates of sorption coefficients (K_d).

When simple ion exchange is the dominant mechanism of sorption, the K_d can be incorporated into the standard ion exchange equation by making the simplifying assumption that the concentration of the sorbing material of interest is very small compared to the competing major ion concentration, (see Comans et al, in press, for the derivation), so that:

$$K_d = \frac{K_c[sites]}{[M^{a+}]} \qquad (11)$$

where K_c is the selectivity coefficient, [sites] is the number of sites in terms of equivalents per gramme of solid and $[M^{a+}]$ is the concentration in solution of the major competitor (with

the same charge as the material of interest) for sites on the solid. A number of studies have found results in agreement with this equation. For example, Comans et al. (1989) confirmed an inverse linear relationship between log K_d^{Cs} and log ammonium ion concentrations in anaerobic sediments.

If radionuclides in the natural environment were carrier free the assumption of trace status would be irrefutable. However, almost all radionuclides have stable analogues, naturally occurring in the environment. Since the concentration of these stable isotopes is considerably higher than the radionuclide concentration, it is possible that the assumption of trace status is not entirely valid. Concentrations of stable caesium and stable strontium were measured in lake waters covering a range of major ion chemistries and the concentrations were compared with the major ions and with measured K_d.

Surface water samples and sediment cores were taken from twenty lakes in the North of England. The lakes were chosen to give as wide a range of potassium and calcium concentrations as possible, in fresh waters. A sub sample of filtrate was analysed for major cations by atomic absorption spectroscopy using a Perkin Elmer instrument. Further subsamples of filtrate were acidified and analysed by ICPMS for stable strontium caesium.

Sediment samples were taken using a Jenkin corer (Ohnstad and Jones, 1982). The core was extruded in the field and the top 1 cm slice was stored in a plastic bag for transport to the laboratory. A sub sample of each sediment was dried at 60°C and the percentage dry weight detemined. K_d measurements were performed as follows: 10 mg of wet sediment was conditioned for 24 hours in 15 ml (≡650 mg/l wet suspended solids) filtered surface water from the same lake. The samples were centrifuged and the pellet dispersed in clean lake water containing a spike of 25 kBq Cs-134 and 25 kBq Sr-85. Samples were agitated for 24 hour. The solid and liquid were then separated by filtration through a 0.45 um membrane filter and the activity on the solid and in the liquid was determined by gamma spectoscopy on a Canberra Packard spectrometer. It was not possible to obtain carrier free samples of these isotopes. Specific activities of the two radioactive isotopes were 431 MBq / mg for Cs-134 and 278 MBq / mg for Sr-85. With the additions used in these experiments, the resulting additional stable isotope concentrations were 3.87 ug/l (29 nM) and 6 ug/l (67 nM) for Cs and Sr repectively.

Stable Cs and Sr concentrations.
Stable strontium concentrations range from 8 - 214 ug/l, which are consistent with values in the literature. A good linear relationship was observed between stable strontium concentrations and the sum of Mg and Ca (stable Sr v (Ca + Mg), i.e. Sr = 0.1166 + 0.6438 (Ca + Mg), (R^2 = 0.825) where the concentrations of (Ca + Mg) and Sr are in mM and uM respectively.

Stable Cs levels in the Northern English lakes varied from 1.3 to 13.5 ng/l. The authors could only locate one publication reporting a value for stable caesium in freshwaters. Seelye (1975) measured concentrations in one lake using activation analysis and reported values of a few ng/l. This is consistent with our data. Unlike the situation for Sr, there appears to be no relationship between stable Cs and any of the major ions or ammonium. A plot of stable caesium versus potassium is given in figure 5.

The effect of stable isotope concentrations on the K_d.

If the assumption of trace radionuclide is not made, i.e. Cs or Sr atoms cover a significant proportion of the exchange sites, then the following equation can be derived (a similar equation holds for Ca^{2+} competition for Sr^{2+}:

$$K_d^{Cs} = \frac{K_c(Cs/K) \cdot FES}{([K^+] + K_c(Cs/K)[Cs^+])} \tag{12}$$

From direct measurement De Preter (1990) reported K_c - Cs^+/K^+ = 1000 for illite. For the sampled sites, K_c (Cs/K) [Cs^+] has been calculated as a proportion of the potassium concentration. Over the range of ionic concentrations observed in this study stable caesium contributes no more than about 1% to the variation in K_d. Hence it is reasonable to assume trace levels in their effect on K_d. Equivalent calculations for Sr^{2+} using K_c (Sr / Ca) = K_c (Sr / Mg) = 1 from a compilation of selectivity coeficients presented by Burggenwert and Kamphorst (1982) show that the maximum value of K_c (Sr/Ca). [Sr^{2+}] is 0.26%. Hence, the trace assumption for stable Sr in natural waters is also reasonable. However, it is worthy of note that, because of the high selectivity of the frayed edge sites for caesium, nanomolar concentrations of caesium are comparable with millimolar concentrations of potassium. In comparison, uM concentrations of Sr have much less effect as a result of its low selectivity coefficient with respect to mM Ca concentrations.

Under the laboratory conditions created by the presence of extra stable Sr due to the carrier (equivalent to 6 ug/l = 67nM) in the determination of K_d , the addition is relatively small compared to the naturally occuring conditions (see above) and the trace assumption still holds. For Cs the high selectivity coefficient relative to K extenuates the effect of carrier Cs (an addition equivalent to 3.87 ug/l = 29 nM) in the laboratory conditions of K_d measurement. This additional concentration of Cs in solution {average = 15nM: $[Cs]_{soln} = [Cs]_{added}$ / (1+ K_d SS), where SS is the suspended solids in the laboratory measurement in kg dry solid l^{-1}} is orders of magnitude greater than the natural concentrations (1-14 ng/l = 0.01-0.102 nM). When the dissolved Cs concentration is multiplied by the selectivity coefficient a factor results which, in many cases, is several times greater than the potassium concentration. As expected from theory there is a reasonable negative relationship between log [K] and log K_d^{Cs} (figure 6a) with an R^2 value of 0.55. However, inclusion of the stable Cs term at a total additional concentration of 29 nM raises the R^2 for the plot of log K_d versus log {[K] + K_c (Cs/K). [carrier Cs]$_{soln}$}to 0.67 (figure 6b). There is an accompanying increase in slope, from -0.69 for potassium alone to -0.87, which is very close to the theoretical slope of -1. About 8% of the total variability is accounted for by the inclusion of K_d into the right hand side of the equation, 2% is due to differences in the water content of the wet sediment used in the laboratory measurements. The other 2% is due to either or both effects and indicates a small co-varience between the K_d and dry solids content.

In order to assess the influence of any ion, other than the primary competitor, on the K_d it is necessary to define the K_d in terms of both the primary and the secondary competitors. Sweeck et al. (1990) proposed a method for achieving this for homovalent competition. An alternative, simpler, derivation was used to obtain a similar equation to (12) for homovalent competition and the method was extended to include divalent - monovalent competition.

Manipulation of data from Brouwer et al., (1983) gives: K_c-(M^{2+}/K^+) = 2.445 x 10^{-10}; K_c-(Na^+/K^+) = 0.015. From De Preter (1990) K_c -NH_4^+/K^+ = 5.85. The bivalent cation - potassium selectivity is so low that bivalent cations have no effect on the K_d for caesium. The concentrations of the secondary competing ions multiplied by the selectivity coefficient with respect to potassium were calculated as a proportion of the potassium concentration. Over the range of chemical conditions found in this study, sodium ions should be as important as potassium in determining the K_d and, even under aerobic conditions, ammonium ions can be dominant. As shown above log-log plot of K_d^{Cs} versus potassium has R^2 = 0.55. Regressions of log ammonium concentration and log sodium concentration versus log K_d separately show weak correlations with R^2= 0.21 and 0.26 respectively. When combined with the potassium concentrations using an extension of equation 1 the regression shows only a marginal improvement (R^2 = 0.57). If the equation includes the additional stable Cs present in the K_d measurement R^2 reduces from 0.67 to 0.63. The implication is that the cumulative errors attained, at this level of complexity in the model, are larger than the effect itself over the relative narrow range of secondary competitor concentrations observed here.

In a review of K_c values for standard ion exchange sites on soils, Bruggenwert and Kamphorst (1979) quoted: K_c (K^+/Ca^{2+}) = 2.04 ; K_c (Na^+/Ca^{2+}) = 0.40 ; K_c (NH_4^+/Ca^{2+}) = 2.04 ; K_c (Mg^{2+}/Ca^{2+}) = 1.01. The coefficients show a much narrower range than those compared to K on frayed edge sites and are within about a factor of 2 above and below 1. As a secondary competitor, Mg follows the simple homovalent equation and contributes about 30% to the total K_d , and, since K_c (Mg/Ca) = 1, the sum (Ca + Mg) can be considered as a single ion. A plot of log K_d^{Sr} v log (Ca + Mg) shows (figure 7) a very high correlation (R^2 = 0.83) with a slope of 0.59. The slope is a little lower than the predicted slope of 1. All three monovalent competitor ions show much lower contributions than would have been the case if the homovalent equation had been valid. Ammonia contributes less than 1% to the K_d compared to Ca. The contribution of K is normally less than 2% and Na is normally contributes less than 50 % compared to Ca. Na, K and NH_4 all show lower correlations with K_d^{Sr} when plotted on log-log form (R^2 = 0.52, 0.32 and 0.26 respectively). Because of the heterovalent form of the competition between Ca and the three monovalent ions (NH_4 , K and Na) it is not possible to develop a simple, single equation to combine all three effects in the same way as is possible for homovalent competition. However, NH_4 and K are likely to have very little effect on the K_d. A plot of the heterovalent combination of (Ca + Mg) and Na has much lower R^2 (=0.529) than the R^2 for (Ca + Mg) alone. This probably results from the cumulative errors outweighing the effect of Na.

It is clear from this study that the nanogram per litre stable Cs concentrations measured in the natural environment are 3 - 4 orders of magnitude lower than the microgram per litre concentrations of stable Sr measured in the same samples. However, because of the large selectivity of Cs with respect to potassium at the FES, very small quantities of stable Cs can affect the value of the K_d . Although no effect was observed in the natural environment, up to 12% in the variability of the measured K_d could be due to this effect under the measurement conditions used in our experiments, where stable carrier was added with the radio-isotope. Conversely, stable Sr carrier showed no such effect due to its much lower selectivity coefficient with respect to Ca at normal ion exchange sites. These data suggest that, for Cs but not for Sr, the use of non-carrier free isotopes in laboratory measurements can result in both increased variability and under-estimation of the K_d. In addition, it appears that, for the range of secondary competitor concentrations covered in this study, the variability of measured K_d's is much greater than the effect of secondary competition in aerobic samples.
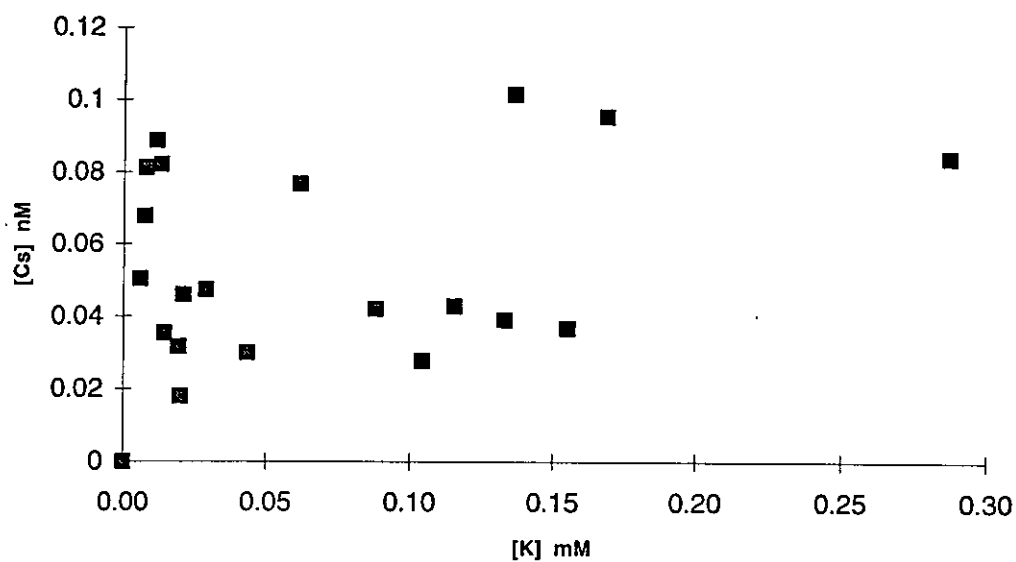
Figure 5. [Stable Cs] v. [K]

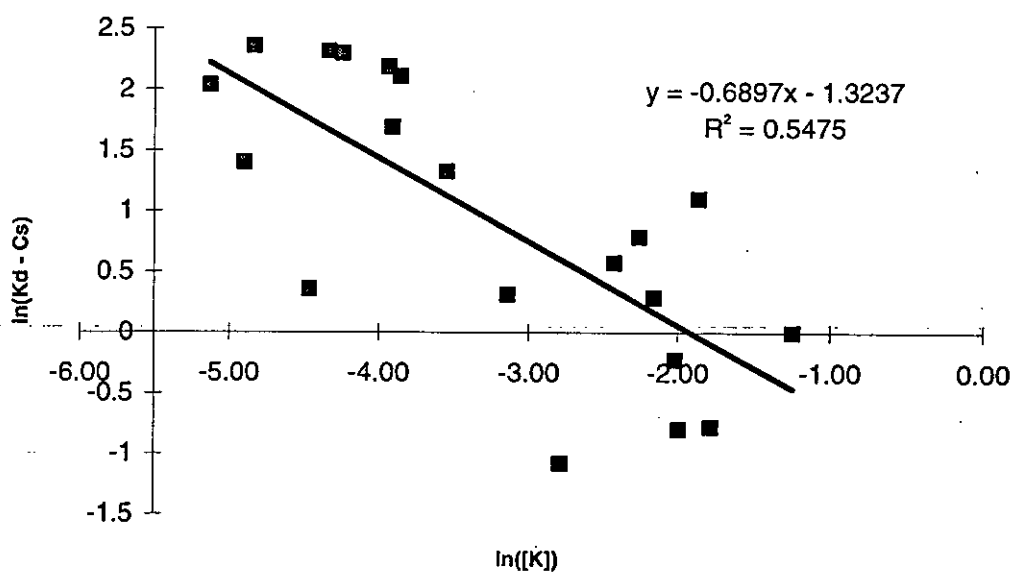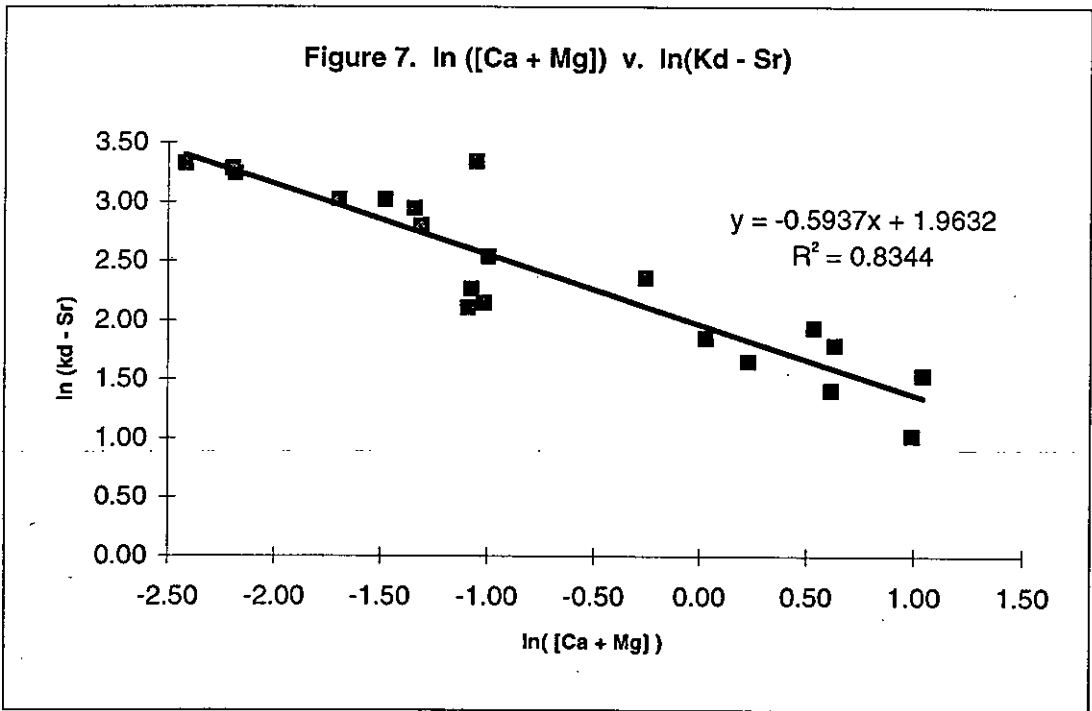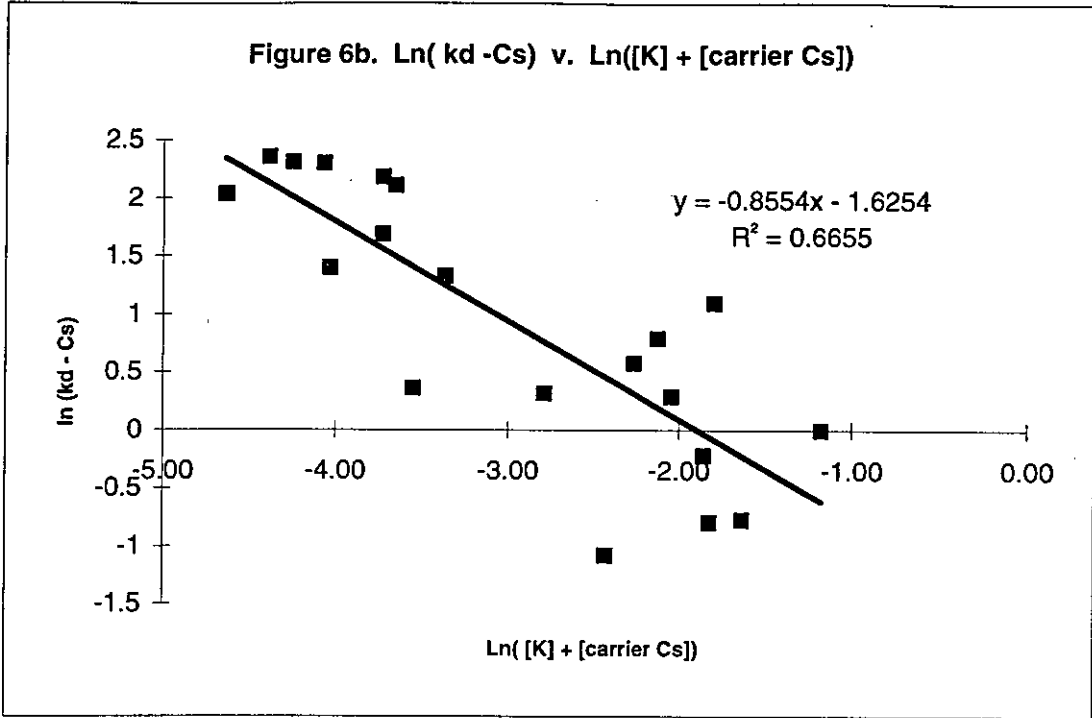Figure 6a. Ln (Kd - Cs) v. ln([K])

$y = -0.6897x - 1.3237$
$R^2 = 0.5475$

Figure 6b. Ln(kd -Cs) v. Ln([K] + [carrier Cs])

$y = -0.8554x - 1.6254$
$R^2 = 0.6655$

Figure 7. ln ([Ca + Mg]) v. ln(Kd - Sr)

$y = -0.5937x + 1.9632$
$R^2 = 0.8344$

References

Berner R.A. (1980) *Early diagenesis.* Princeton University Press.

Brouwer E., Baeyens B., Maes A., and Cremers A. (1983) Cesium and rubidium ion equilibria in illite clay. *J. Phys. Chem.* **87**, 1213-1219.

Bruggenwert, M.G.M and A.Kamphorst. (1979) Survey of experimental information on cation exchange in soil systems. in "Soil Chemistry, B. Physico-chemical models" Ed. G.H.Bolt. Developments in soil Science. Elsevier, Amsterdam, New York.

Comans R.N.J., Middelburg J.J., Zonderhuis J., Woittiez J.R.W., De Lange G.J., Das H.A., Van Der Weijden C.H. (1989) Mobilization of radiocaesium in pore water of lake sediments. *Nature* **339**, 367-369.

Comans R.N.J. and Hockley D.E. (1992) Kinetics of cesium sorption on illite. *Geochim. Cosmochim. Acta* **56**, 1157-1164.

Comans R.N.J., Hilton J., Cremers A, Geelhoed-Bonouvrie P.A., Smith J.T. (1995) Predicting radiocaesium ion-exchange behaviour in freshwater sediments. *Submitted for publication.*

Devol A.H. (1987) 'Verification of flux measurements made with in situ benthic chambers' Deep-Sea Res. 34 Nos. 5/6, 1007-1026.

Evans D.W., Alberts J.J., Clark R.A. (1983) Reversible ion-exchange fixation of cesium-137 leading to mobilization from reservoir sediments. *Geochim. Cosmochim. Acta* **47**, 1041-1049.

Hesslein R.H. (1987) 'Whole-lake Radiotracer Movement in Fertilized Lake Basins' Can. J. Fish. Aquat. Sci. 44 (suppl. 1), 74-82.

Hilton J., F.R. Livens, P. Spezzano and D.R.P. Leonard, (1993) 'Retention of radioactive caesium by different soils in the catchment of a small lake.' Sci. Tot. Env., 129 253-226.

House W.A., Denison F.H., Smith J.T., Armitage P.D. (1994) 'An investigation of the effects of water velocity on inorganic phosphorus influx to a sediment' (in press, J. Environ. Pollut.)

Ohnstad, F.R. and J.G.Jones (1982) The Jenkin surface mud sampler (a users manual). Freshwater Biol. Assoc. Occ. Publ. no.15.

de Preter, P. (1990) Radiocaesium retention in the aquatic, terrestrial and urban environment: a quantitative and unifying analysis. Ph.D thesis. Katholieke Universiteit, Leuven.

Santschi P.H., Bower P., Nyffeler U.P., Azuedo A., Broecker W.S. (1983) 'Estimates of the resistance to chemical transport posed by the deep sea boundary layer' Limnol. Oceanogr. 28 No. 5, 899-912.

Seelye, J.G. (1971) A measurement of low level caesium isotope concnetrations in a freshwater lake. U.S. Atomic Energy Commission Report Coo-1975-7, 38p.

Smith J.T. & Comans R.N.J. (1995) 'Modelling the diffusive transport and remobilisation of ^{137}Cs in sediments: the effects of sorption kinetics and reversibility' Geochim. et Cosmochim. Acta (accepted for publication).

Sweeck, L., J.Wauters, E.Valcke and A.Cremers. (1990) The specific interception potential of soils for radiocaesium, in: "Transfer of radionuclides in Natural and Semi-natural environments." 249-258. Ed. G.Desmet, P.Nassimbeni and M.Belli. Elsevier Applied Science.

List of publications

Hilton J., F.R. Livens, P. Spezzano and D.R.P. Leonard, (1993) 'Retention of radioactive caesium by different soils in the catchment of a small lake.' Sci. Tot. Env., 129 253-226.

Davison, W., Hilton J., Hamilton-Taylor, J., Livens F., Kelly M. (1993) 'Measurement, interpretation and modelling of Cs-137 transport through two freshwater lakes after Chernobyl. *J. Environmen. Radioactivity* **19**, 213-232.

Spezzano, P., Hilton, J., Lishman, J.P. and Carrick, T.R. (1993) The variability of Chernobyl

Cs retention in the water column of lakes in the English Lake District, two years and four years after deposition. *J. Environ. Radioactivity* **19**, 213-232.

Hilton, J. and Spezzano, P. (1994) An investigation of possible processes of radiocaesium release from organic upland soils to water bodies. *Wat. Res.* **25**, 975-983. publication.

Hilton, J. (1993) Vulnerable aquatic systems and the location of nuclear power stations. Proceedings of the Workship: Hydrological Impact of Nuclear Power Plant systems. UNESCO, Paris, Sept. 23-25. 1992. UNESCO SC-93/WS.

Hilton, J., Davison, W., Hamilton-Taylor, J., Kelly, M., Livens, F., Rigg, E. and Singleton, D.L. (1994) Similarities in the the behaviour of Chernobyl derived Ru-103 and Ru-106 in two freshwater lakes. *Aquatic Sciences.* **56(2)**, 133-144.

Hilton, J. Dispersion of radionuclides in aquatic systems. Chapter for book by IUR request. IUR Radioecology text book. Submitted for publication.

Hilton, J., Rigg, E., Davison, W., Hamilton-Taylor, J., Kelly, M., Livens, F.R., and Singleton, D.L. (in press) Modelling and interpreting element ratios in water and sediments: a sensitivity analysis of post-Chernobyl Ru, Cs ratios. *Limnol. Oceanogr.*

Hilton, J. (Submitted, 1994) Aquatic radioecology post Chernobyl - a review of the past and a look to the future. *Sci. Tot. Environ.*

Smith J.T. & Comans R.N.J. (1995) 'Modelling the diffusive transport and remobilisation of ^{137}Cs in sediments: the effects of sorption kinetics and reversibility' Geochim. et Cosmochim. Acta (accepted for publication).

Scientist Responsible of Project 2: A.Ortins de Bettencourt

Head of Project 2: Maria Carolina Vaz Carreiro

Research Team: Maria Carolina Vaz Carreiro
Maria José B. Madruga
José Alberto G. Corisco

1) PHYSICO-CHEMICAL BEHAVIOUR OF RADIONUCLIDES IN FRESHWATER SEDIMENTS

II. Objectives

1. Study of the effect of ionic composition, sediment drying and temperature on radiocaesium fixation in sediments;

2. Study of the solid-phase speciation of radiocaesium and radiostrontium in sediments;

3. Characterization of suspended matter (Fratel dam) in terms of relevant parameters for the short-term prediction of solid/liquid partitioning of radiocaesium.

III. Progress achieved including publications

1. Factors influencing the radiocaesium fixation in sediments

Ionic composition

On the basis of a rather consistent and coherent caesium selectivity pattern in the frayed edge sites (FES) of the sediments, it was accepted that the FES in the various sediment systems are essentially similar structures, although this is an oversimplification considering the erratic and unpredictable irreversibility pattern of radiocaesium sorption in various systems. Such diversity in behaviour could eventually be connected, with weathering effects. In the protocols followed before to radiocaesium irreversibility studies, the radiocaesium contamination of the systems was carried out on the system as such (i.e. in the ionic state as sampled) without pretreatment. However, it should be considered the effect of the sediment ionic composition and that of the overlying water column.

Two scenarios were considered:

a) Sediments homoionically saturated with various ions

A comparison was made between the potassium, sodium, and calcium forms of the sediment, Tejo river (T1<63μm, T2<500μm) and Tejo estuary (A<212μm, S<212μm) and their natural conditions. Homoionic systems (1g/10ml) (K $2x10^{-3}$M; Na $2x10^{-3}$M; Ca 10^{-3}M) were labelled with radiocaesium in a 10^{-5} M KCl ^{137}Cs labelled solution and allowed to age for 4 and 52 days. They were subsequently dispersed in 200ml of 10^{-3}M NH₄Cl containing a dialysis membrane with giese (ammonium copper

hexacyanoferrate) granulate ("Infinite Bath" method). Desorption progress was monitored by counting the adsorbent (fresh adsorbent is used after each sampling).

Fig.1.1 summarizes the results obtained in terms of a comparison of plateau fixation levels in the various systems studied for the natural, potassium, sodium and calcium states and for 4 days aging time. In spite of some minor differences, a very consistent pattern in the behaviour of all systems is observed. It is seen that, fixation levels decrease from the natural conditions to the K-state; fixation levels increase in the sodium state; the highest fixation being found in the Ca-state. It appears that the action of strongly hydrated ions (Na, Mg, Ca) leads to (structural) configurations unfavorable for radiocaesium desorption within a very short time scale (days). Possibly, the presence of strongly hydrated ions in the FES pool may lead to a wedge-effect, allowing for a deeper penetration of radiocaesium into the solid, resulting in a dramatic drop in subsequent desorption levels. This may be confirmed by the difference in fixation behaviour between the freshwater (T1 and T2) and estuarine sediments (A and S), showing a higher fixation level in the systems with the lower FES capacity. However, the higher fixation levels are very likely related to differences in ionic composition. When the various sediments were submitted to an aging time process (52 days) the differences in fixation behaviour become less pronounced and the Ca-saturated sediments scarcely show any aging effects.
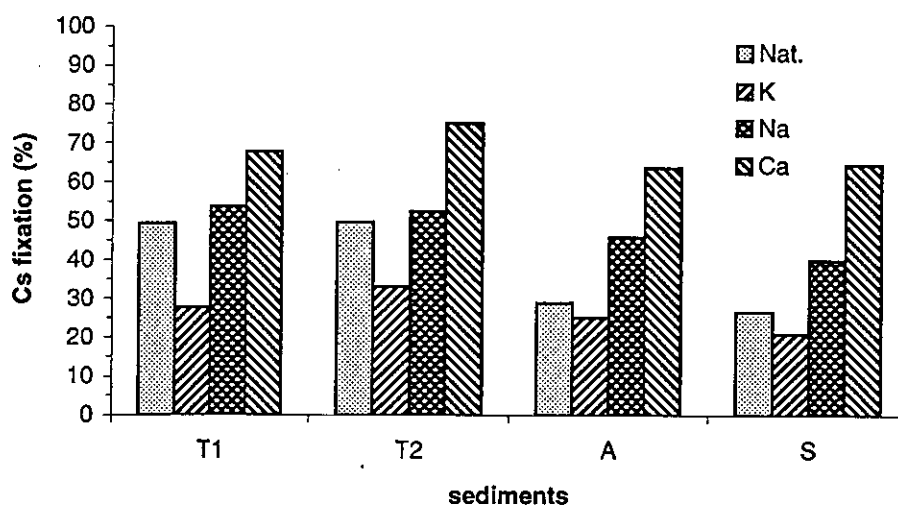

Fig. 1.1 - Effect of K, Na and Ca ions on radiocaesium fixation for Tejo river sediments (T1, T2, A, S) and 4 days aging time.

b) Mixed potassium-calcium solutions

The possible effect of ionic concentration was investigated in a homoionic (K) and a mixed (K-Ca) scenario. For the first case, sediment samples (T2) were preconditioned homoionically at 4 different potassium concentrations (0.1, 0.5, 1 and 2 meq.l^{-1}), ^{137}Cs labelled in the same solutions and aged for 2 and 165 days. They were subsequently dispersed in 200ml of 10^{-3}M NH$_4$Cl containing a dialysis membrane with giese granulate ("Infinite Bath" method). Desorption progress was monitored by counting the adsorbent (fresh adsorbent is used after each sampling).

For the K-Ca scenario, sediment samples (T2) were preconditioned with three solutions at the same potassium adsorption ratio (0.08) but increasing total concentrations. The compositions studied were (in meq.l^{-1}): K=0.1, Ca=3; K=0.5, Ca=75; K=1, Ca=300. The systems were ^{137}Cs labelled in these conditions, aged for 2, 129 and 165 days and submitted to the same desorption protocol.

Results are shown in Fig. 1.2 and Fig. 1.3 for the homoionic and mixed scenarios respectively.
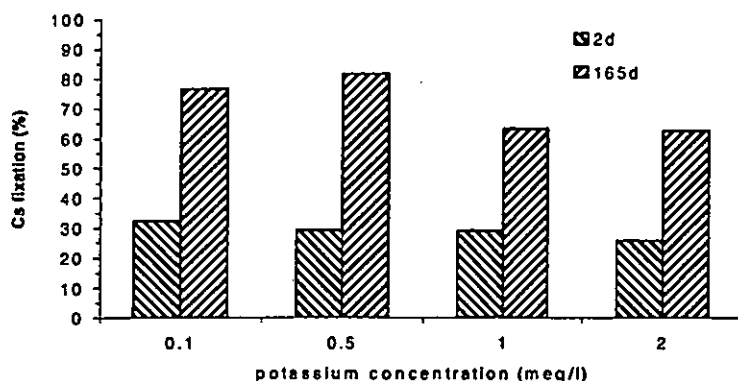

Fig. 1.2 - Effect of potassium concentrations on radiocaesium fixation for T2 sediment, at different aging times (2 and 165 days).

For the potassium scenario (Fig.1.2), there are only a very small trend towards fixation promotion at lower concentration. The fixation levels increase by a factor of about two up to 165 days aging, for all potassium concentrations. In the case of the K-Ca system, the effect of total concentration is more pronounced, particularly at longer aging times (a factor of about 1.5).
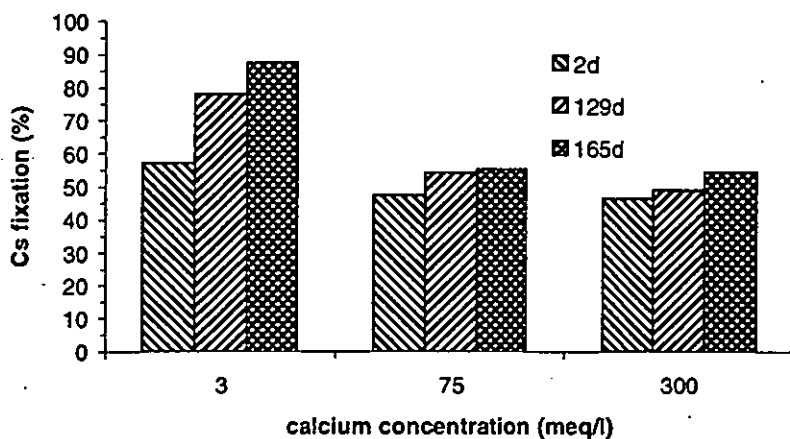

Fig.1.3 - Effect of potassium-calcium concentrations on radiocaesium fixation for T2 sediment, at different aging times (2, 129 and 165 days).

It is concluded that the cationic composition of the liquid phase (and therefore the solid) plays a key role in the radiocaesium fixation behaviour: strongly hydrated cations (Ca, Mg, Na) lead to a pronounced enhancement of radiocaesium fixation in the solid phases; poorly hydrated ions (K, NH_4) have the opposite effect and promote sorption reversibility.

Sediment drying and temperature

In sediment sampling methodology is important to know if a sediment should be dried and, if so, at what temperature and what is the possible effect on the desorption behaviour of radiocaesium. Another question which raises to soils sampling is how important are aging effects in dry conditions. These issues are being addressed here.

Sediment samples ($\approx$1g) were weighted in aluminium plates and contaminated using 2.5ml 10^{-5}M KCl ^{137}Cs labelled solution. These systems were submitted to 5 drying-wetting cycles at 25°C using 2.5ml bidistilled water. The entire procedure took 4 days.

Another set of samples were labelled with ^{137}Cs, using the same procedure, dried at 25°C and left to age for 48 days. The effect of temperature was studied by oven-drying the ^{137}Cs contaminated samples at 110°C and left to age for 4 and 48 days.

In parallel, reference samples were contaminated with ^{137}Cs and left to age at room temperature (25°C) in wet conditions for 4 and 48 days.

For the desorption protocol all the samples were dispersed in 200ml 10^{-3}M NH_4Cl using the giese granulate in a dialysis membrane.

These procedures were carried out to Tejo river (T1, T2) and Tejo estuary (A) sediments.

The results obtained are summarized in Table 1.1 in terms of fixation levels as obtained from the desorption plateaus, for 4 and 48 days aging times.

From Table 1.1 it is seen that, for short aging times (4 days) the wetting/drying cycles have a limited effect on radiocaesium fixation, except for sediment A, as compared with the reference samples left to age for 4 days under wet conditions. Submitting the systems to a drying procedure at 110°C leads to a significant increase in fixation levels.

In what concerns the aging effects, an increase in fixation levels by a factor of about 2, for wet systems, was observed. However, the most important is the finding that in the dried systems, aging leads to minimal changes in fixation levels. It means that, when sediments (or soils) are air-dried after sampling, aging effects are interrupted and, if one is interested in studying radiocaesium desorption yields, the picture obtained relates in fact to the date of sampling. Moroever, these data show very clearly that drying the system at high temperature should in any case be avoided.

It is concluded that, drying a sediment at room temperature has a very limited effect on fixation but appears to put a brake on the aging effects.

Table 1.1 - Effect of sediment drying and temperature on radiocaesium fixation for 4 and 48 days aging times.

Aging time days	Sediments	Wet	Dry (25°C)	Dry (110°C)
4	T1	41.5	44.6 *	66.7
	T2	41.4	54.3 *	-
	A	26	47.8 *	59.6
48	T1	75.9	49.3	63
	T2	74.7	50.7	-
	A	39.7	33.1	55.5

* 5 wetting/drying cycles

2. Solid-phase speciation of radiocaesium and radiostrontium in sediments

It is commonly thought that the fraction of sediment-bound radiostrontium and radiocaesium, dispersed in 1M ammonium solutions -the ion exchangeable pool- is associated with the "regular" part of the ion exchange complex (the planar and easily exchangeable sites). A study on radiostrontium and radiocaesium sorption reversibility, covering a range of sediments and desorption agents (complex ions, KCl, NH_4Cl, $MgCl_2$, $CaCl_2$, $Sr(NO_3)_2$), demonstrated that radiostrontium and radiocaesium are associated with different exchange sites in the solid. On the basis of this different behaviour a sequential ion exchange displacement protocol was developed which allows the quantitative separation of the ion exchangeable fractions of the two radionuclides.

Sediment samples ($\approx$1g) inside dialysis membranes were thoroughly equilibrated with mixed K-Ca solutions (10^{-5} M KCl, 10^{-5} M $CaCl_2$) which were double labelled with ^{137}Cs and ^{90}Sr. After three days equilibration ^{137}Cs radioactivity in the dialysate was counted by gamma spectrometry and the amount of ^{137}Cs adsorbed was calculated. For ^{90}Sr, dialysate samples were counted by beta spectrometry after 16 days (allowing a stationary state of the ^{90}Y daughter nuclide), and ^{90}Sr radioactivity adsorbed on the sediments was calculated. Appropriate corrections were made for the ^{137}Cs interference (maximum energy of 0.51 MeV) in the liquid scintillation counting assays of ^{90}Sr (maximum energy of 0.54 MeV).

Radiostrontium desorption was carried out by transferring the dialysis membranes to 50ml 1N $SrCl_2$ (end-over-end shaking, 24 hours); ^{90}Sr and ^{137}Cs activities were monitored in the dialysate (taking appropriate time delays and corrections as described). From such measurements, desorption levels of both radiostrontium and radiocaesium could be calculated. Finally, dialysis membranes were transferred to a

vessel containing 12g (dry) giese granulate in 200ml 10^{-3}M NH$_4$Cl, and the radiocaesium desorption was monitored by regular gamma counting of the adsorbent.

In addition, reference desorption experiments were carried out on the various sediments (using single labelling), applying the 1N SrCl$_2$ and the "Infinite Bath" protocol (10^{-3}M NH$_4$Cl, giese granulate).

The results are summarized in Table 1.2 for the studied sediments. Five data series are shown: the ^{90}Sr desorption levels obtained with 1N SrCl$_2$ (double labelled systems), ^{137}Cs desorption levels in 1N SrCl$_2$ (double labelled), cumulative ^{137}Cs desorption levels (obtained as the plateau values after 11 days of desorption) using the "Infinite Bath" technique (double labelled), ^{90}Sr desorption levels in 1N SrCl$_2$ (single labelled) and ^{137}Cs desorption levels (single labelled) with the "Infinite Bath" technique.

It is seen that in all systems (double and single labelled), ^{90}Sr desorption is nearly quantitative (96-100%), clearly demonstrating complete reversibility. The ^{137}Cs displacements in the 1N SrCl$_2$ treatment are quite low (1-3%) showing that ^{137}Cs is not at all present in sites accessible to strontium. The desorption levels obtained for ^{137}Cs, after having been submitted to a 1N SrCl$_2$ treatment are seen to be significantly lower (a factor of about 1.5) than the values obtained in the single labelled systems (no 1N SrCl$_2$ treatment). This effect should be due to the enhancement of fixation, resulting from the effect of concentrated solutions of strontium, as shown before to calcium.

Table 1.2 - Radiostrontium and radiocaesium desorption yields (%) for T1, T2, A and S sediments, in the presence of 1N SrCl$_2$ and 10^{-3}M NH$_4$Cl giese ("Infinite Bath" protocol). Standard deviations are given in parenthesis.

Sed.	Mixed "Infinite Bath"			^{90}Sr 1N SrCl$_2$	^{137}Cs 10^{-3} M NH$_4$ giese
	^{90}Sr 1N SrCl$_2$	^{137}Cs 1N SrCl$_2$	^{137}Cs 10^{-3} M NH$_4$ giese		
T1	98.4 (±0.3)	2.7 (±0)	33.4 (±0.5)	95.6 (±0.1)	49.3 (±0.5)
T2	99.3 (±0.2)	3.3 (±0.1)	28.2 (±0.8)	97.3 (±0.6)	46.5 (±0.1)
A	96.4 (±0.2)	1.3 (±0)	39.6 (±0)	96.8 (±0.1)	61.9 (±0.2)
S	97.1 (±0.4)	1.3 (±0.1)	40.2 (±0.2)	97.3 (±0.1)	67.5 (±0)

It is concluded that the ion exchangeable fractions of ^{90}Sr and ^{137}Cs can be rather well separated, the procedure making use of the fact that the radionuclides are associated with different sites of the solid phase. Radiocaesium is quantitatively associated with the FES and its desorption is only partially reversible; radiostrontium is quantitatively associated with the regular ion exchange complex and its adsorption is completely reversible.

3. Short-term prediction of radiocaesium solid/liquid partitioning to suspended matter (Fratel dam)

Suspended matter samples (grain size <106μm) from Fratel dam (Tejo river) collected at 1m (FU) and 10m (FL) depth, were characterized in terms of cation exchange capacity (CEC), organic matter content (OM) and potassium and ammonium radiocaesium interception potential, $K_d m_K$ and $K_d m_{NH4}$ respectively (Table 1.3). The results obtained for the various parameters are in good agreement with those obtained to other freshwater sediments (Madruga, 1993) and show that the two suspended matter samples have very similar properties.

Table 1.3 - Relevant parameters for the suspended matter samples.

Suspended matter	CEC meq.100g^{-1}	OM %	$K_d m_K$ meq.g^{-1}	$K_d m_{NH4}$ meq.g^{-1}	K_c (NH$_4$/K)
FU	39.4	22.8	2.8 ± 0.3	0.73 ± 0.04	3.8
FL	37.8	18.2	3.0 ± 0.1	0.81 ± 0.05	3.7

The solid phase characteristics relevant for the specific sorption of radiocaesium ($K_d m_K$ and $K_d m_{NH4}$) have been determined in the presence of a masking agent (silver thiourea). However, it is of interest to test if the radiocaesium adsorption is exclusively confined to the FES. Such predictions could be confirmed by experimental data for scenarios in which the entire ion exchange complex is accessible to radiocaesium.

Predictions of the radiocaesium partitioning for field scenarios can be made using the following equation:

$$K_d(Cs) = \frac{\left[K_d(Cs).m_K \right]}{K_c(NH_4 / K).m_{NH4} + m_K}$$

where the denominator expresses the total competitive effect of K and NH$_4$ ions, multiplied by its weight factor, obtained from [$K_d m_K$] /[$K_d m_{NH4}$] ratios. Taking into account the values in Table 1.3 and the water column composition (Fratel dam) in terms of K (69 μeq.l^{-1}) and NH$_4$ (17 μeq.l^{-1}) concentrations, the distribution coefficients obtained are 2.1×10^4 and 2.3×10^4 ml.g^{-1} for FU and FL respectively. These values are higher by a factor of two than those obtained "in situ" (1.1×10^4 ml.g^{-1}). The same calculations were made to bottom sediments and also based on the predictions, a higher K_d (6.3×10^3 ml.g^{-1}) than "in situ" K_d (2.8×10^3 ml.g^{-1}) was obtained. Consequently, it may be concluded that in spite of the higher K_d values the solid/liquid partitioning of radiocaesium in field scenarios can reliably be predicted on the basis of sediment laboratory characterizations and column water composition.

The radiocaesium fixation levels at short time period, for the suspended matter were also evaluated. Suspended matter samples (FU, FL) (solid/liquid ratio=1g/25ml) were first preequilibrated (three times) with water from Fratel dam. The radiocaesium

adsorbed on the suspended matter was determined after the samples equilibration (one day, end-over-end shaking) with the same water ^{137}Cs labelled. The labelled suspended matter samples were dispersed in 1M NH$_4$Cl shaken and centrifuged at each sampling time. The procedure was repeated four times and desorption yields expressed in cumulative terms. The results obtained show fixation levels of about 22%. These values are lower than those obtained for bottom sediments (about 50%). It can be concluded that for the same aquatic environment and short aging times the suspended matter plays a more important role than the bottom sediments in what concerns the radiocaesium desorption.

Publications

- Madruga, M.J. Adsorption-desorption behaviour of radiocaesium and radiostrontium in sediments. PhD thesis, K.U. Leuven, Belgium, October 1993.

- Madruga, M.J. On the differential binding mechanisms of radiostrontium and radiocaesium in sediments. Presented on the "International Seminar on Freshwater and Estuarine Radioecology", Lisbon 21-25 March 1994. In publication on the journal "Science of the Total Environment".

- Wauters, J, Madruga, M.J., Vidal, M., Cremers, A. Solid phase speciation of radiocaesium in freshwater sediments. Presented on the "International Seminar on Freshwater and Estuarine Radioecology", Lisbon 21-25 March 1994. In publication on the journal "Science of the Total Environment".

2) BIOLOGICAL PROCESSES

II. Objectives

Radiocaesium bioaccumulation shows a large variability in nature, being higher in oligotrophic lakes, with low potassium concentration, and lower in freshwaters with high potassium content. More recently, after the Chernobyl accident, very high ^{137}Cs concentrations in freshwater fishes were found, mainly in lakes in Northern Europe, with large differences from lake to lake. Temperature is another environmental factor, which is referred in literature as affecting the bioaccumulation of radionuclides by fish.

The objective is the evaluation of the effects of changing environmental parameters which affect the variability of concentrations and transfer factors.

a) Under the assumption that it is not only the K$^+$ concentration in water that affects the radiocaesium accumulation by fish, but also the K$^+$-Cs$^+$ balance, series of experiments were programmed to study the effect of the K$^+$-Cs$^+$ in water, on radiocaesium accumulation and retention by the Cyprinid fish *Chondrostoma polypepis polylepis*.

b) To study the combined effect of different K$^+$ concentrations and different temperatures in water on radiocaesium accumulation by the same fish species.

III. Progress achieved including publications

MATERIALS AND METHODS

All the experiments were performed in small aquaria with 5 liters of an artificial freshwater medium, without water filtration system, but with aeration and artificial light during 8 hours a day, except for weekends (continous lighting). Artificial medium was composed of distilled water to which some salts were added, in order to get a basic cationic composition similar to the one found in Tejo River at the site of Fratel dam. Ca^{2+}, Mg^{2+}, Na^+ and K^+ concentrations were, respectively, 36, 11, 25 and 3.3 mg l^{-1}. Only K^+ concentration was changed and the values used were 0.35, 3.5 and 35 mg l^{-1}. ^{134}Cs was in the chloride form, in a solution 0.1 M of chloridric acid, with a massic concentration of 2 μg Cs^+ml^{-1}. Water was changed once a week and the contaminated feccal pelets were daily separated by screening, to prevent their ingestion by fish.

Small specimens of the cyprinid fish *Chondrostoma polylepis polylepis*, aged of about 1 year and weighing about 2g, were used and fed 5 days a week with milled soft parts of bivalves (containing 0.9 mg K^+ per gramme), each meal representing about 5% of the total fish weigth. Each group was previously acclimated to the artificial medium, for 2 weeks, before contamination with radiocaesium.

During the uptake phase fishes were fed in separated aquaria, with uncontaminated media, to avoid fish contamination from the food pathway.

Radioactivity measurements were made on pre-weighed living fishes, anaesthetized in an aqueous solution of 0.3 g.l^{-1} of MS-222 (Sandoz). To measure ^{134}Cs concentration in the liquid phase during the uptake, 5 ml samples of labelled water were filtered through membranes (0.45 μm).

The measuring equipment was based on a well-type NaI(Tl) detector, associated with a multi-channel analyser.

The first set of experiments at the temperature of $20° \pm 2°C$ had the objective of studying the balance of potassium-stable caesium. Table 2.1 shows the concentrations of stable Cs^+, K^+ and also of $^{134}Cs^+$ added during the uptake phase.

Table 2.1 Concentrations of K^+, stable Cs^+ and radioactive Cs^+ in the artificial medium, at 20°C

(ppm)

	K^+	stable Cs^+	radio Cs^+ **
group 1	0.35	5.8E-04	6.16E-04 to 6.28E-04
group 2	3.5	5.8E-04	6.16E-04 to 6.28E-04
group 3	35	5.8E-04	6.16E-04 to 6.28E-04
group 4	5.8E-04	0.35	6.56E-04 to 6.64E-04
group 5	5.8E-04	3.5	6.56E-04 to 6.64E-04
group 6	5.8E-04	35	6.88E-04 to 7.04E-04

** only for uptake phase

The second and third sets of experiments were carried out at the temperatures of $12° \pm 2°C$ and $5° \pm 1°C$, but being the temperature effect the aim of the experiment, the same three different K^+ concentrations were used and stable caesium was kept constant, 5.8×10^{-4} mg l^{-1}. Very similar conditions as described in Table 2.1 for groups 1,2 and 3, were settled.

RESULTS AND DISCUSSION

Data expressed in Bq g^{-1} of fish (fresh weight) are affected by a confidence interval of 0.95. Concentration Factor, CF_t, the ratio Bq g^{-1} (fish) / Bq ml^{-1} (water), was computed considering the mean value of water radioactivity for all the uptake period. Retention, R_t, was computed considering the mean total radioactivity of fishes, so that data would not be affected by the biological dillution of radiocaesium, due to the weight increase of fishes. Retention data represent the percentage of the initial radioactivity of fishes during the elimination phase and is based upon a multicompartmental analysis. Biological half-life, T_b, means the time needed for a retention compartment to loose 50% of its radioactive content.

In order to be comparable, all the uptake kinetic curves are fitted to power functions, because for the lowest temperature retention analysis could not yet be completed, but for those already completed the results are also presented according to the treatment described by Garnier-Laplace (1991) and Badie *et al.* (1985), where the elimination rate is taken into account.

Potassium-stable caesium effect

[134]Cs concentration in fishes during 4 weeks of direct uptake, has increased in all six groups without reaching a steady state. Figs. 2.1 and 2.2 show the CF_t experimental data and the adjusted uptake functions for groups 1, 2, 3 and 4, 5, 6, respectively.

Keeping a low stable Cs^+ concentration of 5.8 E-04 mg l^{-1} in the artificial medium (groups 1, 2 and 3), it can be easily verified that the higher the K^+ concentration in water the lower the radioactive contamination of fishes, Figure 2.1. The same happens when, on the contrary, there is a low K^+ concentration of 5.8 E-04 mg l^{-1} and stable Cs^+ is present as a major cation (groups 4,5, and 6) Fig. 2.2.

Analysis of variance reveals that, for CF_t experimental data, variances for groups 2 and 3 are not significantly different at the significance level of 0.95, but both are different of group 1, while groups 4, 5 and 6 are significantly different. The same analysis applied to the retention data reveals that groups 1, 2 and 3 are not significantly different, and the same for groups 4, 5 and 6.

The $[K^+]/[Cs^+]$ balance appears to be determinant on the [134]Cs uptake by fishes, and there seems to be a resemblance of Cs^+ and K^+ behaviour when their relative concentrations in medium are inversed.

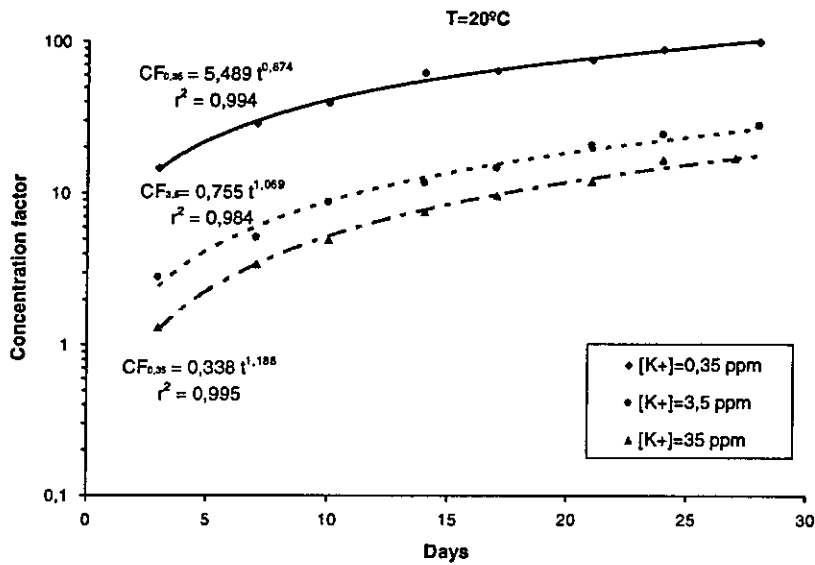It is important to enhance that at K^+ concentration of 3.5 ppm and at the same concentration of Cs^+, CFs are quite similar.

Fig. 2.1 [134]Cs uptake by a freshwater fish from water with different K^+ concentrations, at 20°C

Uptake curves based on the treatment used by Garnier- Laplace (1991) and Badie *et al.* (1985):

$$0.35 \text{ ppm: } CF_t = 419 (1-e^{-0.009\,t}) + 7 (1-e^{-0.183\,t})$$
$$3.5 \text{ ppm: } CF_t = 96 (1-e^{-0.011\,t}) + 0.15 (1-e^{-0.161\,t})$$
$$35 \text{ ppm: } CF_t = 50 (1-e^{-0.013\,t}) + 1.3 (1-e^{-0.114\,t})$$

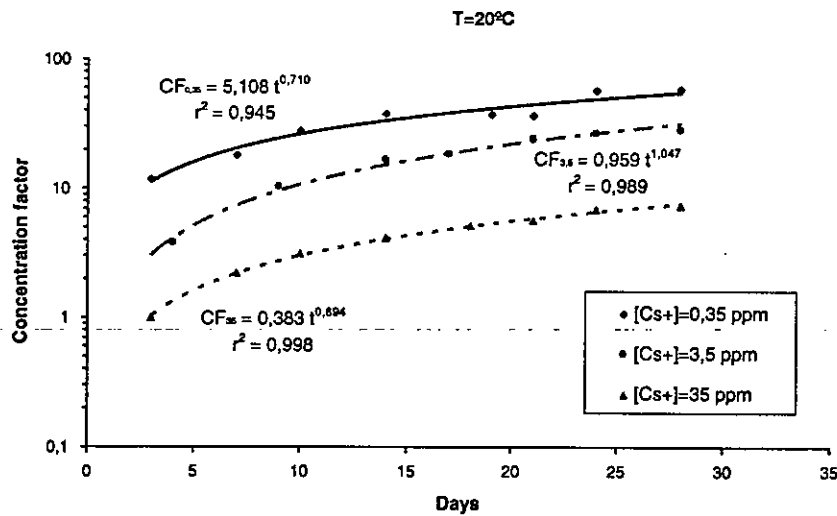Fig. 2.2 [134]Cs uptake by a freshwater fish from water with different Cs^+ concentrations, at 20°C

Uptake curves based on the treatment used by Garnier- Laplace (1991) and Badie *et al.* (1985):

$$0.35\ ppm: CF_t = 653\ (1\text{-}e^{-0.003\ t})$$
$$3.5\ ppm: CF_t = 227\ (1\text{-}e^{-0.005\ t}) + 0.24\ (1\text{-}e^{-9.61\ t})$$
$$35\ ppm: CF_t = 232\ (1\text{-}e^{-0.001\ t}) + 1.1\ (1\text{-}e^{-0.126\ t})$$

Rt(0,35) = 6 exp (-0,183 t)+ 94 exp (-0,009 t)

Rt(3,5) = 14 exp (-0,161 t)+ 86 exp (-0,011 t)

Rt(35) = 11 exp (-0,114 t)+ 89 exp (-0,013 t)

□ [K+]=0.35 ppm
◇ [K+]=3.5 ppm
× [k+]=35 ppm
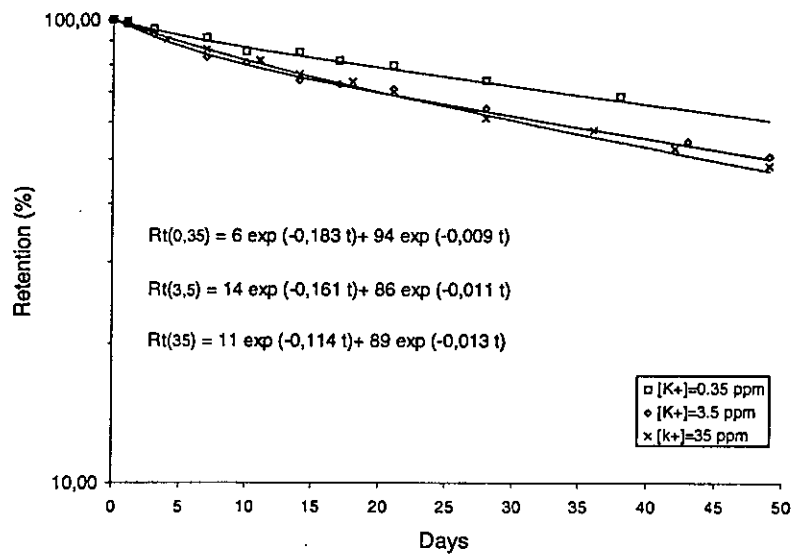
Fig. 2.3 [134] Cs retention by a freshwater fish at different K^+ concentrations in water

Rt(0,35)=100 exp (-0,003 t)

Rt(3,5) = 3 exp (-9,6 t) + 97 exp (-0,005 t)

Rt(35) = 7 exp (-0,126 t) + 93 exp (-0,001 t)

□ [Cs+]=0.35 ppm
◇ [Cs+]=3.5 ppm
× [Cs+]=35 ppm
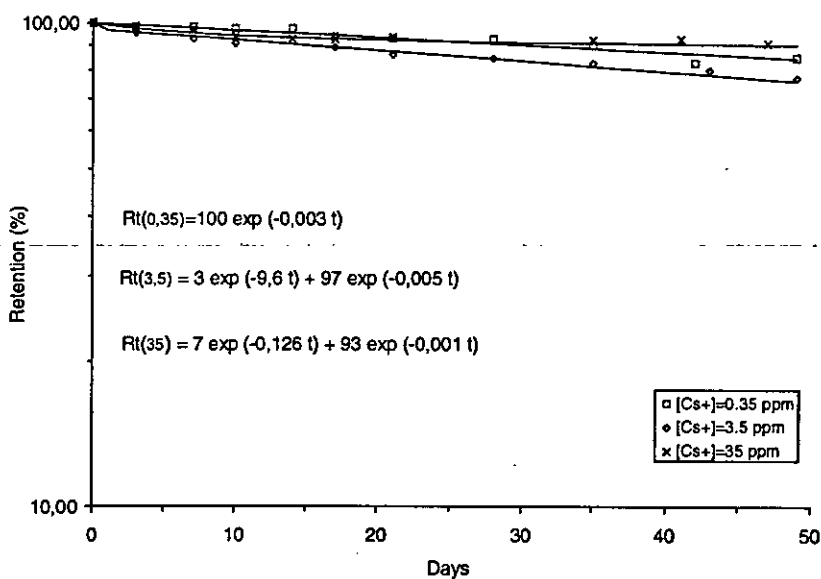
Fig. 2.4 [134] Cs retention by a freshwater fish at different Cs^+ concentrations in water

However, the retention curves show that the removal of radioactive caesium by stable caesium is not as efficient as it is by potassium (Figures 2.3 and 2.4). In fact, comparing retention functions, all the long term retention components of groups 4, 5 and 6, exhibit longer biological half-lives than their respective pairs, ranging from 139 to 693 days. While at the three K^+ concentrations used in water the longer biological half-life varies from 53 days (at 35 ppm) to 77 days (at 0.35 ppm).

One possible explanation is that practicaly no more exchange is possible between the radiocaesium in fish and the potassium in water, as in this case it is only in a tracer amount, and fish must keep constant the internal K^+ concentration (homeostatic regulation).

Potassium concentration and temperature effect

An interesting point to enhance is that the K^+ concentration effect remains approximately the same, at the temperatures of $20°$ and $12°C$, Figs. 2.1 and 2.5. Variance analysis does not reveal for both temperatures (see page 11) significant difference on radiocaesium uptake kinetics for K^+ concentations of 3.5 and 35 ppm, although at $12°$ C it was observed that these uptake kinetics curves are "inverted", Fig.25. In fact following the treatment used by Garnier-Laplace (1991) and Badie *et al.* (1985), they are superposed, which for the moment can not be explained.

However the elimination at $12°$ C is much different than at $20°C$. Not only the biological half-lives are longer, what could be expectable (0.35ppm K^+: $Tb_1=17$ days, $Tb_2=305$ days; 3.5ppm K^+: $Tb_1=14$ days, $Tb_2=167$ days; 35ppm K^+: $Tb_1=16$ days, $Tb_2=105$ days), but the elimination at 35ppm K^+ is faster. This fact seems to mean that the higher K^+ concentation favorizes radiocaesium elimination.

At the temperature of $5°C$, Fig. 2.6, the different K^+ concentrations did not affect differently the radiocaesium accumulation. The three uptake kinetics curves of ^{134}Cs are not significantly different. (Fishes are not very active and they feed at a very low rate).

So, it is noticed that at the temperatures of $20°$ and $12°$ C, there is actually an inverse relation between K^+ concentation in water and radiocaesium concentration factor (CF). Based on the values at the end of each experiment, the three different values of CF obtained according to the three potassium concentrations in water, at the temperature of $20°C$, show the following trend:

$$CF = 70.33\ [\ K^+]^{-0.368} \qquad R^2 = 0.92 \qquad (1)$$

At the temperature of $12°C$ the trend is similar, although the correlation is not so good:

$$CF = 21.15\ [\ K^+]^{-0.444} \qquad R^2 = 0.67 \qquad (2)$$

At the temperature of $5°C$ it is not possible to establish such kind of relation.
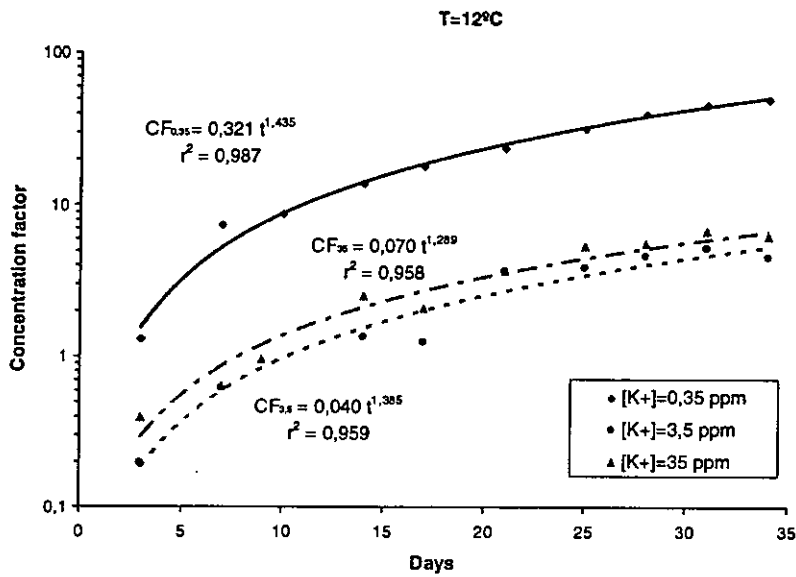
Fig. 2.5 [134] Cs uptake by a freshwater fish from water with different K^+ concentrations at 12 °C

Uptake curves based on the treatment used by Garnier- Laplace (1991) and Badie *et al.* (1985):

$$0.35 \text{ ppm: } CF_t = 313 \ (1\text{-}e^{-0.005 \ t})$$
$$3.5 \text{ ppm: } CF_t = 24.4(1\text{-}e^{-0.006 \ t})$$
$$35 \text{ ppm: } CF_t = 24.3 \ (1\text{-}e^{-0.009 \ t})$$
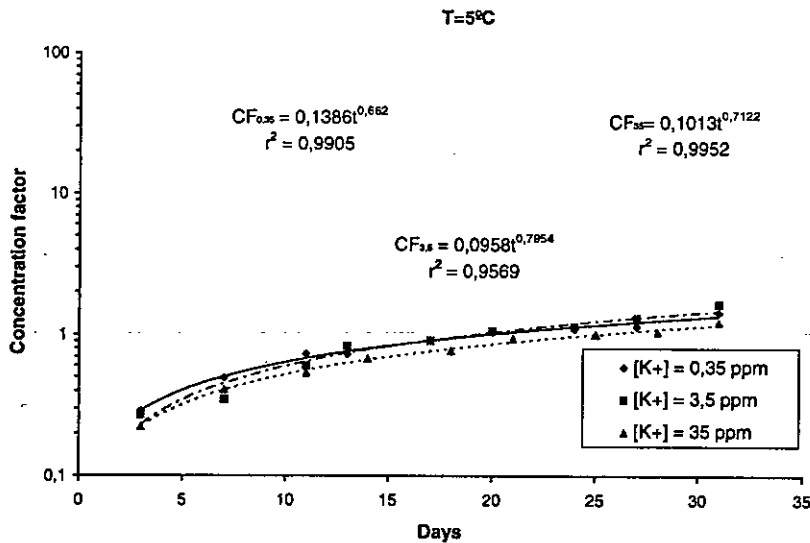

Fig. 2.6 [134] Cs uptake by a freshwater fish from water with different K^+ concentrations at 5 °C

These adjusted exponential functions, with only one term, mean very likely that the accumulation was still far from the equilibrium, in a phase of steep slope, when the process is very well described by a power function (coefficient correlations are about 0.99), and that might respond to the fast component of the elimination curve. So, when adjusting the uptake function, according to the retention study (> 250 days), that first part of the uptake is meaningless and only one exponential term is obtained.

Comparing Figs. 2.1., 2.5 and 2.6 and Cfs equations, it may be seen that: Cfs at equilibrium, at the lower K^+ concentration, represent 73% and 2.2% of the CF at 20°C, at 12°C and 5°C respectively. For the "normal" K^+ concentration, 3.5 ppm, they are reduced to 25% and 8%, at 12° and 5°C respectively, and at the higher K^+ concentration they represent 47% and 11% at the same temperatures respectively.

It must be stressed that the retention experiment was stopped at the 35th day because some deaths occurred and the number of remaining fish was not enough to continue the experiment.

CONCLUSIONS

Potassium-stable caesium effect

According to the proposed objective, it appears that $[K^+]$ / $[Cs^+]$ balance is determinant on the ^{134} Cs uptake by fishes, and there seems to be a resemblance of Cs^+ and K^+ behaviour when their relative concentrations in medium are inverted.

The high stable caesium concentrations in the medium cause a decrease in radiocaesium concentration factor, but at long term the decrease brought about by potassium is stronger. These results suggest a stable caesium descrimination by fish physiology.

The elimination of radiocaesium by fish seems to be independent of the external K^+ concentration (conclusion from an only 50 days experiment).

Potassium concentration and temperature effect

Decreasing temperatures at different K^+ concentrations in water decreases the radiocaesium accumulation, the pattern being almost the same at 20° and 12° C. At 5°C it is completely different, and it seems possible to say that there is no influence of the K^+ concentration in water on the radiocaesium uptake. CF equations show that the highest K^+ concentration influence on radiocaesium accumulation is at 20°C, where the Cf_{eq} at 35 ppm K^+ is 53% of the CF_{eq} at "normal" K^+ concentrations (3.5 ppm).

It was previously concluded, at 20° C, that different K^+ concentrations in water did not seem to affect the radiocaesium elimination rate, as well as at 5°C, but these former experiments lasted only 50 and 35 days respectively, while those ones at 12° C lasted for 250 days. In this case, at higher K^+ concentration in water, the elimination is faster, the exchange rate is higher, and the longer biological half-life is lower. Therefore, it

raises the question as to whether a long time experiment influences the goodness of results.

Publications

- Corisco, J.A.G.; Carreiro, M.C.V.
  Potassium- stable caesium effect on the radiocaesium uptake and loss by the Cyprinid fish *Chondrostoma polylepis polylepis* Steindachner. Presented on the "International Seminar on Freshwater and Estuarine Radioecology", Lisbon 21-25 March 1994. In publication on the journal "Science of the Total Environment".

- Corisco, J.A.G.; Carreiro, M.C.V.
  ^{60}Co transfer in a freshwater simplified trophic chain. III Accumulation and retention by the fish *Chondrostoma polylepis polylepis* Steindachner (to be published)

- Fernandez, J. A.; Heredia, M. A.; Garcia-Sanchez, M. J.; Corisco, J. A .G.; Carreiro, M.C.V.; Rios, A. D. de los
  Mechanisms of radiocesium uptake and accumulation in *Riccia fluitans* (to be published)

Head of Project 3: A. CREMERS

II. Objectives for the reporting period

1. Speciation of radiocaesium in freshwater sediments
2. A simplified procedure of specific site characterization for radiocesium sorption
3. Prediction of K_D for radiocaesium in sediments and soils
4. Radiocaesium uptake in microalgae: effect of K concentration
5. Characterization of sapropell sediments

III. Progress achieved including publications

1. Speciation of radiocaesium in freshwater sediments

In earlier reports, various approaches have been presented for assessing the solid-phase speciation of radiocaesium in sediments. One of these methods is based on the difference in caesium sorption selectivity in the Regular Exchange Complex (REC) and the illitic Frayed Edge Sites (FES) responsible for the very selective sorption of radiocaesium. In particular, it is well known that the K and NH_4 ions are equally competitive with radiocaesium in the REC; in contrast, NH_4 is about 4-7 times more competitive than K for Cs sorption in the FES. Theoretical basis and experimental procedure have been described earlier. In short, the method is based on the measurement of the $K_D(Cs)$ response to NH_4 injection in systems preequilibrated with a mixed Ca-K solution (Ca: 100mM; K: 10 mM). If radiocaesium is intercepted in the REC, then $K_D(Cs)$ should remain invariant to the increase in NH_4 concentration. If it is present in the FES, then K_D should decrease according to the equation

$$\frac{K_D \quad (Ca/K)}{K_D \quad (Ca/K/N)} = 1 + K_c \quad (N/K) \quad \frac{m_N}{m_K}$$

in which $K_D(Ca/K)$ and $K_D(Ca/K/N)$ refer to $K_D(Cs)$ in the Ca/K and Ca/K/NH_4 scenarios, $K_c(N/K)$ to the N/K selectivity coefficient in the FES and m_N/m_K to the ratio of N/K concentrations in the liquid phase. This procedure has been applied to a set of 19 sediments originating from various sources in Europe (Rhône, Moselle, Loire, Vienne, Meuse, Rhine, Garonne, Seine, Tejo, Po, Ravenglass, Lake Devoke and Zoete Waters Lake (Belgium). Systems cover a very wide range in textural properties (% clay + fine silt 5-80%), cation exchange capacities (1-26 meq/100g) and specific sorption potentials. The results are summarized in figure 1 in terms of the averages of $K_D(Cs)$ ratios (and standard deviations) in the two scenarios, $K_D(Ca/K)$ / $K_D(Ca/K/N)$ versus m_N/m_K. Data can be described in terms of the linear regression equation:

$$\frac{K_D \quad (Ca/K)}{K_D \quad (Ca/K/N)} = 1.12 + 7.17 \quad \frac{m_N}{m_K}$$

All individual systems show slopes in the range of 6-8, i.e. the $K_D(Cs)$ response for all systems to increasing NH_4 levels is identical to what is found for illite clay, thus demonstrating quantitative interception of radiocaesium in the FES. This means that reliable predictions of $K_D(Cs)$ can be made on the basis of FES specific sorption potentials and water composition (see below).

2. A simplified procedure of specific sorption potential for radiocaesium sorption

The fact that radiocaesium is, in the very large majority of field scenarios, quantitatively intercepted in the FES group, makes the quantitative assessment of this sorption pool of paramount importance if we wish to make K_D predictions. In the early stages, the specific sorption potential, defined as the product of FES capacity and trace Cs to K selectivity coefficient (formally represented by the symbol $[K_D.m_K]$ was measured on the basis of an elaborate silver-thiourea masking procedure. The principle of a new and simple protocol, eligible for routine applications was introduced in the K_D workshop at the 1984 Lisbon freshwater ecology meeting. It was presented in our 1984 progress report and applied to a limited number of systems. In short, it is based on a single $K_D(Cs)$ measurement in systems preequilibrated with a Ca/K mixed solution (Ca:100mM); K:.5mM) i.e. a PAR (Potassium Adsorption Ratio $m_K/\sqrt{m_{Ca}}$) of 0.05. At this low PAR value, K ions are (nearly) exclusively confined to the FES. This procedure has now been extended to over one hundred sediment (and soil) samples of a wide range in textural properties, cation exchange capacity and organic matter content. Figure 2 shows the correspondance between results obtained by the masking procedure and the simplified PAR protocol. The agreement is essentially perfect: the linear regression yields

$$[K_D.m_K]^{PAR} = -0.083 + 1.01 [K_D.m_K]^{AgTU} \qquad\qquad R^2 = 0.85$$

An additional demonstration of the nature of the agreement between the elaborate masking technique and the PAR protocol is based on a comparison of $[K_D.m_K]$ and $[K_D.m_N]$ values. Figure 3 shows the results.
Both procedures are in excellent agreement in demonstrating the highe competitivity of NH4 as compared to K. The linear regressions are:

$$[K_D.m_K]^{PAR} = -0.11 + 5.12 [K_D.m_K]^{PAR} \qquad\qquad R^2 = 0.90$$
$$n=105$$

$$[K_D.m_K]^{AgTU} = -0.065 + 5.70 [K_D.m_K]^{AgTU} \qquad\qquad R^2 = 0.92 \qquad n= 116$$

$$[K_D.m_K]^{All} = -0.046 + 5.28 [K_D.m_K]^{All} \qquad\qquad R^2 = 0.91$$
$$n= 221$$

It thus appears that the sorption characteristic, necessary for making K_D predictions is obtainable from a single measurement using simple laboratory procedures readily available.

The reliability of predictions based on such characterizations is demonstrated in the section below.

3. Prediction of K_D(Cs) in sediments and soils

Predictive capabilities were tested on a broad range of systems using the following equation

$$K_D \ (Cs) = \frac{[K_D \ m_K]}{m_K + 5.3 \ m_N + 0.02 \ m_{Na}}$$

in which 5.3 and 0.2 refer to the N/K and Na/K selectivity coefficients in the FES. The following tests were carried out:(1) fifty freshwater sediments were thoroughly preequilibrated with a (modal) synthetic river water ($m_K = 0.15$ mM; $m_N = 0.1$ mM, $m_{Ca} = 2$ mM, $m_{Mg} = 0.5$ mM $m_{Na} = 1$ mM) and K_D(Cs) measured; (2) twenty-five freshwater sediments were equilibrated with the (Cs[137] labelled) water described in (a) and K_D(Cs) measured; liquid phase compositions were measured after equilibration; (3) five estuarine sediments were submitted to tests 1 and to equilibration with synthetic seawater; (4) six widely different soils (texturally) were subjected to 8 different cationic scenarios (Ca = 3.5 mM; Mg = 1.5 mM) varying the K and NH_4 concentration in the range of 0.3 - 2 mM. In total, some 133 systems (combinations of sediments/soils and water compositions) were included in the study. Figure 4 shows the nature of the agreement between predicted K_D(Cs) values (K_D-pred) and experimental findings (K_D-exp). It is seen that K_D values cover a range of three orders of magnitude (50 to 50000 L/Kg) and that the agreement is reasonably good. In general, predictions somewhat overestimate experimental values but 90% of all observations deviate by less than a factor 3 from predictions. On the average it is found that

$$\frac{K_D(\text{exp})}{K_D(pred)} = 1.61 \pm 0.75$$

It may thus be concluded that reasonably reliable predictions of K_D(Cs) can be made on the basis of [$K_D.m_K$] values (obtainable by routine procedures) and liquid phase compositions (K and NH_4, and in saline scenarios, Na ion concentrations).

4. Radiocaesium uptake in algae: effect of K concentrations

The main aim of this study was to assess the nature of the competitive effect of K (covering a range of 0.1 to 10 mM) on TF values for radiocaesium uptake in microalgae (Dunalliella viridis). In a preliminary stage, efforts were directed at: (a) setting up a chemostat cultural system; (b) testing the ability of Dunaliella to grow in media of large differences in K concentration; (c) optimizing counting procedures for TF measurement in microalgae for marine (high conc.) conditions. It was found that the organism could be grown in a K conc. range of 10^{-4} to 10^{-2} M without significant loss in growth rate and photosynthetic activity. Ca concentrations could be varied in a range of 2.10^{-4} to 2.10^{-2}M but growth rate and photosynthetic activity were affected. Cs[137] contents of algae were measured, using glass-fiber filtration for cell harvesting.

K effects on TF were measured in a standard simplified Johnson & Johnson medium labelled with Cs^{137}. Algae were grown (batch culture) for one week in a growth chamber at constant temperature and ligth intensity at 10^{-2}, 10^{-3} and 10^{-4} in K. No significant differences in growth rate were observed. Cs^{137} activity was measured on filters (100 ml suspension for 0.1 g of algae d.w.). The results (averages of three runs) are TF = 0.9($\pm$ 0.15) at 10^{-2} M K, 1.1 ($\pm$ 0.3) at 10^{-3} M and 28.5 ($\pm$ 1.3) at 10^{-4} M. These data, which are relevant for scenarios of low K concentration in freshwaters, clearly show that, at low K concentrations, TF values increase more than proportionally with decreasing K levels. These findings are in agreement with unpublished data (E. Smolders, K.U.Leuven) for higher plants indicating high sensitivity of TF (Cs) below K concentration of 0.25 mM.

5. Characterization of Sapropell sediments

Sapropell refers to sediments containing indigested vegetal and animal residues and which is available in large quantities in lakes in the CIS, particularly in Belarus and the Ukraine. Sapropell has been used in recent years as a countermeasure in radiocontaminated soils. A set of six samples, originating from various lakes in Belarus were characterized in terms of organic matter (OM) content, CEC, ionic composition of the exchange complex, specific sorption potential and fixations properties for radiocaesium.

OM content covers a range of 23 to 73% and CEC values range from 27 to 105 meq/100g. Normalizing CEC values to OM content leads to an average value of 1.24 ($\pm$0.23)meq/g, showing that exchange capacity is nearly exclusively associated with OM. In all samples (except one) NH_4 levels exceed those of K, sometimes by a factor of 10, as could be expected from the anoxic conditons of the sediments. [$K_D.m_K$] values cover a range of 0.1 to 1 meq/g. This is the range commonly found for the soils in the Chernobyl contaminated area. It follows that the beneficial effect, if any, is not connected with the sorption properties of those materials. In contrast, its use as a countermeasure for radiostrontium is predictable, particularly in case of high OM content.

As an experimental test, a series of K_D measurements were carried out on sandy soils originating from the contaminated area with and without sapropell for both radiocaesium and radiostrontium. The effects observed were completely consistent with the relative sorption properties of soils and sapropell amendment for both radiocaesium and radiostrontium.

6. Publications

Submitted (Applied Geochemistry)
Prediction of solid/liquid distribution coefficients of radiocaesium in soils and sediments
- Part one: a simplified procedure for the solid phase characterization
J. Wauters, A. Elsen, A. Cremers, A.V. Konoplev, A.A. Bulgakov and R.N.J.Comans
- Part two: a new procedure for solid phase speciation of radiocaesium
J. Wauters, M. Vidal, A. Elsen and A. Cremers
- Part Three: a quantitative test of a K_D predictive equation
J. Wauters, A. Elsen and A. Cremers

<u>To be submitted</u>
- The use of sapropell as amendment in radio-contaminated soils (Applied Geochemistry)
E. Valcke, L. Moskaltchuk and A. Cremers
- The influence of particle concentration and fixation on radiocaesium sorption (Env.Chem.)
J. Wauters and A. Cremers
- Caesium-specific sorption sites on illite-bearing substrates (Env. Chem)
J. Wauters, A. Dierickx and A. Cremers
- Adsorption Kinetics of radiocaesium in aquatic sediments (Env. Chem.-)
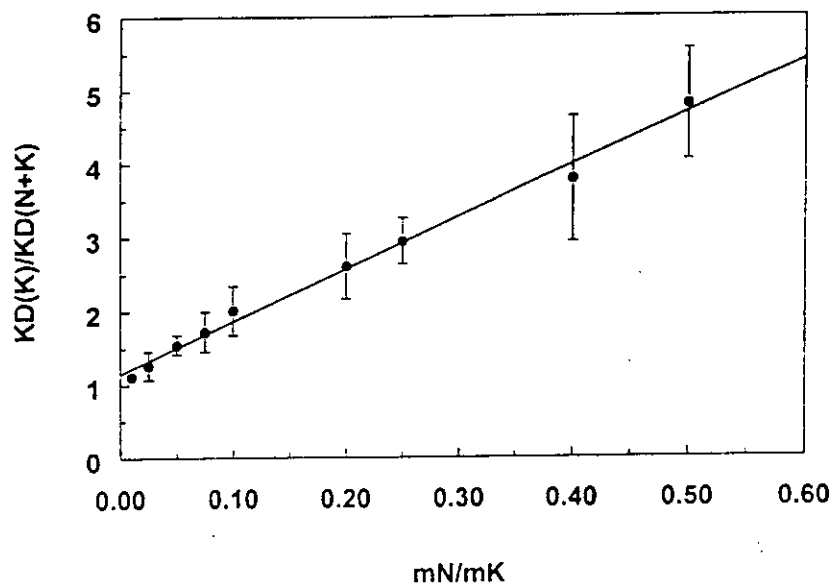*J. Wauters, S. Rampelberg and A. Cremers*

Figure 1. Effect of increasing NH_4 concentration on the K_D ratios (K-Ca/K-N-Ca scenarios) for freshwater sediments
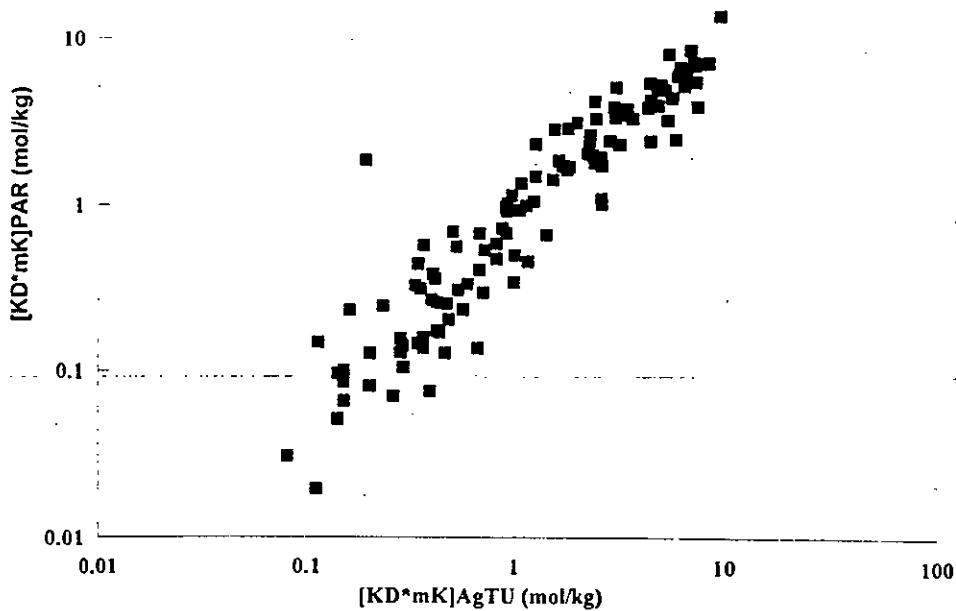

Figure 2. Comparison of $[K_D.m_K]$ values obtained by the AgTU masking technique and the simplified PAR protocol.
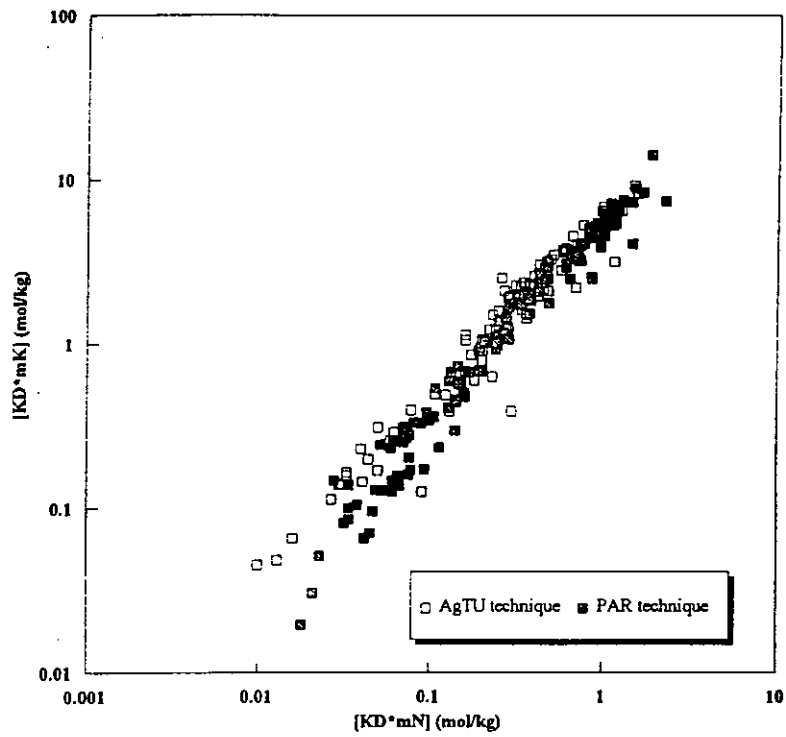
Figure 3. [$K_D.m_K$] versus [$K_D.m_N$] for the AgTU masking technique and the simplified PAR protocol.
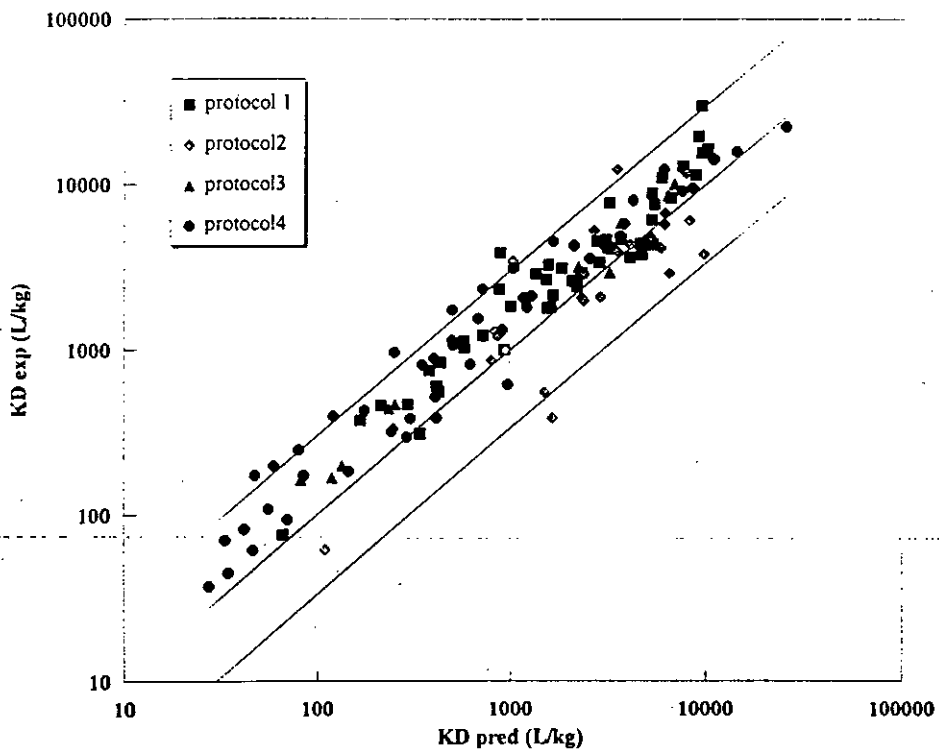

Figure 4. Experimental versus predicted K_D values: upper and lower lines refer to $K_D(exp)$ / $K_D(pred)$ values of 3 and 0.33.

I. head of project 4: Dr. FOULQUIER

II. Objectives.

- The Chernobyl accident showed the importance of cesium 137 in aquatic ecosystems and its fixation in the sediments. In relation with the different source terms (fallout from the atmospheric weapon tests and the Chernobyl accident, liquid wastes from nuclear plants), a review of our knowledge about cesium 137 fixation in the sediment of main french rivers is done.

- The importance of radioruthenium was shown in Chernobyl fallout and in the liquid wastes of reprocessing fuel plants. An experimental work studies the fixation of ruthenium 106 in an aquatic ecosystem.

III. Progress achieved including publications

1) CESIUM IN THE FRENCH RIVERS.

French rivers are an intereting investigation field to study the behaviour of cesium in aquatic ecosystems. Seven rivers are fitted with nuclear power stations (Figure 1): the Rhône with 5 stations (Creys, Bugey, St Alban, Cruas, Tricastin) and the fuel reprocessing plant of Marcoule), the Garonne with 1 station (Golfech), the Loire with 4 stations (Belleville, Dampierre, Saint Laurent, Chinon), the Seine with 1 station (Nogent), the Rhine with 1 station in France (Fessenheim) but under the influence of other stations upstream (Gosgen, Beznau, Liebstat, Muhleberg), the Moselle with Cattenom, the Meuse with Chooz.

Roughly, differences exist between the granulometric composition of the river sediments. Some like Rhône, Meuse, Rhine rivers have silty sediment, others like Moselle, Garonne, Loire have sandy sediments. The percentage of thin particles (lower than 50µm) and the organic matter are given in table 1:

Table 1. Percentage of thin particles, and composition of organic matter in sediments of french rivers.

River	particles <50µm	organic matter (g/kg DW)
Rhône	30-70%	2.6 - 17.5
Meuse	72-75%	7.1 - 7.7
Rhin	50-54%	3.2 - 3.5
Seine	48-57%	2.9 - 9.1
Moselle	11-36%	5.6 - 6.5
Garonne	21-32%	1.7 - 2.1
Loire	18-37%	4.2 - 9.3

The radiocesium concentrations were studied upstream and downstream from every nuclear plants. The concentrations of these nuclides in the different rivers sediments from 1989 to 1993 are given in table 2.

Differences exist between eastern and western rivers which are the consequences of several factors:

-first is that the Chernobyl plume flew mainly over the eastern parts of France.

-other reasons are related with the type of reactors and the hydroelectric equipment of the rivers.

The lowest values of ^{137}Cs concentration are found in the Garonne river sediments ; ^{134}Cs was not detected. The effluents of the Golfech 1300 MWe PWR have a very low radioactive level.

In the Loire and the Seine rivers concentrations of ^{137}Cs are higher because the presence of 900 MWe PWR (which did not retreat their effluents as well as 1300 Mwe power stations) and the graphit-gaz reactors (St Laurent and Chinon).

In the eastern rivers like Meuse, Moselle, Rhin, the concentration of radiocesium in the sediments is higher, showing the effect of the Chernobyl fallouts and of the liquid effluents from the old reactors (from 1970 in Chooz, 1977 in Fessenheim).

Table 2. Concentrations of ^{134}Cs and ^{137}Cs in the different sections of the french rivers. (Bq.kg^{-1} D.W.)

Rivers	sections	^{134}Cs	^{137}Cs
Garonne	upstream Golfech	-	3.9 ± 3.1
	downstream Golfech	-	2.8 ± 3.2
Loire	upstream Belleville	1.1 ± 0.9	13.5 ± 13.3
	Belleville-Dampierre	2.1 ± 1.5	7.8 ± 5.2
	Dampierre St.Laurent	1.8 ±1.1	13.4 ± 7.5
	St-Laurent-Chinon	2.2 ± 1.2	12.7 ± 6.5
	downstream Chinon	9.4 ± 7.0	23.3 ± 21.0
Meuse	upstream Chooz	1.7	31
	downstream Chooz	5.9 ± 1.0	79.5 ± 53.0
Moselle	upstream Cattenom	-	5.5 ± 39.6
	downstream Cattenom	4.8 ± 3.3	16.6 ± 39.6
Rhine	upstream Fessenheim	10.9 ± 5.0	64.7 ± 22.9
	downstream Fessenheim	9.0 ± 6.5	56.0 ± 28.4
Rhône	Geneva lake	8.0 ± 5.8	66.5 ± 40.5
	Geneva-Creys	1.7 ± 1.6	16.6 ± 15.8
	Creys-Bugey	2.1 ± 2.2	24.0 ± 16.2
	Bugey-St.Alban	2.8 ± 1.9	19.0 ± 17.9
	St.Alban-Cruas	3.5 ± 1.6	31.1 ± 12.5
	Cruas-Tricastin	5.6 ± 5.3	36.8 ± 25.3
	Tricastin-Marcoule	3.1 ± 2.5	32.0 ± 21.7
	Marcoule-Camargue	28.6 ± 13.7	253 ± 72
	Grand Rhône	8.5 ± 5.2	75 ± 33
	Petit Rhône	11.5 ± 3.9	195 ± 91
	Camargue delta	1.3 ± 0.4	16.1 ± 7.3
Seine	uptream Nogent	1.1 ± 0.7	13.3 ± 6.0
	downstream Nogent	3.7 ± 4.1	16.0 ± 18.9

The Rhône river presents several aspects. In the lake of Geneva the sediments have 66 Bq/kg DW of ^{137}Cs showing the characteristic of lakes with large catchment area and slow renewal flux.

In the upper Rhone, the sandy sediments have a concentration of around 20 Bq/.kg^{-1} DW. From Lyon to Marcoule the ^{137}Cs activity is about 30 Bq.kg^{-1} and 250 downstream from the reprocessing fuel plant of Marcoule and less in the two arms of the river (Grand-Rhône and Petit-Rhône) surrounding the delta of Camargue.

The same comments could be made for ^{134}Cs which shows concentrations 10 times lower than ^{137}Cs.

Radiocesium concentrations are well correlated with sediment thin particles and organic matter.

Multivariated analysis were done on these field data. For example figure 2 shows a graphical representation of a Principal Component Analysis (PCA) done with 9 parameters on 26 samples of sediment of upper Rhône.

The first graph shows the projection of the parameters on the factorial plan constructed with the first two axis that represent 70% of the total variability.
The correlation circle shows that the best correlated parameters in the principal plan are ^{137}Cs (-0,94), thin silts (-0,89), thick silts (-0,84) and thick sands (+0,79)

The parameters having correlations close to the circle (-1, +1) are the best variables represented on the principle plan. Axis 1 explains 50% of the variability, it could, roughly represent the sediment granulometry.

When two variables are in the same direction, their evolutions are correlated. So 137Cs is a function of the percentage of thin particles, and specially silts (and it is in opposite with percentage of sands).

Axis 2 explains 20% of the variability and it does not give interesting informations.

The second graph shows the projection of the different samples on the factorial plan. One could see different populations:

- on the left are the samples characterised by a high percentage of thin particles ; they are the sediments on the dam reservoirs, and two samples downstream from Lyon.

- on the upper part of the diagram are the samples from Bugey area, where sandy sediment is found. - the last population is composed by the sediments sampled between the Geneva lake and the area of Creys, with sandy sediments.

When several parameters are in the same direction it is possible to draw the regression graph between them. For example figure 3 shows the relation between the percentage of thin particles and the cesium concentration in the sediments from upper Rhône.

In conclusion, this study shows that the concentration of radiocesium in river sediment can be related whith the different source terms and with the granulometric characteristics of the sediments.

2) RUTHENIUM 106 EXPERIMENTAL TRANSFER MODEL.

A research program was undertaken on evaluation, modeling and analysis of ^{106}Ru transfer in a fresh water trophic net. The reason was that ^{106}Ru was found in Tchernobyl fallout and constituted 95% of liquid wastes of the reprocessing fuel plant of Marcoule. It was the subject of Françoise Vray PhD. Her thesis defence occured on november 24th 1994. 72 experimentations

studying the transfer of [106]Ru in a freshwater ecosystem including 2 abiotic compartments and 10 species from 3 trophic levels were done.

The CEC-DG XII cofinanced a part of the experimentations concerning the following components:
- Water sampled in the Rhône river, upstream from the Cruas power station.
- Primary productors, which are two species of algae abundant in freshwater ecosystems (Scenedesmus,Chlorella). These two species present differences in morphology, size, and digestibility by their consumers.
- First order consumers, (Daphnia magna) which is a planctonic crustacea important in fish diets.
- Second order consumers (Gambusia) which is chosen because its small size, used as a food for young trouts.
- Third order consumer (Salmo trutta) which is a ichtyophagus fish.

Experiments are done in plastic tanks (1 to 10 liters, according to the size of the organisms), temperature is fixed at 18°C, oxygenation is made with air pumps. For the direct transfers from water, contamination with [106]Ru (RuCl₃, in HCl) is realized in a single time, one or two days before introducing organisms. For the trophic transfers, food is previously contaminated and rinced in inactive water before it is given to predators. Sampling and radioactive measuring is done regularly. For water, samples of 5 and 10 ml are taken, part is measured non filtered, an . other one after filtration at 0.45 μm.

Algae are sampled by filtration on 0.45 μm membrane, biomass is evaluated in a Malassez cell.
Daphnids are sampled by filtering the water on a nylon sieve. They are rinced in inactive water then dried on blotting paper.
Fish are sampled with a spoon net, they are anesthetized, then put in plastic tubes. Radioactivity is measured by gamma spectrometry on a NaI cristal.

2.1 TRANSFER FROM WATER TO ALGAE.
The contamination of the two species was done at several ages of the population (0, 6, 13, 26 days).
Figure 4 shows the simulation of the concentration factor evolution for a constant concentration of water and without cellular divisions.

The transfer of [106]Ru to phytoplancton is characterized by an intensive accumulation (FC#800). It is influenced by the morphology of the cells, or by physiological characteristics (mucus). [106]Ru does not seem to go inside the cell but only adsorbed on the membrane. Depuration is slow in relation with the biological dilution. So, algae are an important vector of contamination for their predators.

2.2 TRANSFER FROM WATER TO DAPHNID
Uptake and depuration were realised for two different levels of contamination (70 and 370 Bq.ml^{-1}). Figure 5 shows accumulation and depuration curves of daphnids concentrations. The CF is 120 to 140 at the steady state (11 days). Elimination is characterized by two biological half-lives : 4 hours and 48 hours.

2.3. TRANSFER FROM ALGAE TO DAPHNIDS.

After 14 days of culture, algae were contaminated with 500 $Bq.ml^{-1}$ of ^{106}Ru. After 3 to 5 days, algal cells were filtered and given to daphnids as one meal a day. The radioactivity of food was estimated by comparison of filtered and unfiltered culture medium and numeration of algae.

The parameters computed were the trophic transfer factor (TTF) which measures the bioaccumulation of ruthenium during accumulation phase (concentration in daphnia/concentration in algae) and the retention factor (R) in depuration phase (C_t/C_0).

Figure 6 shows the transfer of ruthenium to daphnids via *Scenedesmus* and *Chlorella*. The growth of daphnids and the transfer of ruthenium are higher with *Scenedesmus* than *Chlorella*. In fact the concentration of ^{106}Ru in daphnids is in relation with the concentration in algae and with the number of cells absorbed.

The elimination curve is similar with the two species of algae (figure 7). The transfer factor is 0.21 with Chlorella and 0.23 with Scenedesmus.

2.4. TRANSFER FROM WATER TO GAMBUSIA.

14 fish were put in the contamination tank for 40 days. No weight growth was observed as they were adult fish, in spite they were fed. Figure 8 shows the ^{106}Ru concentration in the water and in the fish. The medium was renewed twice (12 and 26 days). The activity of ^{106}Ru was between 500 and 300 Bq/ml. Figure 9 shows the depuration : gambusia lost 58% of their ^{106}Ru concentration after 14 days.

Figure 10 shows simulations for adult gambusiae in a steady water concentration and the retention of the nuclide when contamination stops. The concentration factor reaches 1.1 after 120 days ; 2 biological half lives exist in depuration phase, respectively 16 hours and 21 days .

2.5. TRANSFER FROM WATER TO TROUTS.

Trouts were fed with midge larvae ; the fish weight increased from 5 to 8 g during the 49 days of experimentation. Figure 11 shows the ^{106}Ru concentration in filtered water -which was renewed every week- and in the fish. Figure 12 shows the simulation of the trout concentration factor for a steady water concentration and the nuclide retention when contamination stops. The concentration factor reaches a value of 1.4 at 140 days. Depuration shows 2 biological half lives of 2 and 36 days.

2.6. TRANSFER FROM GAMBUSIA TO TROUTS.

Trouts were fed with *Gambusiae* in order to have a rapid growth. The concentration of ^{106}Ru in the food shows very important variations. The concentration in predators is proportional to this of preys. The depuration of the ^{106}Ru from trout is going through 14 days. The simulation of the trophic transfers from food to trouts for a constant feeding rate and a steady concentration in food is shown on figure 13. The trophic transfer factor at a steady state is $4.1.10^{-3}$. The retention factor after 60 days is less than 0.5%.

2.7. CONCLUSION.

This table shows the values of all the [106]Ru transfer parameters obtained from the several experimentations :

Experimentation	FC	FTT	Tb1	Tb2
water-chlorella	710	-	220 j	-
water-Scenedesmus	830	-	100 j	-
water-daphnia	170	-	4 h	2 j
algae-daphnia	-	0.2	15 h	-
water-Gambusia	1	-	16 h	21 j
water-Salmo	1.3	-	2 j	36 j
Gambusia-Salmo	-	0.004	6 h	24 h

Experimental results were expressed mathematically so they could be included in a global model which was tested in two different situations with the shell-fish called *Dreissena* and the carp. The comparison of the available data concerning the *in situ* measured concentrations to the corresponding computed values validated the procedure (Vray, 1994).

IV. Papers published or in press resulting from this work

FOULQUIER L. & BAUDIN-JAULENT Y. (1992). Impact radioécologique de l'accident de Tchernobyl sur les écosystèmes aquatiques continentaux. *C.C.E. RADIATION - PROTECTION-58* : 392 p.

FOULQUIER L., GARNIER-LAPLACE J., LAMBRECHTS A., CHARMASSON S. & PALLY M. (1993). The impact of nuclear power stations and of a fuel reprocessing plant on the Rhone river and its prodelta. In: *Environmental impact of nuclear installations. Proceedings of the joint seminary from september 15th to 18th 1992 at the university of Fribourg (Suisse), organised by the Société Française de Radioprotection and the German-Swiss Fachverband für Strahlenschutz.* : 263-270.

FOULQUIER L., LAMBRECHTS A. (1994). Radioecology assessment in waterways in France with nuclear facilities (1989-1993). *International seminar on freshwater and estuarine radioecology, Lisbon, Portugal, 21-25 march 1994* : 7p.

LAMBRECHTS A., FOULQUIER L. & PALLY M. (1992). Synthèse des connaissances sur la radioéologie du Rhône. *Comité de bassin Rhône Méditerranée Corse. Groupe de travail "Qualité des eaux du Rhône" sous groupe "Micropollution toxique"* : 172 p.

VRAY F., SVADLENKOVA M. & BAUDIN J.P. (1993). Accumulation et élimination du [106]Ru par *Daphnia magna* Strauss. Etude des voies directe et trophique. *Annls. Limnol.* **29** (3-4) : 281-293.

VRAY F. (1994) Evaluation, modélisation et analyse des transferts expérimentaux du [106]Ru au sein d'un réseau trophique d'eau douce. Université se Montpellier II, Sciences et techniques du Languedoc, Thèse de doctorat (spécialité Biologie des populations et écologie) 24/11/94 : 377p
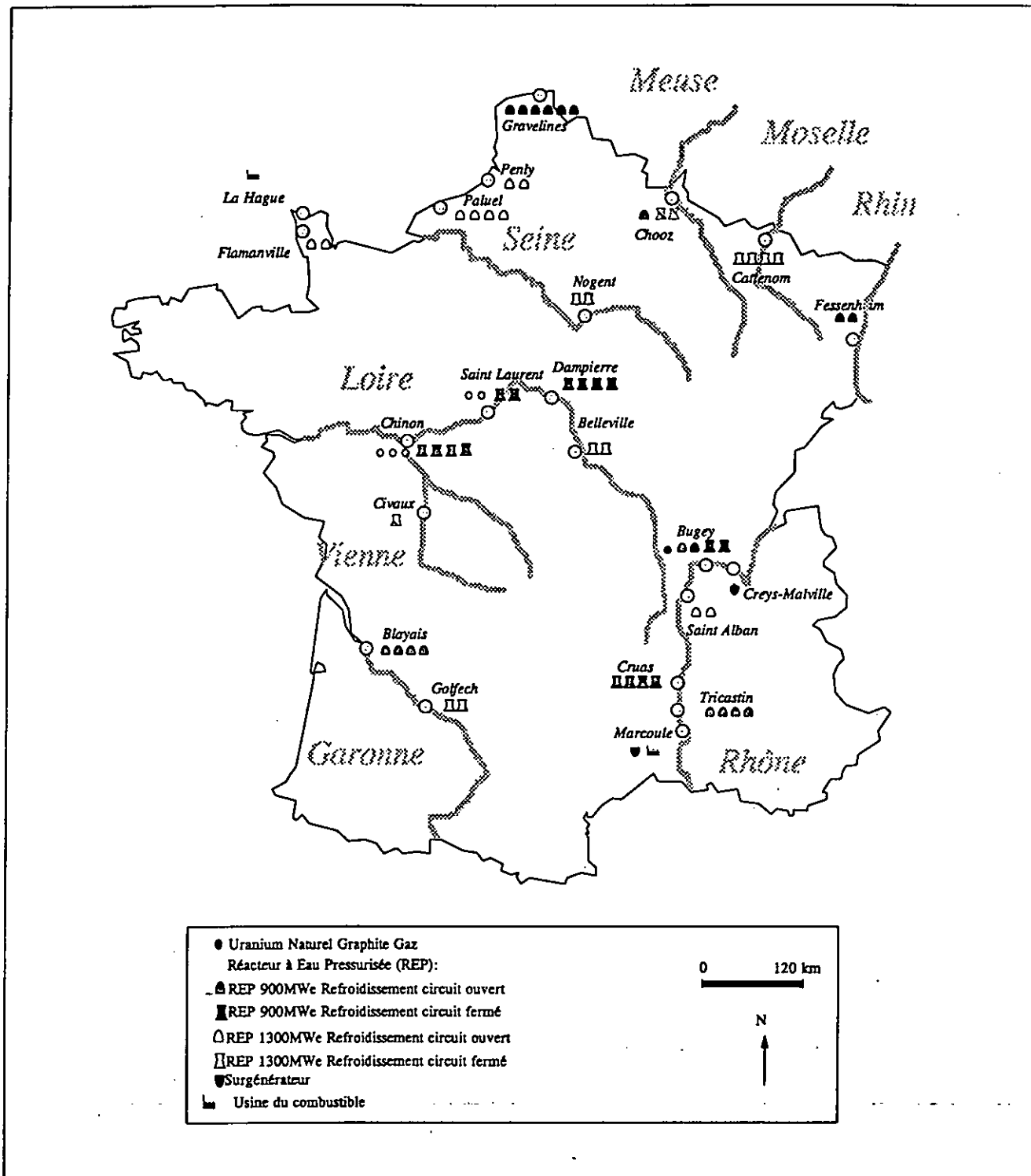
La Hague

Flamanville

Gravelines

Penly

Paluel

Chooz

Cattenom

Fessenheim

Seine

Nogent

Loire

Saint Laurent Dampierre

Chinon

Belleville

Civaux

Bugey

Creys-Malville

Saint Alban

Blayais

Cruas

Golfech

Tricastin

Marcoule

Vienne

Garonne

Rhône

Meuse

Moselle

Rhin

● Uranium Naturel Graphite Gaz
Réacteur à Eau Pressurisée (REP):
▲ REP 900MWe Refroidissement circuit ouvert
▌REP 900MWe Refroidissement circuit fermé
◊ REP 1300MWe Refroidissement circuit ouvert
▯ REP 1300MWe Refroidissement circuit fermé
▼ Surgénérateur
▙ Usine du combustible

0   120 km

N

Fig 1. Installations nucléaires françaises
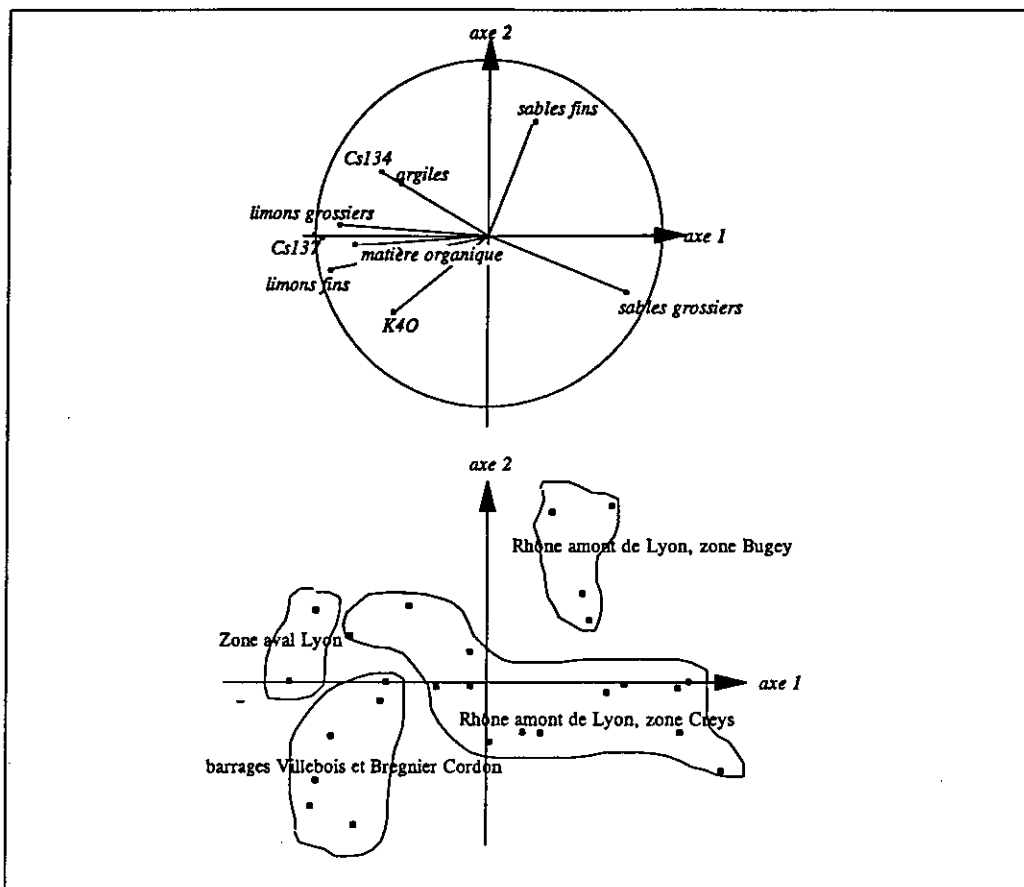
Fig.1. French nuclear facilities

Fig.2: A.C.P. sur les sédiments du Haut-Rhône Français
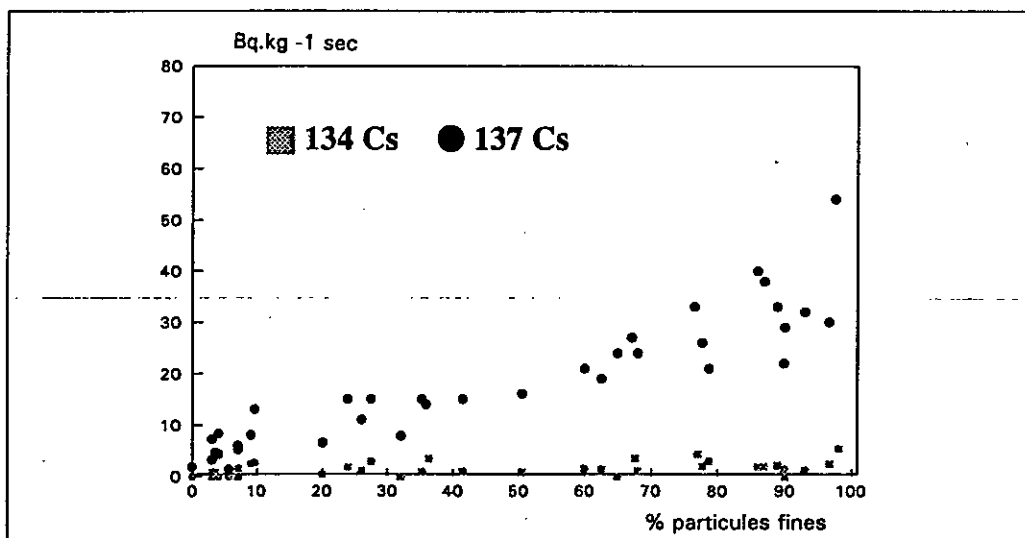*Fig.2 : P.C.A. on french upper Rhone sediments*

Fig.3: Relations entre radiocésium et particules $< 50 \mu$m dans
les sédiments du Haut-Rhône Français
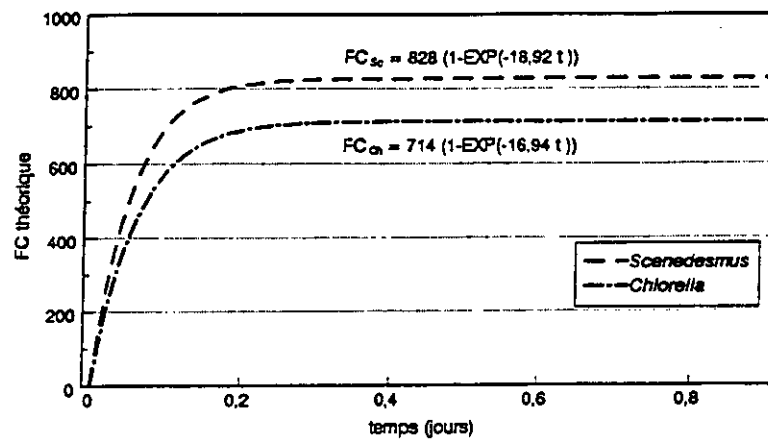*Fig.3: relations between radiocesium and particles $< 50 \mu m$ in
french upper Rhone sediments*

Fig. 4 : Simulation de l'évolution du facteur de concentration (FC) du ^{106}Ru par les algues en l'absence de divisions cellulaires et pour une concentration du radionucléide dans l'eau constante.

Fig.4 : simulation of algae ^{106}Ru concentration factor evolution for a constant water concentration and without cellular divisions
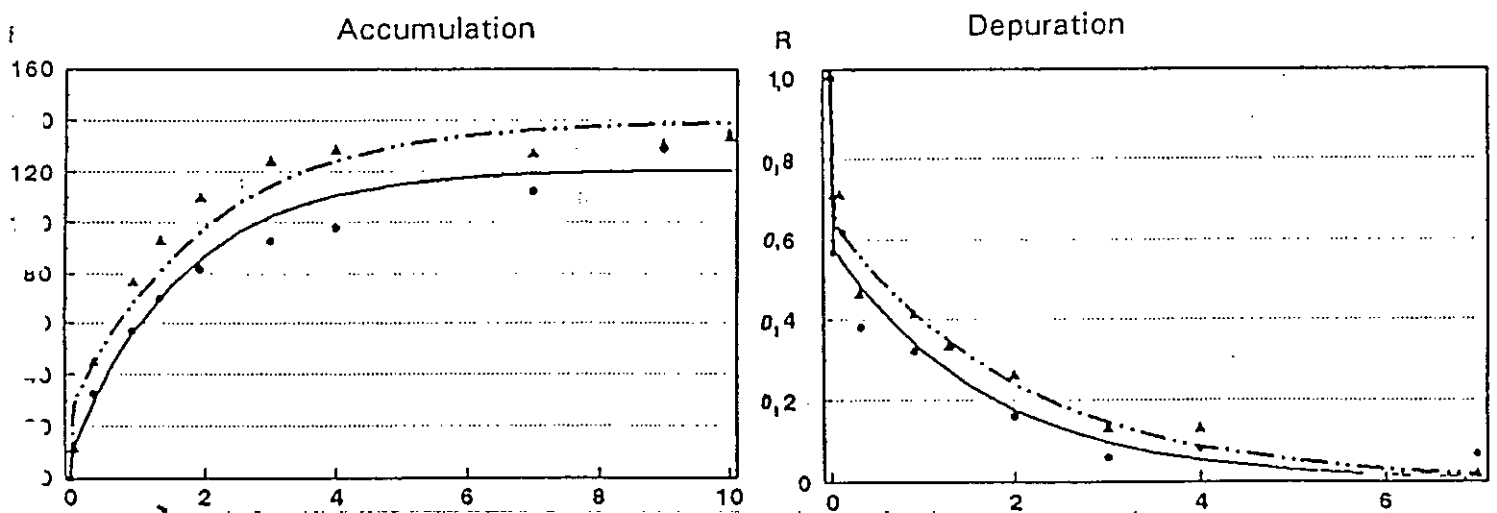

Fig. 5 : transfert du ^{106}Ru de l'eau aux daphnies (accumulation et élimination)

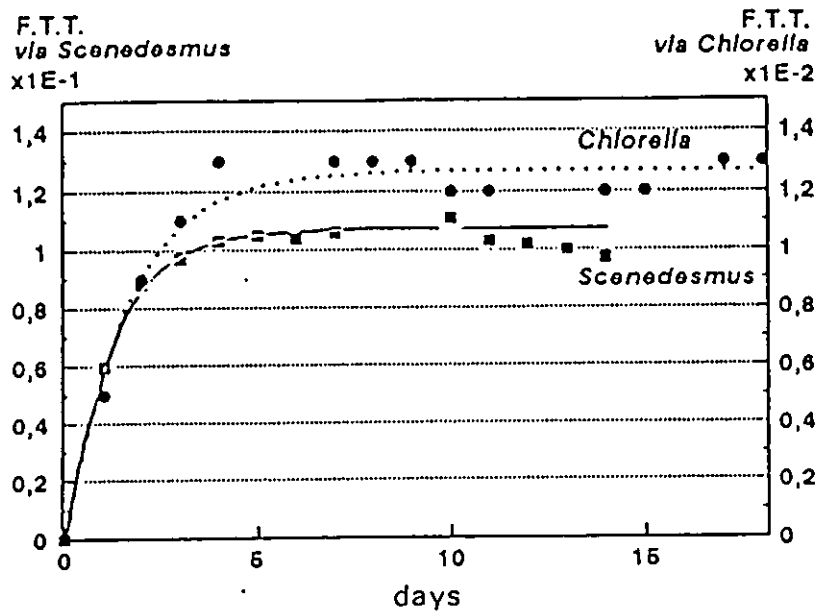*Fig 5 : transfer of ^{106}Ru from water to daphnids (accumulation and depuration).*

Fig 6 : transfert du [106]Ru des algues contaminées aux daphnies

Fig 6 : transfer of [106]Ru from algae to daphnids

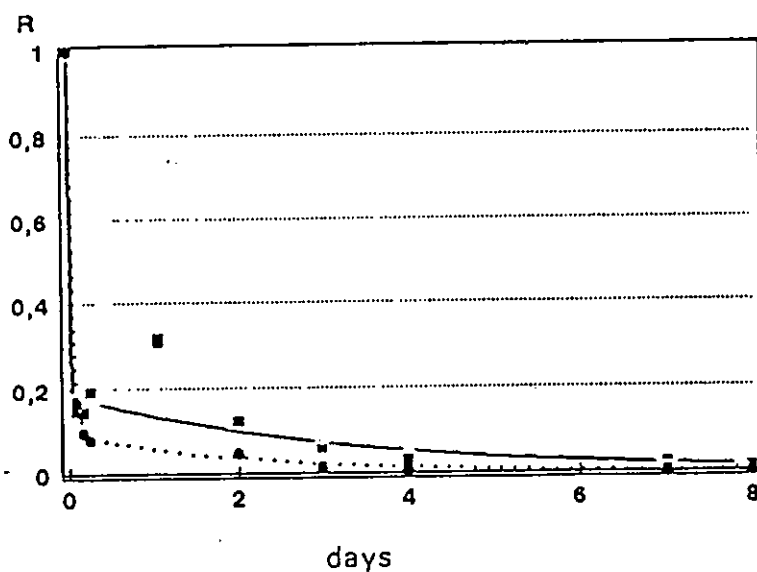

Fig 7 : élimination du [106]Ru des daphies aprés leur contamination par la nourriture

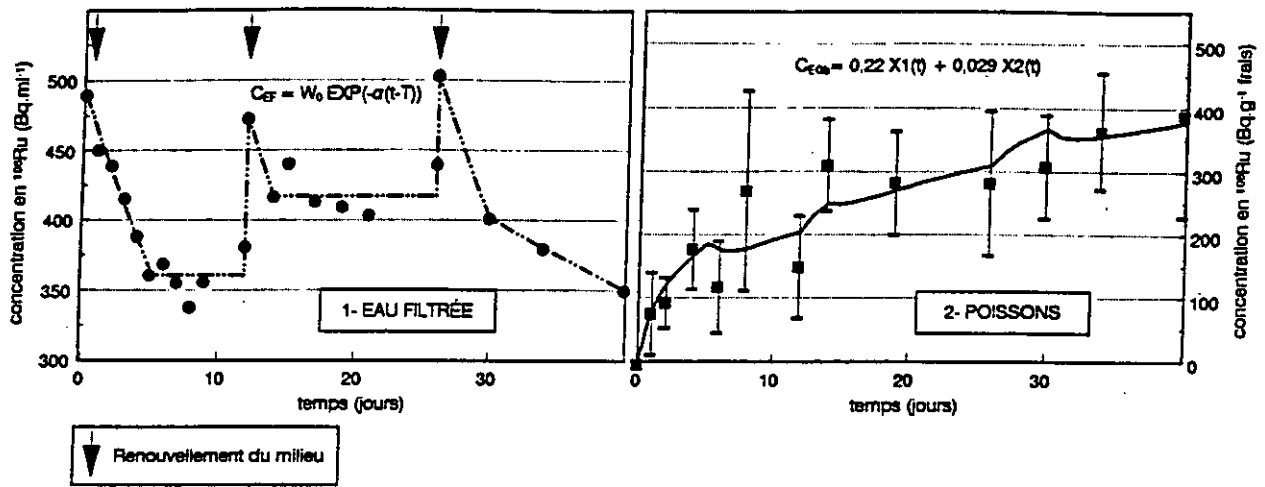*Fig 7 : depuration of daphnids after their contamination with food*

Fig 8 : transfert du ^{106}Ru de l'eau aux gambusies

Fig 8 : transfer of ^{106}Ru from water to gambusiae

Fig 9.: élimination du ^{106}Ru par les gambusies

Fig 9 : depuration of ^{106}Ru from gambusiae
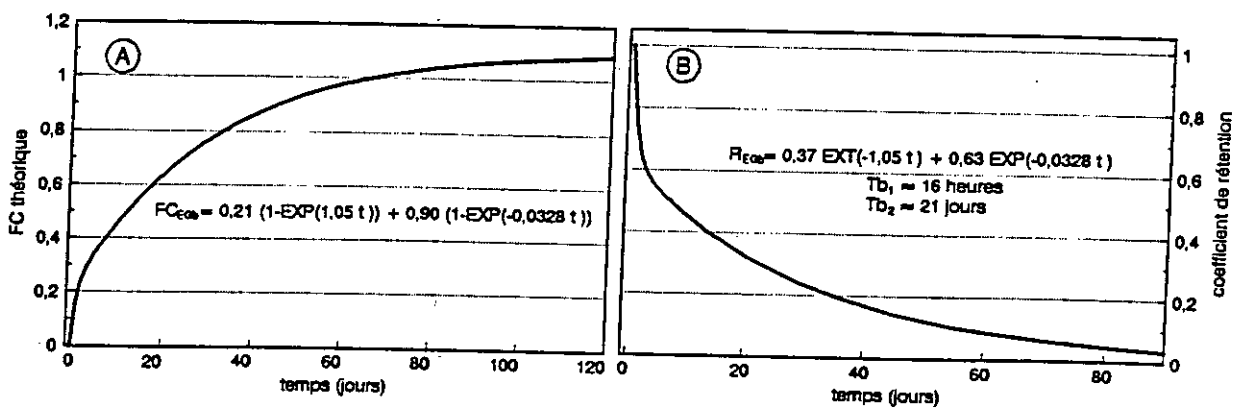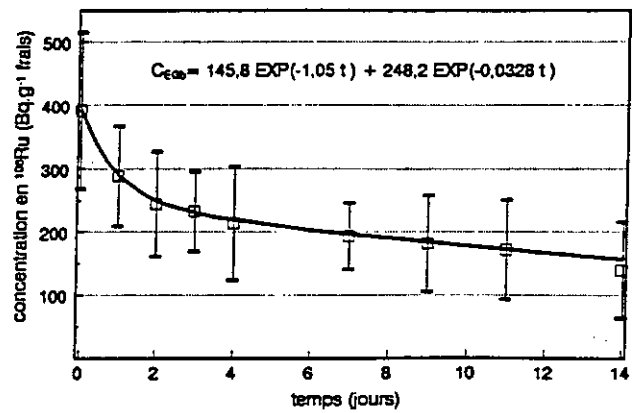

Fig 10 : simulation de l'évolution du facteur de concentration (FC) du ^{106}Ru par des gambusies pour une concentration dans l'eau stable (A) et rétention du radionucléide à l'arrêt de la contamination (B).

Fig 10 : simulation of gambusiae ^{106}Ru concentration factor evolution for a constant water concentration (A) and retention of nuclide in fish after contamination (B)
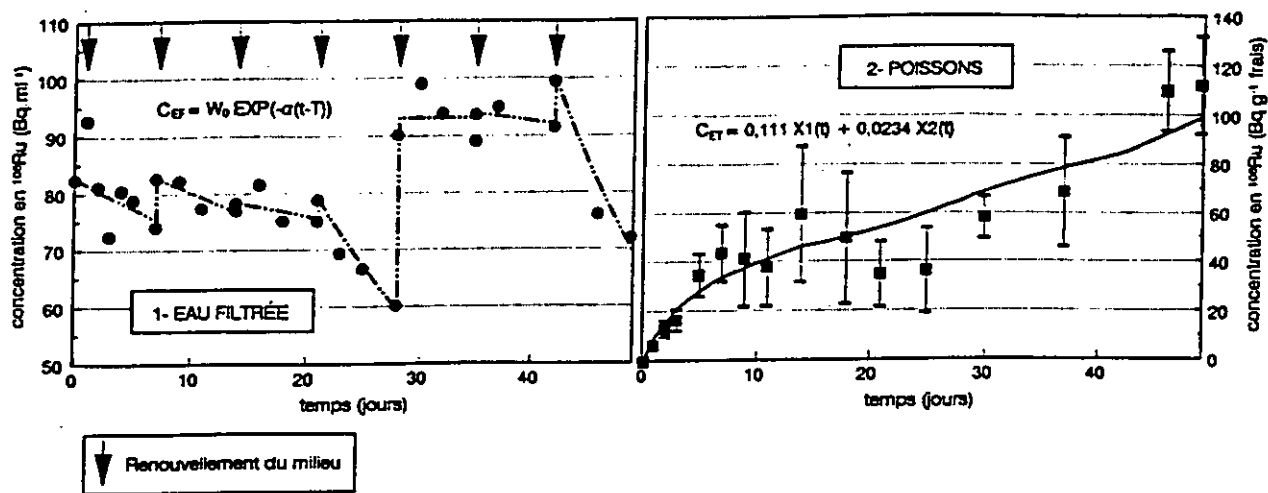
Fig. 11 : transfert du ^{106}Ru de l'eau aux truites

Fig. 11 : transfert of ^{106}Ru from water to trouts
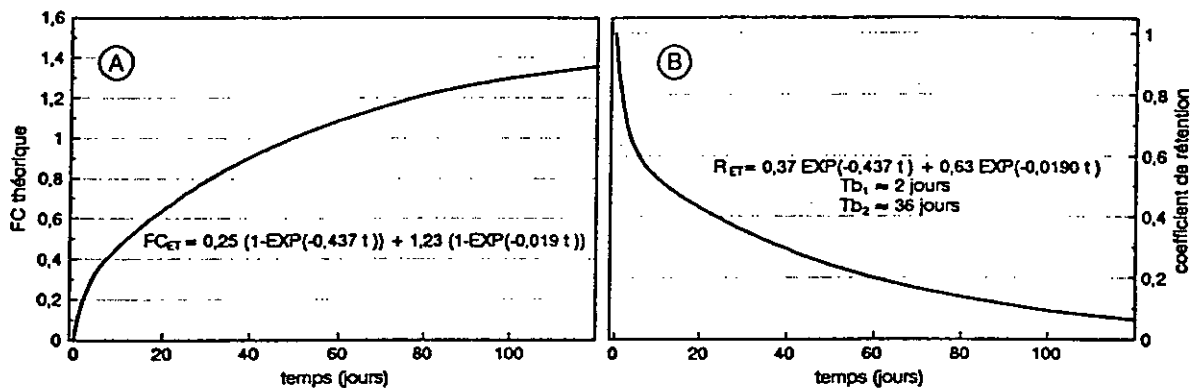
Fig. 12 : Simulation de l'évolution du facteur de concentration (FC) du ^{106}Ru par la truite pour une concentration dans l'eau constante (A) Rétention du radionucléide à l'arrêt de la contamination (B)

Fig. 12 : Simulation of ^{106}Ru concentration factor (CF) evolution for trout in a steady water concentration (A). Retention of the nuclide when contamination stops (B)..
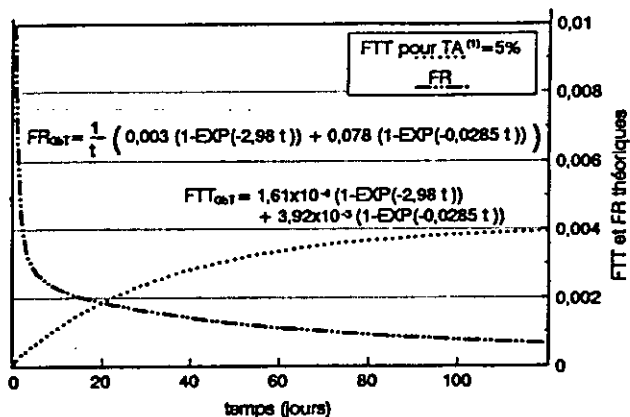
Fig. 13. Simulation de l'évolution du facteur de transfert trophique (FTT) et de rétention (FR) du ^{106}Ru à la truite liés à l'ingestion de gambusies contaminées.

Fig. 13. Simulation of trophic transfer factor (TTF) and retention factor (RF) of ^{106}Ru for trout ingesting contaminated gambusiae.

II. Objectives

The main objective of this project is to study the role of particulate phase of a spring river in the transport of radiocaesium. In particular the study was focused on the distribution of radionuclides between solid and liquid phases because this is one of the most important parameters involved in the migration and fate of radionuclides in surface waters.

The experimental activities were carried out on a spring river (Stella river) located in the Friuli-Venezia Giulia region (north-eastern part of Italy). This site was selected because during our researches in the earlier EC contract, relatively high caesium concentration was observed in the sediments at the Stella mouth and this fact seemed to be in contrast with the regimen of the river (spring river) [1]. In fact the solid solid flow of this river has been always considered scarce owing to its spring characteristics. For this reason time series of solid measurement are lacking.

III. Progress achieved including publications

In the Friuli Plain, all the rivers with a mountain drainage basin loose their water discharge after a few kilometres due to the gravelly deposits of the high plain. Downwards the spring-line, in low plain characterized by sandy and silty deposits, rivers receive waters from ground-water table. Only during main floods, particularly in spring and autumn, waters flow all along the river-bed, from mountain area to the sea.

The Stella river (47 Km length) is the most important river flowing into the Lignano basin, the westernmost basin of the Marano lagoon. Its source is formed by a large number of springs located southward the spring-line.

The Stella river slighty erodes the silty-clayed soils of the plain, producing a wide and flat depression, recognizable as far as the lagoon border.

From 1926 until 1950, an average annual discharge of 33.6 m^3 s^{-1}, was calculated. A similar value (32.6 m^3 s^{-1}) was provided during the 1966-1974 period. The monthly average discharge of Stella is quite regular through the year: the minimum value seldom falls under 25 m^3 s^{-1}, while the maximum value is about three folds the average discharge.

By examining and comparing the daily discharge with the rainfall data, it can be noted that the former increases for one or two days after heavy rains (over 25 mm), owing to a rapid drainage.

In order to provide a complete set of enviromental data to characterize such a complex environment, different field activities where carried out from 1992 to 1994.

To assess the exchange processes between river and lagoon environment, the total suspended matter concentrations were measured by filtering 1 dm^3 of water, sampled by means of a Niskin bottle, on a Whatman GF/F fibreglass filter (0.8 μm pore size, 47 mm filter diameter). Elemental particulate organic carbon and nitrogen analyses were performed by combustion in pure oxigen atmosphere, using helium as entrainer by means of a Perkin Elmer 2400 CHN Elemental Analyzer.

The grain-size analyses of the suspended matter were performed by means of a Coulter Multisizer Analyzer, with an orifice tube of 140 µm.

The mineralogical composition was performed on a Siemens D 500 diffractometer, using CuKα radiation; scanning interval ranged between 2° and 35° of 2 Θ, pitch 0.1°, 2 seconds of computation per pitch. Quali-quantitative computation of the mineralogical phases were done using the diffractogram height of peaks.

Samplings of water and suspended matter for radiocaesium determination were carried out at the same depth (about 1 m from water surface) using two device capable of performing size fractionation of suspended solids using cartridge filters of 40, 10 and 0.45 µm porosity and filtering large amount of water (more than 500 dm^3). Each system was equipped with resin columns (ammonium exocyanocobaltferrate, NCFN) to fix radiocaesium dissolved in water. To determine the efficiency of the resins, two resins columns (diameter of 20 mm and height of 160 and 80 mm respectively) connected in series were used. ^{137}Cs concentrations were determined in samples by gamma-spectrometry using high purity Germanium detectors (HPGe).

Results

The mean grain size distribution of the total suspended material concentrations in the Stella river, from 1985 to 1993, show that the most frequent concentrations range between 5-10 mg dm^{-3}; whereas concentrations between 10 and 30 mg dm^{-3} are observed in more than one third of cases. Concentrations higher than 60 mg dm^{-3}, measured only during flood tide, can be considered exceptional.

The following table reports the mean elemental particulate organic carbon and nitrogen content on suspended particles performed by means of a Perkin Elmer 2400 CHN Elemental Analyzer on samples collected during the contract period.

	µg/l	sd
C (n=5)	436	43
N (n=5)	43	12
C/N (mol) (n=5)	12.4	3

The average mineralogical composition of the Stella river suspended material results as follows (in percent): calcite (14 ± 3), dolomite (50 ± 9), quartz (18 ± 10), feldspar (3 ± 1), illite (7 ± 4), kaolinite (2 ± 2), clorite (6 ± 3).

Dolomite is the most important mineral, followed by quartz and calcite. The sum of clay mineral percentages can reach 15 %; illite and chlorite content are almost equal, kaolinite is lower. Montmorillonite or other expandable clay minerals were not detected.

Following are reported the values of the main ions measued in the water of the Stella river.

Ca (mg/l)	Mg (mg/l)	K (mg/l)
70.3	24.6	0.94

In the following table are given the mean "in situ" Kd values for suspended material from the Stella river measured from 1992 to 1994. The partitioning of ^{137}Cs between soluble and particulate phases is here defined as the ratio of ^{137}Cs sorbed in the particulate phase to the concentration of this radionuclide in solution.

The table reports the mean ^{137}Cs Kd evaluated for the the different grain size of suspended particles and the totat Kd (40+10+0.45 µm) assessed considering the ^{137}Cs concentrations in the different fractions of suspended particles as follows:

$$\text{Total Kd}_{(40+10+0.45\mu m)} = [(\Sigma\, C_i\, a_i) \cdot (\Sigma a_i)^{-1}] - C^{-1}_{water}$$

where C_i is the ^{137}Cs concentration in suspended particles with size i;
a_i is the concentration of this size of particles in water and
C_{water} represents the ^{137}Cs dissolved in water.

Filter Size µm	Mean ^{137}Cs Kd l/g	Coefficient of Variation %
40 (n=5)	151±29	19
10 (n=5)	169±51	30
0.45 (n=5)	243±73	30
(40+10+0.45)	166±36	22
0.45 (n=12)	151±51	34

In the same table is reported the mean value of the total ^{137}Cs "in situ" Kd evaluated filtering the water only with 0.45 µm size filter.

Discussion and conclusions

The data of elemental particulate organic carbon and nitrogen content on suspended particles allow to define the relations between the suspended material and the surrounding environment (predominance of the detrital component over the living one).

Molar ratios of C/N less than 5 indicate that metabolic phenomena are established due to the presence of bacteria responsible of a more rapid degradation of the organic carbon. Values ranging around 6 are characteristics of living phytoplanktonic communities. Higher C/N values are found when the organic detrital component are prevailing over the living component, or when there is a remarkable contribution of eroded material. The suspended material collected in the Stella river shows a C/N mean value of 12.4±3 and indicates the presence of material derived from erosion processes.

The ^{137}Cs concentration in the water of the Stella river was quite uniform from 1992 to 1994, since it ranged between 4.1×10^{-4} and 12.0×10^{-4} with a mean of 8×10^{-4} Bq l^{-1}. A low variability it is also observed in the ^{137}Cs concentrations measured in the suspended material collected in the same period.

The ^{137}Cs "in situ" Kd values evaluated for the different grain size of suspended particles show higher values for the grain collected on filter of 0.45μm size. The values are higher (about one order of magnitude) if compared with measurements carried out by other Authors [2] in laboratory experiments. Our values could be explained considering the presence of significant concentrations of clay minerals (about 15 %) in particles transported by the Stella river. The Stella river in fact slighty erodes the silty-clayed soils of the plain located southward the spring-line. The high Kd values could be attributable to the aging effect of Chernobyl caesium. In this case, the long time elapsed from deposition has as result a partially irreversible binding of radiocaesium in the clay minerals. The high ^{137}Cs Kd values are also in agreement with the low amount of K^+ found in the water of the Stella river (0.94 mg/l).

The total ^{137}Cs Kd (40+10+0.45 μm) assessed considering the ^{137}Cs concentrations in the different fractions of suspended particles (166±36 l/g) and the mean value of the total "in situ" ^{137}Cs Kd evaluated filtering the water only with 0.45 μm size filter (151±51l/g) are in agreement. This confirm, that the devices developed by ANPA to perform size fractionation of suspended particles on large amount of water, do not influence, with regards to radiocaesium, the distribution between liquid and solid phases.

Finally, combining the average suspended matter concentration with the average annual discharge of the Stella river, it is possible to evaluate the amount of suspended material and ^{137}Cs transported into the lagoon. Assuming a mean concentration of suspended matter of 10 mg dm^{-3}, the corresponding annual amount cannot be lower than 10000 ton y^{-1}, leading to an input of 10^8 Bq y^{-1} of ^{137}Cs discharged into the lagoon. In contrast with the regimen of the Stella river (spring river), the transport of suspended material cannot be considered negligible. The relatively high radiocaesium concentration found in the sediments at the mouth of the river is attributable to the continuous deposition of materials eroded from the silty-clayed soils of the plain.

References

M. Belli, E. Colizza, G.P. Fanzutti, F. Finocchiaro, R. Melis, R. Piani, U. Sansone (1994). The role of a spring river as source of radiocaesium in a lagoonal environment: the case of Stella river (Marano lagoon, Northern Adriatic Sea). Presented at the "International Seminar on Freshwater and Estuarine Radioecology", Lisbon, 21-25 March 1994.

P. Benes, M. Cernik, P. Lam Ramos. (1992). Factors affecting interaction of radiocaesium with freshwater solids. Jour. of radioch. and nuclear chem., 159, 2. 201-218.

Head of project 7: Dr. Blust

II. Objectives:

Development of mechanistic concepts and models for radionuclide uptake in aquatic organisms based upon a fundamental appreciation of chemical and biological processes. The research focused on the effect of environmental conditions on the uptake of radiocaesium and cobalt using the carp, *Cyprinus carpio* as a model organism. The results obtained have been used to construct a pharmacokinetic model for radionuclide uptake by aquatic organisms that can be used to predict the effect of changes in water composition and radionuclide speciation on accumulation kinetics.

III. Progress achieved including publications:

Radionuclide speciation analysis and modelling

In aquatic systems, radionuclides do not occur as single entities, but as a set of different chemical species distributed among soluble, colloidal and solid reservoirs. The biological availability of a radionuclide is largely determined by the chemical speciation of the metal in the environment. Since the speciation of a radionuclide is one of the most important factors to consider when assessing the environmental impact of a radionuclide, it is evident that accurate assessment requires knowledge of both its concentration and speciation. While methods to measure concentrations are well established, methods for speciation analysis are still being developed. .

The speciation of radionuclides in solutions strongly depends on the composition of the water. Inorganic species such as chloride, carbonate and phosphate that can interact with metals are easily measured and their interactions with the metals characterised. Organic ligands, however, present a different situation. They occur in an almost infinite variety and can interact with the metals in a multitude of fashions. Natural sources contribute the bulk of the organic matter present in most surface waters. Humic and fulvic acids, which are important complexing agents for metals, constitute the majority of the organic matter.

The speciation of a metal in solution is represented most simply by a set of equilibrium expressions, ($M+nL=ML_n$ and $K=[ML_n]/[M][L]^n$). A number of values are needed to characterise these relationships. The concentration of the metal ions, the concentrations of the ligand, the stoichiometry of the reactions and the corresponding stability constant. The concentration of the free ligand in the solution is referred to as the complexation capacity. For multi-ligand systems the measured stability constant will not be that for a single ligand but an average value which is the result of the overall extent of complexation. The measured stability constant is actually a conditional stability constant. That is, the constant is measured under a set of limiting conditions (hardness, temperature, hydrogen ion activity), which makes the value different from the thermodynamic stability constant. The thermodynamic stability constant can be calculated provided that the dependence of the equilibria on the conditions are known.

One of the most promising methods for chemical speciation are metal-ligand competition solvent extraction equilibration procedures. The extent of complexation of the metal depends on the concentration of the ligands normally present in the system and an added ligand used as a competitor. The competitor forms complexes with the radionuclides which partition between the aqueous and organic phase. If the partitioning of the radionuclide between the aqueous and organic phase is measured at different metal and competitor concentrations, then the stability constants and concentrations of the natural ligand can be calculated. The technique is based on the thermodynamic rather than the kinetic properties of the reactions considered. The method is thermodynamically well characterised and involves a minimum of operationally defined conditions. The results of these measurements have been used as input in a newly developed chemical speciation model to calculate the chemical speciation of radionuclides in aquatic systems (SOLUTION).

Pharmacokinetics of radionuclide uptake by fish

The design of most radionuclide uptake and elimination experiments with aquatic organisms assumes constant exposure regimes. Constancy of exposure greatly simplifies analysis of uptake kinetics and enables simple estimation of steady state concentrations. However, constant exposures are rare in the real world and often difficult to realise in the laboratory. Clearance constant-based pharmacokinetic models are unique in that model parameters represent discrete physiological processes, i.e. absorption, metabolism, excretion, whereas model parameters in the more conventional rate constant-based models can be a function of more than one physiological process. Thus, it is possible to gain insight into absorption rate-limiting processes from the magnitude of the absorption clearance constant. Additionally, the model-predicted pharmacokinetic parameters can be used to make predictions regarding the bioconcentration factor and the expected concentration in the fish at steady state.

Pharamacokinetic analysis indicated that in the most simple form the fish could be treated as a one-compartment open model for uptake of radionuclides with changes in the rate of radionuclide uptake by complexation and loss to container walls (see appendix). The models developed can be used to analyse data involving non-constant exposure to radionuclides in natural environments. In more complex situations a two compartment model should be used but the principals are the same. The clearance of radionuclides depends on a number of factors which can be related to 1) the concentration and chemical speciation of the radionuclide in the water and other sources and 2) the kinetics and selectivity of the transport systems involved in the uptake and elimination of the radionuclide by the organism. A convenient model to describe these effects and incorporate them in the pharmacokinetic model is the Michaelis-Menten model for enzyme kinetics. Instead of a single parameter describing clearance two parameters are required, Clearance=$V_{max}/(K_m+S)$ in which S is the concentration of the radionuclide in the environment and V_{max} and K_m are the maximal uptake rate and K_m is the dissociation constant.

The uptake of radionuclides is a mediated process in which the radionuclide interacts with the transport systems to form a temporary association. In its most simple form this process can be presented by the following model:

$$S_{out} + T \overset{k_1}{\underset{k_{-1}}{\Longleftrightarrow}} ST \overset{k_2}{\longrightarrow} T + S_{in}$$
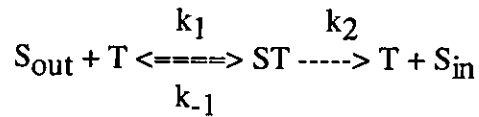
Where k_1 and k_{-1} are the rate constant for the forward and reverse complex formation reactions and k_2 the rate constant of the irreversible translocation reaction. The kinetics of the uptake process can be described by the Michaelis-Menten equation:

$$V = V_{max} * S / (K_M + S) \text{ with } K_M = (k_{-1} + k_2) / k_1$$

where Vmax is the maximum uptake rate, S the radionuclide concentration, and K_M the half-saturation constant. This is the concentration of the radionuclide at which $V = 1/2 Vmax$. When the concentration of the radionuclide is small relative to K_M then the transport kinetics are first order:

$$V = V_{max} * S / K_M$$

Values of Vmax and K_M have been determined by measuring uptake rate for carps exposed to a wide range of caesium and cobalt concentrations. The concentration of potassium in freshwater environments is a critical factor determining the uptake of ^{137}Cs by aquatic organisms. The uptake of caesium decreases with increasing potassium concentration in the water, which results from the competition of potassium and caesium for the same transport system. Similar interactions account for the effect of calcium on cobalt uptake. These interactions can be described by a competitive inhibition model:

$$V = V_{max} * S / (K_M * (1 + i/K_i (+S)))$$

where K_M is the Michaelis constant of the uninhibited process and K_i is the dissociation constant of the inhibitor-transporter complex. The effect of a competitive inhibitor is therefore to decrease the apparent affinity of the radionuclide for the transporter. The latter equation substitutes for the uptake rate (k_1) in the kinetic model for radionuclide accumulation. This results in a new model that accounts for changes in water composition on radionuclide uptake.

The effect of organic complexation on the uptake of cobalt by carps has been studied in chemically defined environments with ligands of different thermodynamic stability. Complexation decreases the uptake of the radionuclide which is in agreement with the general view that the availability of metals to aquatic organisms depends on the activity of the free metal ion in the solution. There is no evidence that the direct uptake of complexes is of any significance. This means that the effect of chemical speciation on the uptake of cobalt from the water can be described by one single variable, the free metal ion activity in the solution. This means that radionuclide uptake does not depend on the concentration of the radionuclide in the water but on the activity of the radionulide species that are taken up by the organisms, i.e. the free metal ion.

A clear decrease in cobalt uptake was also observed with increasing calcium concentrations, but not with magnesium concentrations is observed. The effect of calcium in the water of acclimation is significant but much less than the direct effect of calcium in the exposure water. Since uptake kinetics of both cobalt and calcium show similar results for influx in body, gills and blood, and both elements inhibit each others uptake, the effect of calcium on cobalt uptake is due to a direct interaction at the membrane translocation system. An increase in ionic strength reduces cobalt uptake and this effect is fully explained by the effect of ionic strength on the activity coefficient of the free metal ion.

As an illustration the pharmacokinetic model for the uptake of radionuclides by carp has been used to model the accumulation of caesium and cobalt by carp in different potassium and calcium regimes, respectively (Fig 1-4). In the examples given the concentrations of the radionuclides in food have been fixed to better show the effect of water composition on the relative importance of water and food in radionuclide uptake. In the natural environment however this will not be the case and food contamination will also change with exposure conditions. As expected the model for caesium predicts that the uptake of caesium from water is of minor importance and only becomes a potential concern in very low potassium regimes. For cobalt the situation is more complex, since both water and food are important sources of the radionuclide, water being the main source in soft waters and food the main source in hard waters. In general these models explain more than 90 % of the variation observed under experimental conditions.

Conclusions

The research on the effects of environmental conditions on the uptake of radionuclides by carp has cumulated in the construction of a general mechanistic model for the accumulation of radionuclides in aquatic organisms. The key feature is the linkage of a chemical speciation model to a model for the transport of radionuclides across biological interfaces. As such it has been proved possible to model the effect of changes in the ionic composition and complexation capacity of the environment on the accumulation of radionuclides by biota. The models are much more robust than the ones being used today to predict the fate of radionuclides in aquatic ecosystems since processes are described in terms of mechanisms rather than correlations. The research has also identified many major gaps in the fundamental understanding of radionuclide accumulation in food chains. In general there is a lack of good quality data which can be used to construct mechanistic models for the effect of environmental conditons on radionuclide transfer. The major problem which remains is the lack of information on the uptake of radionuclides at lower trophic levels, especially invertebrates, which make it difficult to model the concentration of radionuclides in the food of predators in a variable environment.

Publications

Comhaire, S., Blust, R., Van Ginneken, L., Vanderborght, O. 1994. Cobalt uptake across the gills of the common carp, *Cyprinus carpio*, as a function of calcium concentration in the water of acclimation and exposure. Comparative Biochemistry and Physiology, 1, 63-76.

Van Ginneken, L. and Blust, R. 1995. Sequential determination of a combined gamma/beta and pure beta emitter by gamma and liquid scintillation counting: application to the transport of metals across fish gills. Analytical Biochemistry, 224, 92-99.

Comhaire, S. Blust, R. Van Ginneken, L., D'Haeseleer, F., Vanderborght, O. Environmental calcium influences radio-cobalt uptake by the common carp, *Cyprinus carpio*. Science of the Total Environment, In Press.

Blust, R., Van Ginneken, L., Comhaire, S. Vanderborght, O. Uptake of radio-cobalt by the common carp, *Cyprinus carpio* in complexing environments. Science of the Total Environment, In Press.

Comhaire, S., Blust, R., Van Ginneken, L., Verbost, P., Vanderborght, O. Branchial uptake by the carp, *Cyprinus carpio*: Partial involvement of the calcium uptake system. Journal of Experimental Biology, Submitted.

Comhaire, S., Blust, R., Vanderborght, O. Branchial cobalt uptake is competitively inhibited by waterborne calcium in carp. Journal of Experimental Biology, Submitted.

Blust, R., Comhaire, S, Van Ginneken, L.. A Michaelis-Menten pharmacokinetic model for the accumulation of cobalt by carp. Environmental Chemistry and Toxicology, Submitted

Fig 1: Accumulation of ^{137}Cs by carp from solution and food in a 0.01 mM K$^+$ environent. The water contains 1Bq.l^{-1} and the food 100 Bq.kg^{-1} of ^{137}Cs. The food ration equals 5 % of the body weight per day.
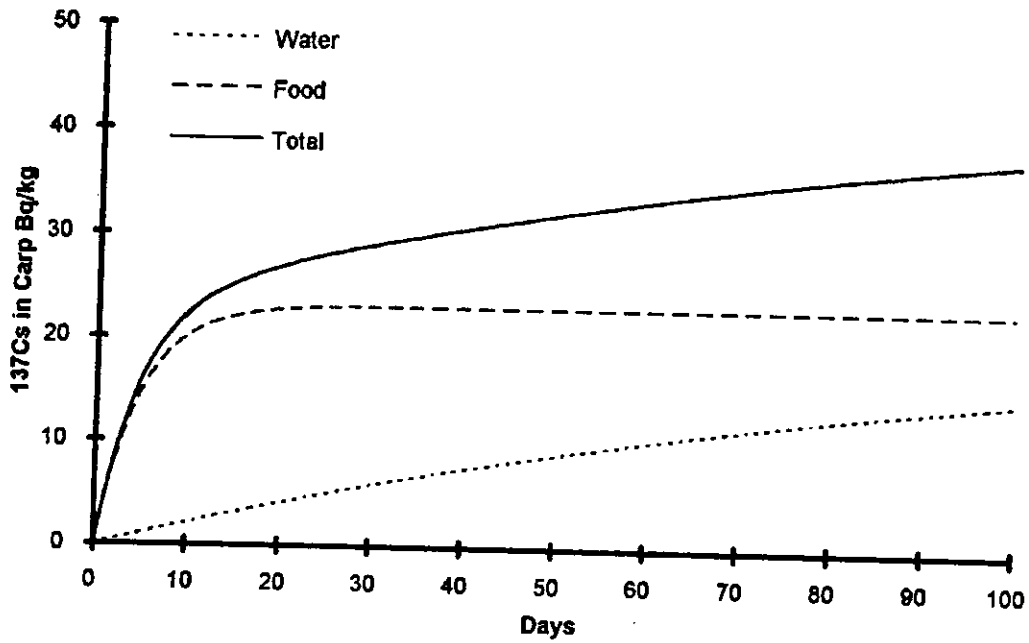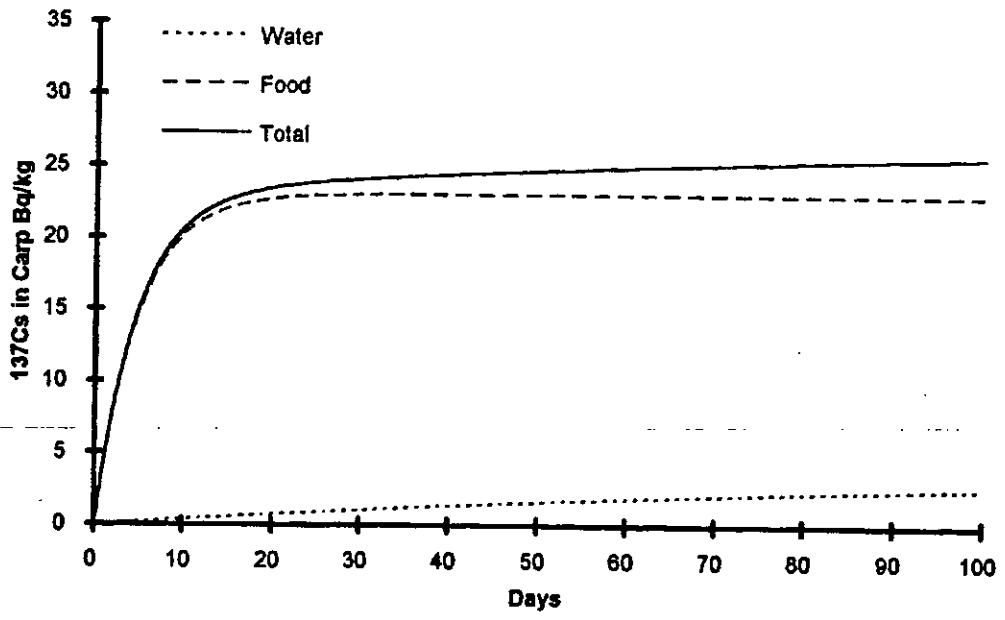

Fig 2: Accumulation of ^{137}Cs by carp from solution and food in a 0.1 mM K$^+$ environent. The water contains 1Bq.l^{-1} and the food 100 Bq.kg^{-1} of ^{137}Cs. The food ration equals 5 % of the body weight per day.

Fig 3: Accumulation of ^{60}Co by carp from solution and food in a 0.1 mM Ca^{2+} environent. The water contains 0.1Bq.l^{-1} and the food 100 Bq.kg^{-1} of ^{137}Cs. The food ration equals 5 % of the body weight per day.

Fig 4: Accumulation of ^{60}Co by carp from solution and food in a 1 mM Ca^{2+} environent. The water contains 0.1Bq.l^{-1} and the food 100 Bq.kg^{-1} of ^{137}Cs. The food ration equals 5 % of the body weight per day.

Appendix:

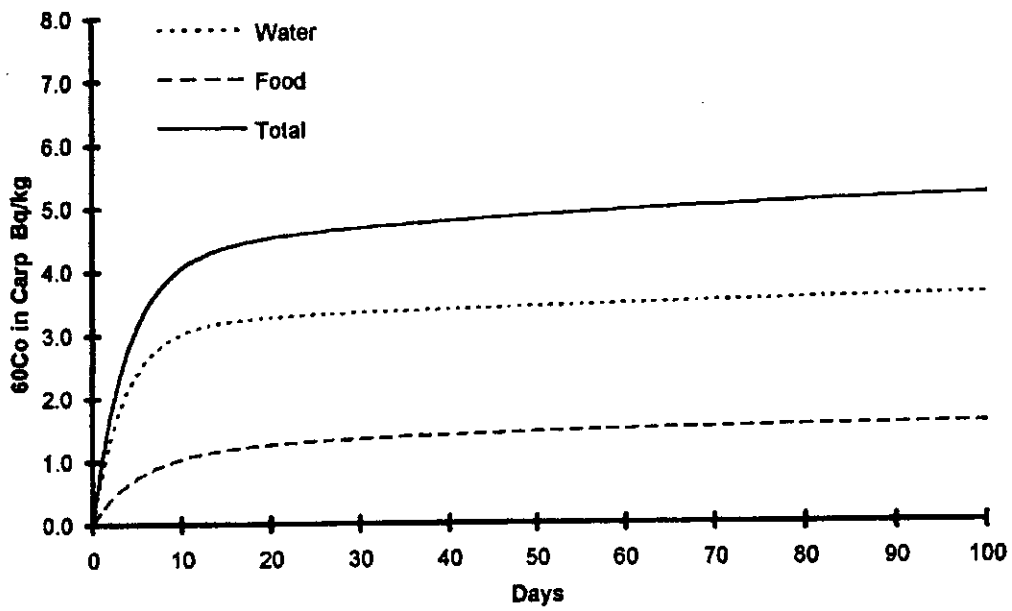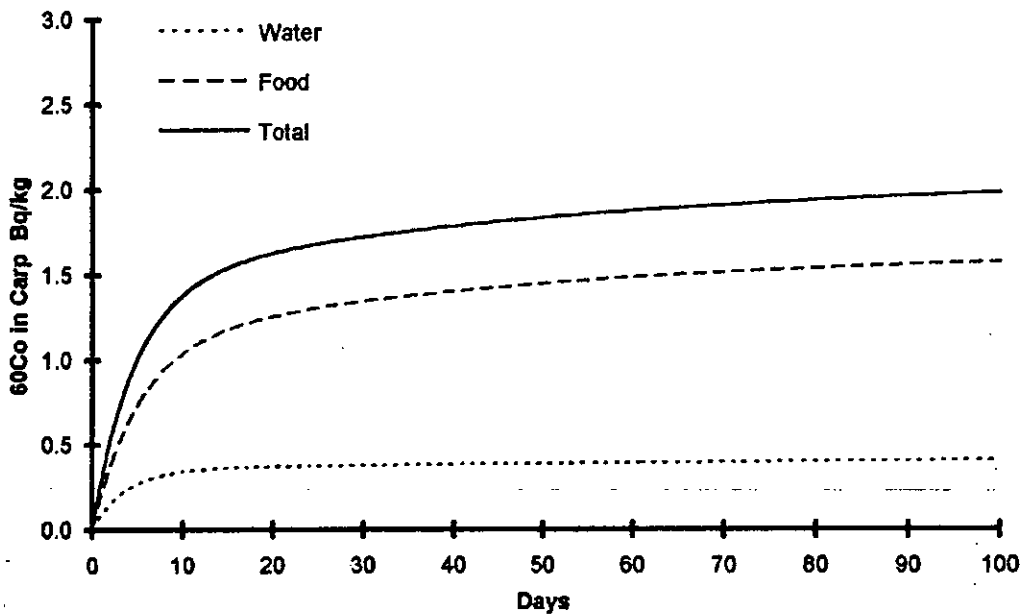One-compartment open model for uptake of radionuclide by fish with loss to container walls.

Rate of change in the amount of radionuclide in the fish

$$dX_f/dt = CL_a(C_w - C_f) \qquad (1)$$

CL_a = absorption clearance constant

C_w = concentration of radionuclide in water

C_f = concentration of radionuclide in body water of the fish

The apparent volume of distribution (V_d), is the proportionality constant that relates the amount of radionuclide in the body to its concentration in the body water of the fish.

$$dX_f/dt = CL_a(C_w - X_f/V_d) \qquad (2)$$

Rate of change in the concentration of radionuclide in water:

$$dC_w/dt = (CL_a \cdot FW/V_0) \cdot [(X_f/V_d) - C_w] - (k_1 \cdot C_w) \qquad (3)$$

FW = mean fish weight

V_0 = volume of water in tank.

Integration of (2) and (3) gives:

$$X_f = [(CL_a \cdot C_w^0)/(\beta - \alpha)]e^{-\alpha t} + [(CL_a \cdot C_w^0/(\alpha - \beta)]e^{-\beta t} \qquad (4)$$

$$C_w = [C_w^0((CL_a/V_d) - \alpha)/(\beta - \alpha)]e^{-\alpha t} + [C_w^0((CL_a/V_d) - \beta)/(\alpha - \beta)]e^{-\beta t} \qquad (5)$$

C_w^0 is the initial concentration in water.

α and β are hybrid rate constants that are defined in terms of model parameters.

$$\alpha + \beta = CL_a/V_d + (CL_a \cdot FW)/V_0 + k_1 = x \qquad (6)$$

$$\alpha \cdot \beta = (CL_a \cdot k_1)/V_d = y \qquad (7)$$

Equations (4) and (5) are fitted simultaneously to the experimental data to obtain values for the model parameters CL_a, V_d and k_1. Estimates for the hybrid rate constants were obtained as secundary parameters by using the quadratic solution to: $\alpha^2 - x\alpha + y = 0$

Input required to model the system:

C_w^0 is the initial concentration of radionuclide in water.

C_w is concentration of radionuclide in water at time t.

FW is mean fish weight.

V_0 is volume of water in tank.

X_f amount of radionuclide in fish.

t is time of incubation.

Head of project 8: Dr. Fernández

II. Objectives

The objective of this project was to study the mechanisms of uptake and accumulation of radiocesium in freshwater plants, taking *Riccia fluitans* as plant type. The initial hypothesis was to consider the mechanisms of transport and accumulation of potassium as the possible ways for transport and accumulation of radiocaesium in aquatic plants. Once these mechanisms were investigated, the influence of some selected environmental variables was studied in order to define the major control variables influencing the mentioned processes. The data obtained were used to define a mechanistic kinetic model that could be of general application in the most conspicuous freshwater plants. Finally the kinetic parameters obtained were integrated in a general mathematical model to predict the flow of radiocaesium through freshwater ecosystems.

III. Progress achieved including publications

Depending on the concentration of potassium in the environment, freshwater plants incorporate potassium in two different ways (Fernández et al., in press; Sanders et al, in prep.). Under potassium sufficiency (plants growing at an overall external potassium concentration around 0.1 mM), potassium is transported at plasmalemma level through potassium channels. This transport system is diffusive, the driving force being the electrochemical potential gradient for potassium at both sides of the membrane:

$$\Delta\mu_{K^+}/F = z \ (Em - E_N^{K^+}) \qquad \text{Eqn. 1}$$

where z is the charge of potassium, Em is the membrane potential, and $E_N^{K^+}$ is the Nernst potential for potassium.

The diffusive constant for such a transport is defined by the membrane permeability for potassium. This intrinsic membrane characteristic is roughly uniform for most freshwater plants, and is accounted for the abundance, activity and conductivity of the potassium channels in the plasmalemma. Potassium channels in plants are not perfectly selective for potassium (Bentrup, 1990). There is a series of positive monovalent ions that enters the cells through potassium channels. Ordered from the most permeable ion i.e. potassium, to the less permeable one, caesium, a general series for freshwater plants could be: $K^+ > Rb^+ > NH_4^+ > Na^+ > Li^+ > Cs^+$. Being the relative permeability of Cs^+ with respect to K^+ around 0.6 in the case of *R. fluitans* (Fernández et al. in press).
Under potassium deficiency (plants growing at an overall potassium concentration around 0.01 mM), *R. fluitans*, and probably most freshwater plants exhibit an active transport system for potassium (Sanders et al. in prep.). This system has higher affinity for potassium ($k_s = 25 \ \mu M$) and exhibits a Michaelis-Menten type uptake kinetic, compared with channel transport that exhibit, over the concentration range assayed, a lower affinity and a linear uptake kinetic. Cytoplasmic pH (pHc) measurements performed by using pH sensitive microelectrodes (for a complete description of this technic see Felle and Bertl, 1986), indicate that a transient acidification of pHc takes

place upon the addition of micromolar amounts of potassium or caesium (figure 1). These results suggest that potassium and caesium enter the cells in a proton cotransport, the driving force being the electrochemical gradient for protons. Such a gradient being generated by the operation of a proton pump present in the plasmalemma of green plants. As expected, this system does not work in the presence of inhibitors of dark respiration as CCCP, azide, cyanide, or in the presence of inhibitors of the proton pump as vanadate or eritrosine b.

Radiocaesium is transported by means of both mechanism. In the figure 2, the uptake kinetics for caesium in *R. fluitans* plants, submitted to potassium sufficiency (linear kinetic) and deficiency (Michaelis-Menten kinetic). The transport efficiency of the active system being ten times higher than the efficiency of the passive (diffusive) system. In addition both system exhibit a different capacity for radiocesium accumulation (figure 3). Channel transport, in plants submitted to potassium sufficiency, yields a CF for radiocesium of 51 ± 2 (n=8), in contrast, active system for potassium yields a CF for radiocesium of 1329 ± 128 (n=5).

Plants submodel.

Kinetic data obtained in the experiments mentioned above were used for building up a tentative mathematical model, to predict the CF for radiocesium in freshwater plant as a function of the most conspicuous variable affecting to the processes of radiocesium uptake and accumulation. Since caesium uses the same transport systems than potassium for entering the cells, uptake rate and CF for caesium are dramatically affected by the external concentration of potassium at two levels: instantaneous, because potassium compete with caesium for the transport system and the integrated effect of the overall external potassium concentration during the life of the plant.

For modelling purposes we assumed a threshold of 0.1 mM of external potassium concentration to define plants submitted to potassium sufficiency (plants living at potassium concentration equal or higher than 0.1 mM) and plants submitted to potassium deficiency (plants living at external potassium concentrations below 0.1 mM). This figure can be used as the threshold to predicting CF from the kinetic parameters obtained for the diffusive transport or from those obtained for the active transport of radiocaesium.

Potassium sufficiency

Under potassium sufficiency, radiocesium is accumulated in plants through potassium channels. The amount of caesium accumulated in the equilibrium, can be expressed as a millivoltage by using the Nernst equation,

$$E_N^{Cs} = RT/zF \cdot \ln Cs^+_o/Cs^+_i \qquad \text{Eqn 2.}$$

where R is the gas constant, T the absolute temperature, z the electrical charge of caesium, F the Faraday constant, Cs^+_o is the concentration of caesium in the water and Cs^+_i is the concentration of caesium inside the cells. Since Cs^+_i/Cs^+_o is the concentration factor (CF), equation 1 can be expressed as

$$E_N^{Cs} = RT/zF \cdot \ln CF^{-1} \qquad \text{Eqn 3.}$$

Caesium reaches equilibrium when the Nernst potential for caesium (E_N^{Cs}) equals the membrane potential (Em) thus, by knowing Em, and additionally the response of Em to some fundamental environmental variable, as the potassium concentration in the

water, it is possible to predict CF as a function of Em and additionally as a function of potassium concentration in the water.

For a well known freshwater green plant as *Riccia fluitans*, the relationship between Em and the external potassium concentration has been determined. This relationship can be defined by the equation,

$$Em = E_0 + p \, RT/F \cdot \ln K^+_w \qquad \text{Eqn 4.}$$

where E_0 is the membrane potential for a potassium concentration in the water of 1 mM, p is the selectivity of potassium channels for caesium over potassium, and for this plants takes the value 0.73, and K^+_w is the concentration of potassium in the water. The fitting of this equation to experimental data is $Em = -105 + 18.45 \ln K^+_w$ (r=0.98, n=23).

Since CF can be predicted from Em,

$$CF = 1 \, / \, EXP \, [\, EmzF \, / \, RT \,] \qquad \text{Eqn 5.}$$

and Em can be predicted, according to Eqn 4, from the potassium concentration in the water, it is possible to predict CF as a function of the concentration of potassium in the water,

$$CF = 1 \, / \, EXP \, [\, (E_0zF \, / \, RT) + p \ln K^+_w \qquad \text{Eqn 6.}$$

In the model, CF is assessed by equation 6 when plants are not under potassium deficiency, i.e. when plants grow at a potassium concentration in the water of 0.1 mM or higher. This equation reflects that under these conditions, the only transport mechanism operating in the membranes are potassium channels. Figure 4 shows the agreement between experimental figures (closed circles) for CF obtained for plants submitted to potassium sufficiency at different external potassium concentrations and the prediction of the model (line) based in the Nernst equation approach.

Potassium deficiency.

It is generally accepted that green freshwater plants are submitted to potassium deficiency when they grow under potassium concentrations in the water clearly below 0.1 mM. In these cases, potassium is incorporated actively by plant cells. The uptake mechanism proposed is a cotransport, in which the driving ions are either protons or sodium. These transport systems are also sensitive to caesium, but they exhibit an higher affinity and produce an higher CF than potassium channels. In this case, the uptake kinetic is a Michaelis-Menten type and the selectivity of the transport system is a function of the relative affinity of caesium over potassium for the carrier. Uptake rate (V) can be computed from

$$V = Vmax \cdot Cs_w \, / \, [\, Ks_{Cs} \cdot (1 + K^+_w \, / \, Ks_K)] + Cs_w \qquad \text{Eqn. 7}$$

where Vmax is the maximum rate of transport for caesium, Cs_w is the concentration (total) of caesium in the water, Ks_{Cs} is the half saturation constant for Cs^+ transport and Ks_K is the half saturation constant for potassium.

Elimination has been defined as a function of an average biological half life (BHL) for phytoplankton,

k elimination = ln 2 / BHL $\qquad$ Eqn 8

In the model, the change of the concentration of caesium in the plants (dC/dt) is,

$dC/dt = k$ uptake . Cs_w - k elimin . Cs_p $\qquad$ Eqn. 9

where k uptake is V times Cs_w and k elimin times Cs_p (the concentration of Cs^+ in the plants) is the elimination rate.
Concentration factor of these plants is computed as the concentration of caesium in the plants divided by the concentration of caesium in the water when the model reaches equilibrium. In the figure 5, it is shown a good agreement between experimental data obtained with plants submitted to potassium deficiency (closed circles) and the predicted values of CF as a function of the external potassium concentration (line) by using the kinetic parameters from the Michaelis-Menten approach.

Plants submodel has been developed in collaboration with Dr. Rudie Heling (KEMA, Holland) and integrated in more complex mathematical models used to predict the fate of radiocaesium in lakes of Europe in the VAMP program framework.

References

F.W. Bentrup.1990. Potassium ion channels in the plasmalemma. *Physiologia Plantarum*, 79:705-711.

Felle H. and A Bertl. 1986. The fabrication and use of H^+-selective liquid-membrane micro-electrodes for use in plant cells. *Journal of Experimental Botany*. 37(52): 1416-1428.

Fernández J.A., Heredia M.A., García-Sanchez M.J., Gil J.A., Vaz Carreiro M.C. and Diez de los Rios A. (1994). Mechanisms of radiocesium uptake and accumulation in *Riccia fluitans*. Proceedings of the International Seminar on Freshwater and Estuarine Radioecology. Lisbon. Portugal.

Sanders D., Corzo A. and Fernández J.A. Mechanism of potassium uptake in *Riccia fluitans* submitted to potassium deficiency. Submitted.
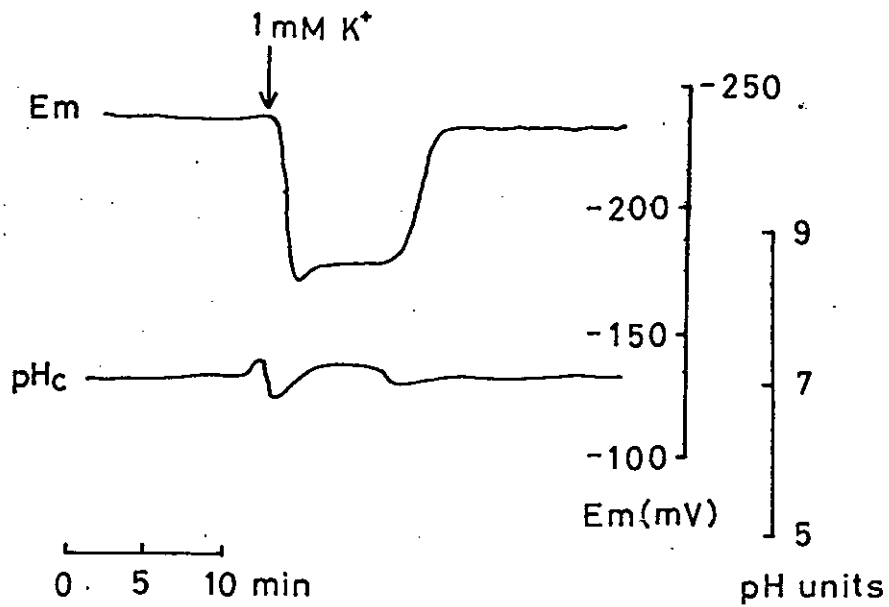
Figure 1.- Continuous recording of membrane potential (Em) and cytoplasmic pH (pHc) in cells of the aquatic liverwort *Riccia fluitans* submitted to potassium deficiency. Addition of 1 mM of KCl is marked by an arrow.
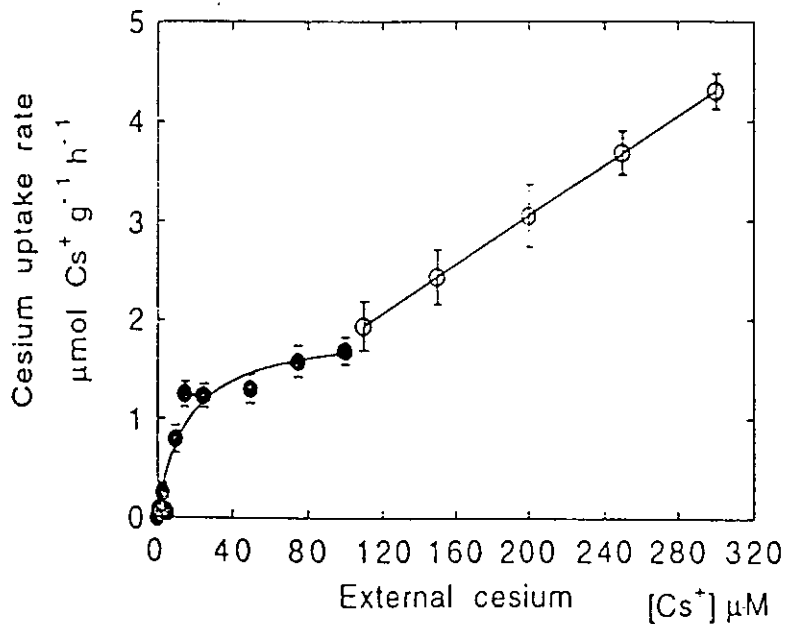
Figure 2.-Dual uptake kinetic of caesium as a function of the external total caesium concentration in *Riccia fluitans*, submitted to potassium deficiency (closed circles) and potassium sufficiency (open circles).
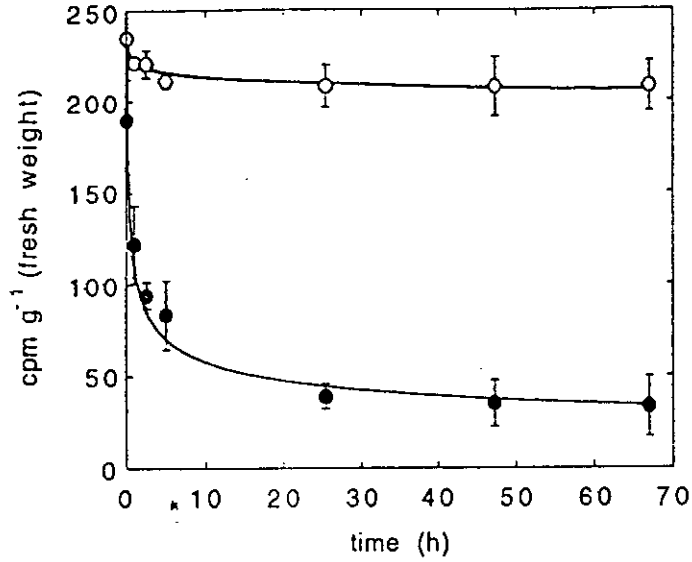
Figure 3.- Time course of the variation of radiocaesium activity in the water, corrected by the biomass of *Riccia fluitans* used in the experiments. Open and closed circles denote plants submitted to potassium sufficiency and deficiency respectively.
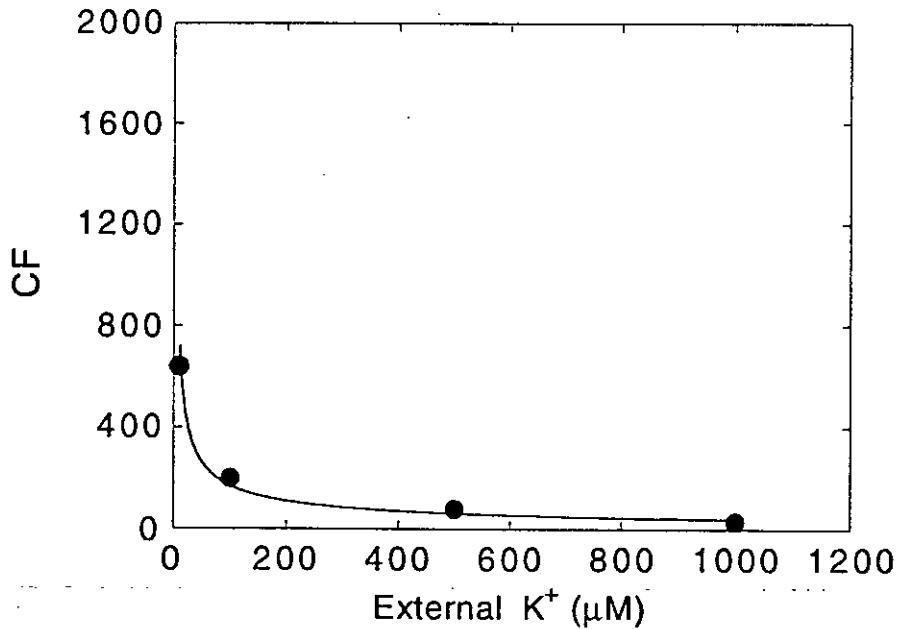
Figure 4.- Comparison between the values of concentration factor for radiocaesium (CF) obtained experimentally in plants submitted to potassium sufficiency (closed circles) with the values predicted by the Nernst equation as a function of the external potassium concentration (line).

Figure 5.- Comparison between the values of concentration factor for radiocaesium (CF) obtained experimentally in plants submitted to potassium deficiency (closed circles) with the values predicted by the Michaelis-Menten kinetic approach as a function of the external potassium concentration (line).

Head of project 10: Dr. R.N.J. Comans

II. Objectives for the reporting period

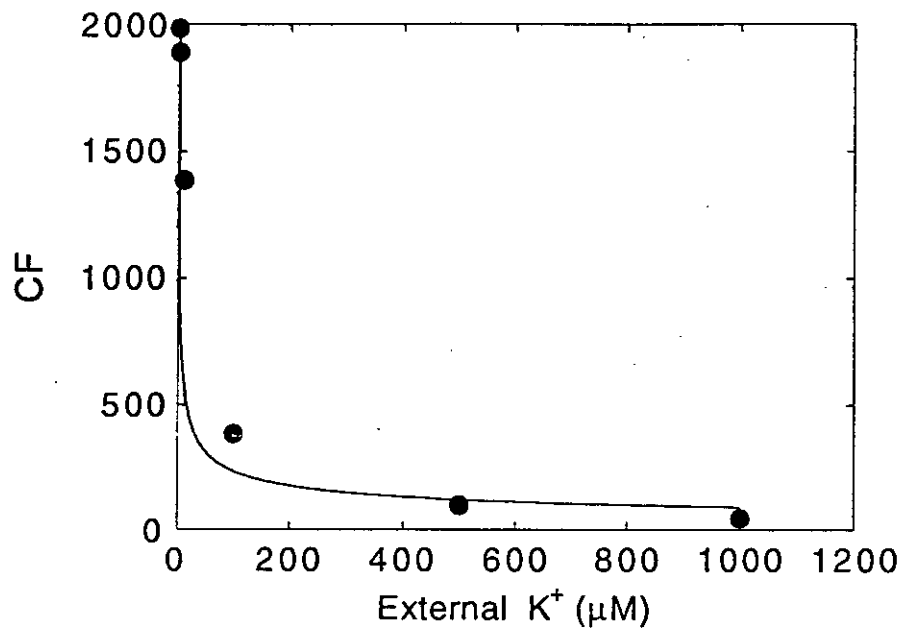1. To test the general validity of the *in-situ* $K_D(^{137}Cs)/NH_4^+$ ion-exchange relationship and its power to predict radiocaesium mobility in (and remobilisation from) freshwater sediments.
2. Determination of "exchangeable" *in-situ* radiocaesium-K_D's, in addition to "total" *in-situ* radiocaesium-K_D's, by multiple extraction of the sediment with NH_4^+-solutions and subsequent preconcentration/low-background measurement of the extracted-^{137}Cs.
3. Search for possibilities (method) to measure the reverse rate constants of radiocaesium sorption (remobilisation) on natural samples, to be included in kinetic models for radiocaesium sorption


III. Progress achieved including publications

Investigation of in-situ K_D-values for radiocaesium

Since the Chernobyl accident, it has become clear that the mobility of radiocaesium is controlled by a highly selective interaction with the frayed particle edges of illitic clay minerals (Cremers et al., 1988), and that competition for these binding sites by the high levels of ammonium in anoxic sediments may partly remobilise sediment-bound ^{137}Cs (Comans et al., 1989). Within the framework of this project, we have investigated a number of widely different W. European freshwater sediments, both in the laboratory and *in-situ*, focusing on the two major factors controlling radiocaesium mobility: the quantity of selective binding sites and the competition for these sites by other cations.

Five sediment profiles from four different freshwater lakes in The Netherlands and the UK (Table 1), which differ widely in their chemical and mineralogical properties, have been carefully sampled and analysed in our laboratories. Sediments were collected in October 1987 (Hollands Diep), November 1987 (Ketelmeer; both prior to the programme), April 1991 and August 1992 (Esthwaite), and February 1992 (Devoke). Sediment collection, slicing at different depths, pore-water extraction, and ultra-low-background ^{137}Cs-counting were done following the strategy outlined in Comans et al. (1989). The treatment of Esthwaite and Devoke sediments was slightly different in that a Mackereth type corer was used and that pore water was separated using high-speed (20,000 x g; 30 min.) refrigerated centrifugation. The *in-situ* distribution of radiocaesium between the sediment particles and the pore water was measured, together with the pore water concentrations of potentially competing major cations as described in Comans et al. (1989). The highly selective binding sites for radiocaesium were measured on the same sediments by Wauters (1994).

Compilation of all *in-situ* K_D-values, measured within the framework of this project to date in Figure 1 (Comans *et al.* 1994), reveals a single relationship between the radiocaesium K_D and the pore-water ammonium concentration. This observation is in agreement with ion-exchange theory in that, among the major ions that compete with caesium for binding sites on illite clays, NH_4^+ outcompetes K^+ in anoxic sediments as it reaches higher concentrations and is about five times more selectively bound. Hence radiocaesium in sediments binds to frayed edge sites (FES) on illite according to the ion-exchange reaction:

$$FES\text{-}NH_4^+ + Cs^+ \quad \overset{K_c^{Cs/NH4}}{\longleftrightarrow} \quad FES\text{-}Cs^+ + NH_4^+$$
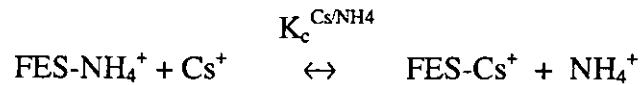
It can be shown that under natural freshwater conditions, with negligible stable caesium concentrations, the radiocaesium K_D (= $[FES\text{-}Cs^+]/[Cs^+]$) is related to the dissolved NH_4^+ concentration, on a log-log basis, according to the linear relationship:

$$\log K_D = -\log[NH_4^+] + \log (K_c^{Cs/NH4}[FES])$$

in which [FES] is the frayed edge site capacity of the sediment (meq/g) and $K_c^{Cs/NH4}$ the selectivity coefficient that describes the preference of the FES for Cs^+ relative to NH_4^+. Figure 1 shows the $\log K_D$ - $\log NH4^+$ plot of the *in-situ* data for the sediments which have been studied in this programme (Table 1; Comans *et al.*, 1994), which clearly indicates that the data follow a straight line with a slope close to (but significantly steeper than) -1. The vertical variation in the plot is about one order of magnitude or less in K_D and suggests that the product of the selectivity coefficient and the concentration of the caesium selective (frayed edge) sites in all of these European sediments would also show a limited variation.

Table 1. Sediments studied for in-situ radiocaesium mobility, with sampling dates and values for the product of the selectivity coefficient and the concentration of caesium-specific sites, i.e. the "radiocaesium interception potential"

Sediment	Sampling date	$K_c^{Cs/NH4}$[FES], meq/g
Hollands Diep, NL	21 October 1987	0.65
Ketelmeer, NL	12 November 1987	0.23
Esthwaite, UK	10 April 1991 & 17 August 1992	0.64
Devoke, UK	28 February 1992	0.24

The intercept $K_c^{Cs/NH4}$[FES] can be independently measured when the FES are "isolated" by blocking all other exchange sites in sediments with AgTU. Using this procedure, Wauters (1994; KU-Leuven) has measured $K_c^{Cs/NH4}$[FES] for all sediments in Figure 1. The results of these measurements are included in Table 1 and show that the values vary indeed by no more than a factor of 3.

We conclude from the above that ^{137}Cs obeys ion-exchange theory and thus allows its solid-liquid distribution coefficient (K_D) in radiological assessment models to be predicted from environmental variables, rather than to be erroneously treated as a constant. The radiocaesium K_D in freshwater sediments can be predicted, within acceptable limits, on the basis of the quantity of highly selective exchange sites and the pore-water NH_4^+ concentration. Figure 1 and Table 1 show that the variation in the former property is limited for widely different W. European sediments indicating that, in situations directly following a nuclear accident, a first estimate of the radiocaesium K_D can be deduced solely from the pore-water ammonium concentration.

Exchangeability of sediment-bound radiocaesium

We have shown earlier (Comans et al., 1991; Comans & Hockley, 1992) that radiocaesium migrates slowly into the interlayers of illite from which it is difficult to displace. This apparent fixation proceeds faster at low levels of competing cations, i.e. at high K_D-values. The same process effectively increases [FES] over time. The effect of this process is apparent in the $logK_D$ - $logNH_4^+$ plot of the in-situ data (Comans et al., 1994) in that the in-situ K_D-values are generally higher than the values predicted on the basis of (short-term) laboratory measurements of $K_c^{Cs/NH4}$[FES]. Moreover, the faster migration into clay interlayers in high-K_D (i.e. low-NH_4) environments may also be reflected in the slope of the data in Fig. 1, which is significantly steeper than -1 (~ -1.4). We also note that the Esthwaite and Devoke sediments, which have relatively low ammonium in their pore waters, deviate more from the predicted K_D-values than the Hollands Diep and Ketelmeer sediments, which have pore-water NH_4 concentrations in the millimolar range and have in-situ K_D's which are quite close to the predicted values.

The exchangeability of sediment-bound radiocaesium has been investigated by extraction of the sediments with 0.1 M NH_4-acetate. These extractions have been performed on all sediment cores that have been studied to date within the framework of this project (Table 1). The sediment samples have been stored frozen (-20 °C) since the pore water separation directly after sampling. Each sediment slice was extracted three times sequentially, each step for 24 hours, with 0.1 M NH_4-acetate at a liquid/solid ratio of 10 L/kg. For each sample the NH_4-acetate from the three extractions was combined. It appeared necessary to remove the ammonium ion from the solution prior to the preconcentration of the radiocaesium on ammoniummolybdophosphate (AMP) as only low recoveries (< 20%) were reached when radiocaesium was preconcentrated directly from the 0.1 M NH_4-acetate solution. Therefore, the extracts were boiled at pH > 10, to remove ammonium as $NH_3(g)$ and the volumes reduced to about 100 mL by evaporation. Radiocaesium preconcentration and measurement by ultra-low background γ-spectrometry was performed as described in Comans et al., 1989).

Results of the exchangeable ^{137}Cs measurements are given in Table 2. The amount of ^{137}Cs that can be released by the three sequential NH_4-extractions from the more mineral sediments of Hollands Diep, Ketelmeer and Esthwaite is very low; on average 2, 3, and 7%, respectively. The more organic-rich sediments of Devoke show a much higher exchangeability of 16%. The values for the three mineral sediments are low if we compare them, for instance, with those of Evans et al. (1983), who have measured ^{137}Cs exchangeabilities (also in 0.1 M NH_4^+) of 10-20% in the sediments of the Par Pond reservoir, 15-20 years after contamination. These

authors attribute their relatively high exchangeabilities to the high kaolinite content of the Par Pond sediments. Western European sediments generally contain illite as the major clay mineral, which likely causes the strong fixation of radiocaesium that has been observed in the Hollands Diep, Ketelmeer and Esthwaite sediments. Devoke apparently behaves more like the Par Pond sediments in that similar amounts of ^{137}Cs are exchangeable.

If we accept that radiocaesium in all four of the above sediments is bound solely to frayed edge sites on illitic clays in the sediments, the up to one order of magnitude differences between the exchangeable fractions of radiocaesium in these sediments is unexpected. The differences are clearly not related to the different contact times of radiocaesium with the sediments, as the lowest values are found for the sediments sampled only 1.5 years after the Chernobyl accident (Hollands Diep and Ketelmeer). Admittedly, the latter sediments have only recently been extracted, but the cores had been stored frozen at -20 °C since the pore water separation directly after sampling. We do not expect caesium migration into the clay interlayers to have progressed much further under those storage conditions.

"Exchangeable" K_D-values for radiocaesium in the sediments, calculated from the exchangeable rather than total amount of ^{137}Cs in the sediments, are included in Figure 1. We would expect "exchangeable" K_D's to correspond better with values predicted on the basis of (short-term) laboratory measurements of $K_c^{Cs/NH4}[FES]$ than the total K_D's. Although this may be the case for the Devoke sediments, total and exchangeable K_D-values for Esthwaite correspond about equally with the predictions, whereas the "exchangeable" K_D's for Hollands Diep and Ketelmeer deviate much more from the predicted values than the total K_D's. These observations strongly suggest that the short-term exchangeability measurements of radiocaesium, especially in the more mineral sediments, underestimate the amount of the radionuclide that is actually taking part in ion-exchange with the pore waters and, hence, is available for remobilisation by high concentrations of ammonium.

The low overall activities of ^{137}Cs in the Hollands Diep and Ketelmeer sediments and in the extractions in particular, have led to large counting errors on the exchangeability data. These sediments contain high levels of NH_4 in their pore waters. The kinetic ion-exchange model (Comans & Hockley, 1992) would predict radiocaesium to be taken up more slowly by clay mineral interlayers under these conditions of high competition, which is inconsistent with the findings above. New measurements on fresh (non-frozen) and larger samples (higher absolute activities) from sediments with high pore-water NH_4 are needed to investigate whether there are significant differences in the long-term exchangeability of radiocaesium in sediments with high and low levels of competing ions. It is also still uncertain what role (the high content of) organic material plays in the relatively high exchangeability of radiocaesium in de sediments of Devoke. This issue clearly needs further investigation because the kinetics of interlayer migration controls the amount of sediment-bound radiocaesium that may be remobilised on the long term. Moreover, knowledge of this process may provide "tools" that allow us to influence the "availability" of particle-bound radiocaesium in order to reduce the bioavailability and risk of remobilisation from sediments.

Table 2. *Total and exchangeable radiocaesium in the different sediment cores.*

Sediment	Depth [cm]	total ^{137}Cs [Bq/kg]	exchangeable ^{137}Cs [Bq/kg]	exchangeable ^{137}Cs [fraction of the total]
Hollands Diep	0.5	249.15	0.85	0.003
	1.5	269.79	0.69	0.003
	3.5	83.05	0.55	0.007
	6.5	5.00	0.50	0.100
	9.5	17.90	-	-
	16.5	46.31	0.51	0.011
	24.5	47.96	1.36	0.028
	31.5	21.31	5.01	*0.235*
	40.4	21.70	-	-
				average $\pm$ *s.d.: 0.022 $\pm$ 0.038*
Ketelmeer	1	115.46	10.06	0.087
	3	124.73	4.33	0.035
	5.5	224.23	5.33	0.024
	8.5	59.07	0.27	0.005
	11.5	37.466	0.76	0.020
	18.5	64.41	0.61	0.009
	25.5	51.79	14.89	*0.288*
	31.5	9.44	2.94	*0.312*
				average $\pm$ *s.d.: 0.030 $\pm$ 0.030*
Esthwaite	0.5	214.80	13.60	0.063
	2.5	330.73	22.12	0.067
	4.5	545.61	32.31	0.059
	6.5	474.14	38.44	0.081
	8.5	353.43	24.93	0.071
	10.5	345.36	18.06	0.052
	12.5	325.69	21.99	0.068
	14.5	266.41	20.31	0.076
	16.5	164.03	15.03	0.092
	18.5	42.73	9.329	*0.218*
	20.5	21.59	4.791	*0.222*
				average $\pm$ *s.d.: 0.070 $\pm$ 0.012*
Devoke	0.5	1813	343.78	0.190
	1.5	1860	401.78	0.216
	2.5	2142	345.69	0.161
	3.5	2598	375.72	0.145
	4.5	3096	363.83	0.118
	5.5	2579	270.93	0.105
	6.5	1524	208.66	0.137
	7.5	1023	237.20	0.232
	8.5	848	174.72	0.206
	9.5	727	181.78	0.250
	10.5	644	140.63	0.218
	11.5	653	44.73	0.068
	12.5	719	108.70	0.151
	13.5	685	94.97	0.139
	14.5	588	81.80	0.139
	15.5	392	58.42	0.149
	16.5	244	103.70	*0.426*
	17.5	146	81.32	*0.558*
	18.5	130	68.18	*0.523*
	19.5	106	56.20	*0.531*
				average $\pm$ *s.d.: 0.164 $\pm$ 0.050*

*average and s.d. values exclude the (unexplained) high exchangeabilities in the bottom sections of each core (indicated in italics)

In the kinetic model we have developed previously on the basis of laboratory sorption experiments of radiocaesium on illite (Comans & Hockley, 1992), we were unable to consider a reverse process of radiocaesium remobilisation from interlayer sites. The equilibration times of up to 4-weeks were too short for the reverse process to become apparent. Nevertheless, the fact that radiocaesium in sediments is still exchangeable to a certain extent after more than 20 years of contact with sediments (Evans et al., 1983), indicates that such a reverse process must exist.

Because of its relevance for the long-term availability of sediment-bound radiocaesium, we have investigated the long-term release of particle-bound radiocaesium in more detail. The primary objective of this part of our study is to estimate the existence and magnitude of a slow remobilisation (reverse rate) of radiocaesium from clay mineral interlayers during contact with a high concentration of competing ions. After the three sequential 0.1 M NH_4-acetate extractions, the sediments have been resuspended for a fourth time in a fresh 0.1 M NH_4-acetate solution and have been allowed to equilibrate for more than one year (400-560 days). Ammonium has been removed from the solution and radiocaesium preconcentrated on AMP and counted on the ultra-low background γ-spectrometer as described above.

Table 3: Average fraction of exchangeable-^{137}Cs in sediments after 3 sequential 24-hr NH_4-extractions and the additional fraction mobilised after a 4th 400/560-d extraction. A reverse rate constant and halve-life for the slow remobilisation of ^{137}Cs from the sediments has been calculated on the basis of the 4th extraction, assuming a first order process.

Sediment	exch. ^{137}Cs after 3x 24-hr extraction [fraction of the total]	additional exch. ^{137}Cs after 400/560-d extraction* [fraction of the total]	reverse rate constant [y^{-1}]	$t_{1/2}$ [y]
Hollands Diep	0.022 ± 0.038	0.0089 ± 0.0050	0.0082	85
Ketelmeer	0.030 ± 0.030	0.0095 ± 0.0030	0.0087	79
Esthwaite	0.070 ± 0.012	(still equilibrating)	-	-
Devoke	0.164 ± 0.050	0.0380 ± 0.0355	0.0220	31

*equilibration time 4th extraction = 400 days for Hollands Diep & Ketelmeer; 560 days for Devoke.

Table 3 shows the average fraction of exchangeable-^{137}Cs in sediments after 3 sequential 24-hr NH_4-extractions and the additional fraction mobilised after the 4th, long-term (400/560-days) extraction. Assuming that (1) all (rapidly) "exchangeable" radiocaesium had been removed by the three prior extractions, and (2) a first order remobilisation process, we can roughly calculate the reverse rate constant that describes the slow remobilisation of ^{137}Cs from the sediments, which we interpret as the slow release of radiocaesium from the interlayer sites (see Comans & Hockley, 1992). Table 3 indicates that the half-life of this reaction is of order 30-80 y^{-1}. Independently, and using a model that includes radiocaesium sorption kinetics to simulate radiocaesium in each of three phases in sediment profiles: aqueous, exchangeably bound and slowly reversible (often termed "fixed"), Smith & Comans (1995) have found evidence for a reverse reaction from the slowly reversible sites of order 10 years. These findings are in fairly close agreement and suggest that radiocaesium on interlayer sites, which

is generally referred to as being "fixed", is not truly immobilised but can, at least partly, be very slowly remobilised.

General conclusions from this study

The *in-situ* K_D-values that have been measured in this study have successfully been related to fundamental properties of the sediments: the concentration of highly selective binding sites for radiocaesium —frayed edge sites on illite— and the concentration of the major ion competing with radiocaesium for these sites —the ammonium ion—. Our results show that the mobility of radiocaesium in sediments follows ion-exchange theory and allow the *in-situ* radiocaesium distribution coefficient to be predicted beyond the conditions under which the measurements were made.

The exchangeability of radiocaesium, measured by 3 sequential rapid (24-hr) extractions is low for the more mineral sediments of Hollands Diep, Ketelmeer and Esthwaite; 2-7% of the total amount in the sediment. For the more organic sediments from Devoke, the exchangeability is significantly higher; 16%. These results would imply "exchangeable" K_D-values for radiocaesium to be down to almost two orders of magnitude lower than the total K_D-values.

Long-term extractions with NH_4, after having first removed the rapidly exchangeable amount, have given evidence for a slow remobilisation of radiocaesium from clay mineral interlayers and indicate that the term "fixed" is not truly appropriate for that particular pool of radiocaesium in sediments. We have been able to estimate a half-live for the slow remobilisation of radiocaesium of 30-80 years. "Exchangeable" K_D-values for radiocaesium in environments where the radionuclide is in contact with (high concentrations of) competing (NH_4) ions for many years would, therefore, be higher than the values measured by short-term extractions.

The good correspondence between total *in-situ* K_D's and values predicted on the basis of ion-exchange theory and the observation that radiocaesium can, after removal of the rapidly-exchangeable amount, still be slowly released from sediments that have been in contact with this radionuclide for up to 6 years, suggest that the amount of radiocaesium in sediments which is available on the long-term is, therefore, likely to be larger than is generally believed.

References

Comans, R.N.J., Middelburg, J.J., Zonderhuis, J., Woittiez, J.R.W., De Lange, G.J., Das, H.A. & Van Der Weijden, C.H. (1989) Mobilization of radiocaesium in pore water of lake sediments. *Nature* **339**, 367-369.

Comans, R.N.J., Haller, M. & De Preter, P. (1991) Sorption of cesium on illite: non-equilibrium behaviour and reversibility. *Geochim. Cosmochim. Acta* **55**, 433-440.

Comans, R.N.J. & Hockley, D.E. (1992) Kinetics of cesium sorption on illite. *Geochim. Cosmochim. Acta* **56**, 1157-1164.

Comans, R.N.J., Hilton, J., Cremers, A., Bonouvrie, P.A. & Smith, J.T. (1994) Predicting radiocaesium ion-exchange behaviour in freshwater sediments. *Report- ECN-RX--93-108. (also submitted for publication).*

Cremers, A., Elsen, A., De Preter, P. & Maes, A. (1988) Quantitative analysis of radiocaesium retention in soils. *Nature* **335**, 247-249.

Evans, D.W., Alberts, J.J. & Clark, R.A. (1983) Reversible ion-exchange fixation of cesium-137 leading to mobilization from reservoir sediments. *Geochim. Cosmochim. Acta* **47**, 1041-1049.

Smith, J.T. & Comans, R.N.J. (1995) Modelling the diffusive transport and remobilisation of ^{137}Cs in sediments: the effects of sorption kinetics and reversibility. *Geochim. Cosmochim. Acta (accepted for publication)*

Wauters, J. (1994) *Radiocaesium in aquatic sediments: sorption, remobilization and fixation.* Ph.D. thesis No. 246, Faculteit Landbouwkundige en Toegepaste Biologische Wetenschappen, Katholieke Universiteit Leuven.

Figure 1. Total (closed symbols), exchangeable (open symbols), and predicted (lines) *in-situ* K_D-values for different w-European lake sediments.
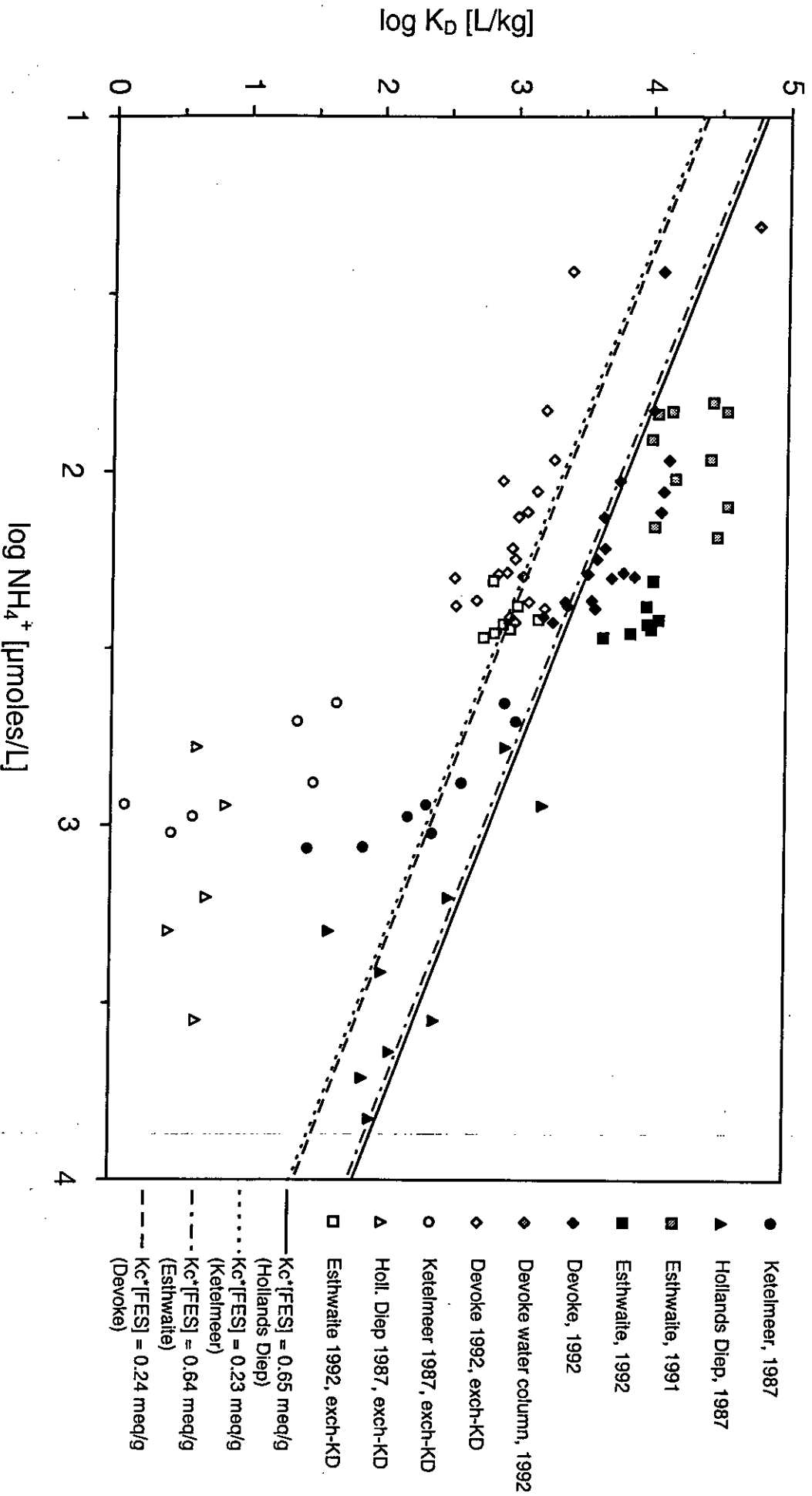
Dynamics of radiocaesium turnover in brown trout: model predictions

NINA, Norway

Aim: To model how environmental and metabolic variables determine radioactivity in brown trout.

The Model

The model is structured by five tiers of equations, each feeding parameters into above levels (Fig. 1). The core equation describes the changes in fish radiocaesium body burden with time. At the level below, equations for radiocaesium excretion and intake provides the input parameters to this equation. Next, a series of equations is given for radioactivity of prey animals and absorption efficiency, feeding rates and growth rates of brown trout that provide parameters for the radiocaesium intake equations. Growth rates determine the body size of brown trout which is an important parameter for feeding rates and radiocaesium excretion. Growth rates are used to quantify feeding rates at levels below maximum feeding. At the lowest level, equations for ambient temperature in lakes provides data necessary for estimating growth rates, feeding rates and radiocaesium excretion rates.

To test the model predictions in a natural setting we compared predicted and measured 137Cs-radioactivity from age-2 to age-4 for the 1985, 1986 and 1989 year-classes of brown trout from the Norwegian Lake Høysjøen. Model performance was evaluated for the period 1987-90, shortly after the Chernobyl fallout when radioactivity in fish and prey declined quite rapidly, and for the period 1991-3 under steady-state-like conditions without major changes in fish and prey radioactivity. Model predictions were made for the dynamic conditions during the first two years after a fallout, and for the subsequent steady-state-like conditions. Predictions for three different lakes with different temperature regimes (data source: temperate: Lake Liavatnet, 59°N, 6°E, 40 m above sea level; boreal: Lake Høysjøen: 63°N, 11°E, 222 m above sea level; and sub-Alpine: Lake Aursjø: 61°N, 8°E, 1085 m above sea level) were made.

Model predictions

Maximum radioactivity attained in brown trout after a fallout is influenced by lake type, time of fallout, fish growth and feeding rates, and fish size. Peak radioactivity is predicted to be considerably higher in the temperate and boreal lakes than in the sub-Alpine lake (Fig. 2). Peak radioactivity increases with increasing feeding and growth rates of the fish. The effects of high feeding rates on caesium accumulation is especially pronounced in the temperate lake where an increase in growth rate, and the accompanying feeding rate, from 80 to100 % of the maximum nearly doubled peak radioactivity. In all lakes a fallout during spring when water temperature is increasing, gives the highest peak radioactivity. In the temperate and boreal lakes a much higher peak radioactivity is predicted for a spring than a summer fallout. Although fallout date is important for peak radioactivity, its influence on the long term development in fish radioactivity for different fallout dates is within 20% of each other.

The relationship between specific radioactivity (S, Bq g^{-1}) and fish size (W, g), $S = aW^b$, changes with time. Shortly after the fallout, the caesium accumulation rate is highest in the small fish with

b-values at approximately -0.2 in all three lake types. After peak radioactivity is reached, the b-values gradually approaches zero. Finally, the relationship between specific radioactivity and fish size became positive with b-values at 0.10-0.15. For the temperate and boreal lakes the relationship changes from negative to positive in the spring one year after the fallout, whereas for the sub-Alpine lake the model predicts that positive b-values occur later during the second summer. Thus, irrespective of lake type radioactivity should increase with fish size in the second year, not decrease as in the year of contamination.

At steady state the model predicts a seasonal variation in biomagnification, with minimum values in late spring and maximum in the autumn. In the temperate and boreal lakes the predicted biomagnification is higher and the seasonal variation more pronounced than in the cold lake. The biomagnification (B_m) at steady state depends on fish size (W, g): $B_m=aW^b$. For the three temperature regimes modelled, there is a negative relationship between fish size and the biomagnification factor at the autumn maximum. The relationship is the most negative in the warmest lake. On the other hand, this relationship is slightly positive at the late spring minimum in the temperate and boreal, but not the sub-Alpine lake.

The model (Fig. 1) where used to develope a quantitative model for biomagnification of radiocaesium in brown trout under steady state conditions. Due to non-linear relationships between maximum biomagnification, body size and growth rate (G, % of maximum growth), we used a polynomial model: $Bm = A (b_0 + b_1W + b_2W^2 + b_3G + b_4G^2 + b_5G^4)$ where A is the absorption efficiency of radiocaesium. Coefficients were estimated for the three different lake types by multiple regressions for brown trout weighing from 5 to 500 g, growing at rates between 20 and 100 % of the maximum at 100% absorption efficiency (A=1).

Biomagnification is highest for small fish in the temperate lake growing and feeding at maximum rates (Fig. 3). At growth and feeding rates below this maximum, the maximum biomagnification is reduced. This reduction is most pronounced in the temperate and boreal lakes, and when the growth rate decreases from 100 to 80% of the maximum.

Model generality
The present model gave reasonable predictions for the radioactivity of brown trout in the Lake Høysjøen, Norway. This holds true both during a period with declining radioactivity after the fallout, and in a period with steady-state-like conditions. Different absorption factors were used, however, in the two situations. To be general, the model should be applicable for brown trout in a wide range of ecological systems, as this species have a wide geographical range. The model application depends strongly upon the generality of the sub-models, which in this case is chiefly based on established, bioenergetic knowledge about brown trout. Experiments have been performed to establish absorption efficenecy and excretion rate (including the size and temperature dependecy) for Arctic charr (*Salvelinus alpinus*, two poulations), bream (*Abramis brama*), whitefish (*Coregonus lavaretus*) and Atlantic salmon (*Salmo salar*, two populations), and the present model may be further developed to be valid for freshwater fishes in general.

There is a growing appreciation for bioenergetically based models in eco-toxicology, as they describe the actual mechanism at work in contaminant accumulation. This approach is most valuable for radiocaesium contamination, and we feel that it is applicable for other cantaminants

as well, given that the rates of intake and excretion can be defined.

List of Figures

Fig 1. Model structure: five tiers of equations (A-D), each feeding parameters into above levels: A: The core equation describing the changes in radiocaesium body burden with time. B: equations for radiocaesium excretion and intake which provides the input parameters to the core equation. C: equations for radioactivity of prey and the brown trout feeding rates, providing parameters for the radiocaesium intake equations. D: the equation for brown trout growth rates. Growth rates determine the body size of the fish which is an important parameter for feeding rates and radiocaesium excretion (at level B). Growth rate are used to quantify feeding rates at levels below maximum feeding. E: equations for ambient water temperature in lakes providing parameters for estimating growth at level D, feeding rates at C and radiocaesium excretion rates at level B.

Fig. 2. Predicted effects of fallout date (from 1 May to 1 August) and fish growth and feedingrates on peak radioactivity of brown trout in different lake types. Results are shown for brown trout weighing 100 g 1 May.

Fig. 3. Predicted biomagnification of ^{137}Cs in brown trout at different growth rates and body sizes, in a situation with stable radioactivity in prey animals. Results are shown for three different lake types and an absorption efficiency at 0.45.
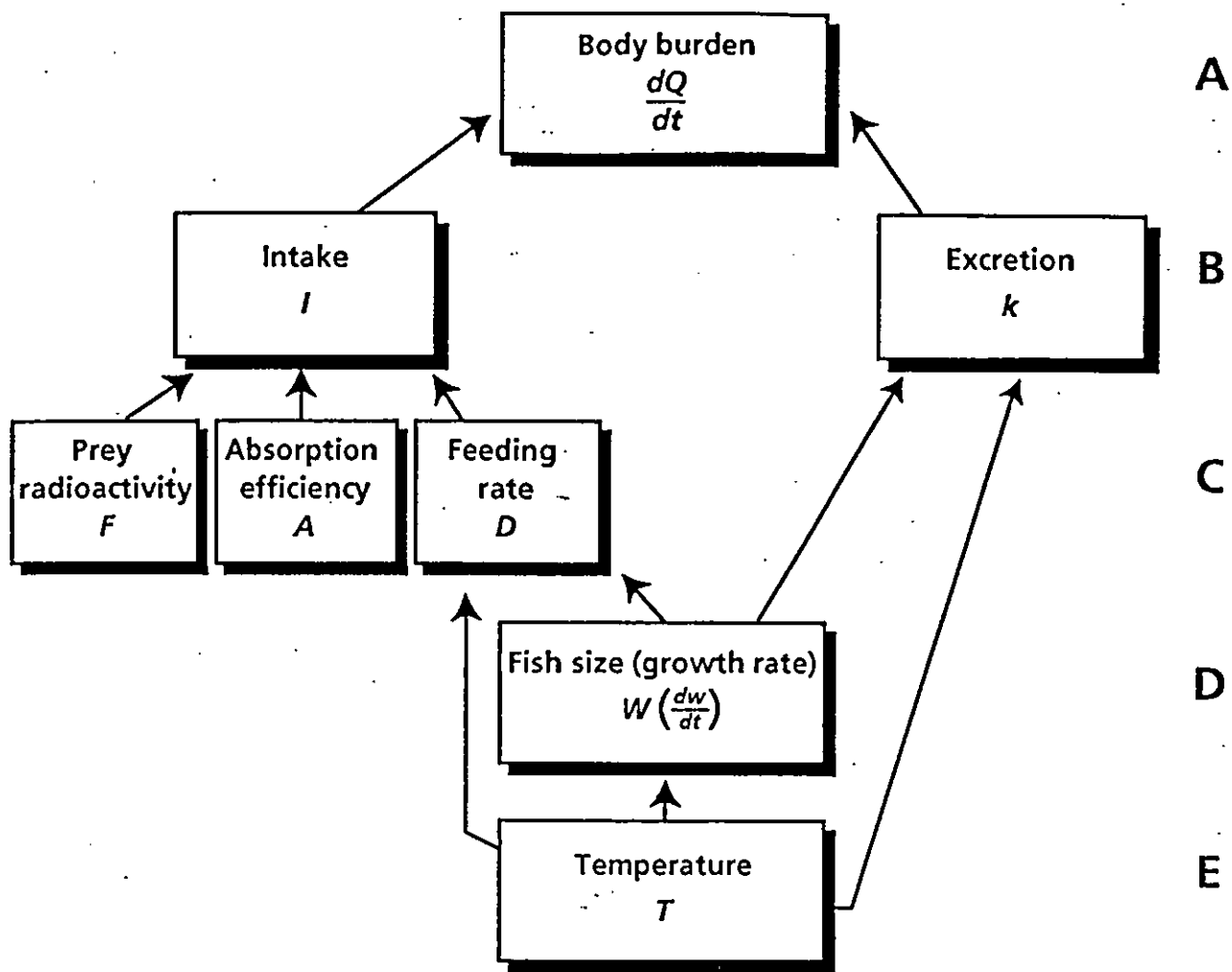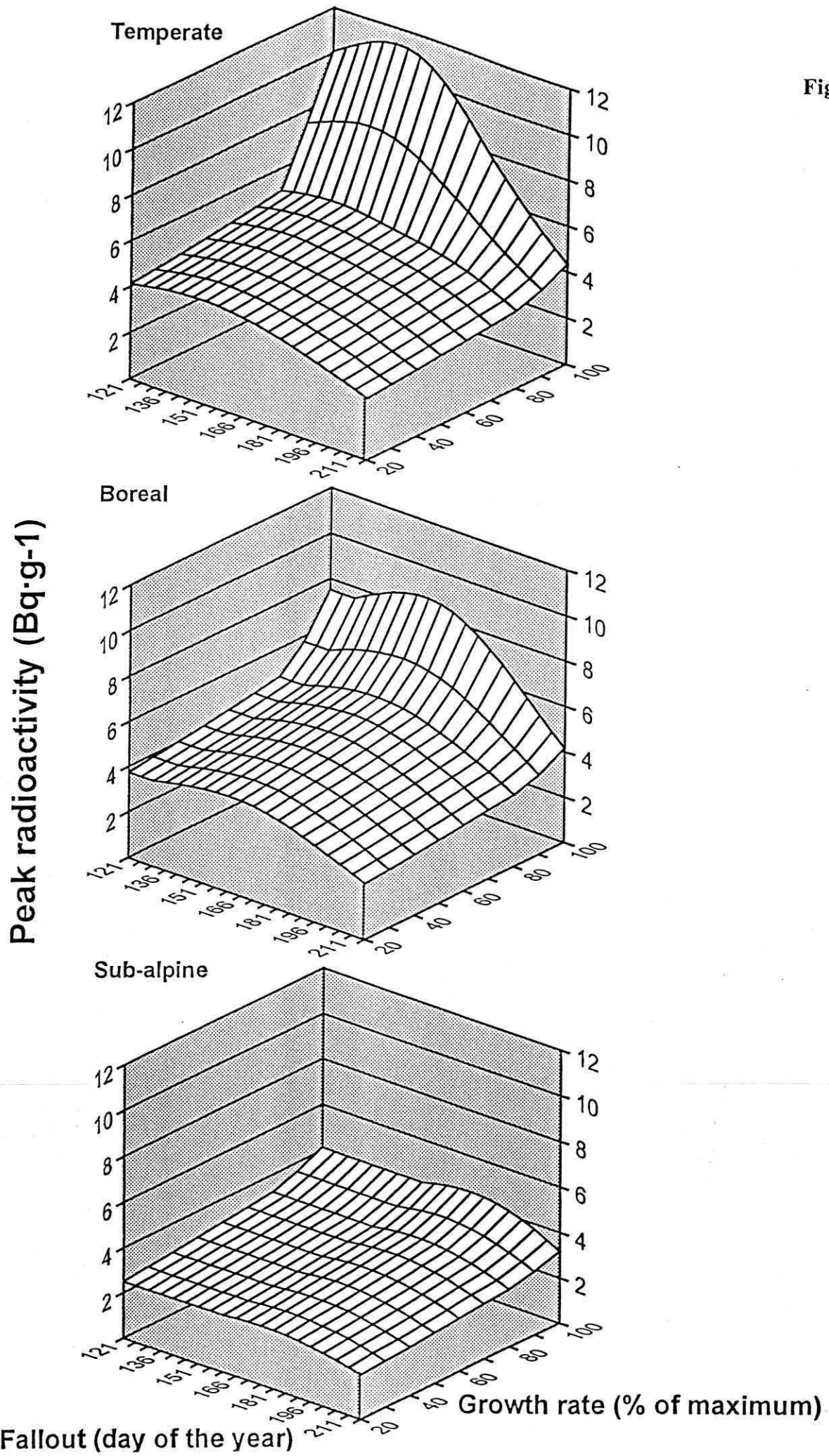
Figure 1.

Fig. 2

Temperate

Boreal

Sub-alpine

Peak radioactivity (Bq·g-1)

Fallout (day of the year)

Growth rate (% of maximum)

Fig. 3

Temperate

Boreal

Sub-alpine

Biomagnification

Body size (g)   Growth rate (% of maximum)